

International Collaborative Research Project

Report

May 2024 - January 2025



Foreword

We are pleased to present this collection of research reports, marking the successful completion of another year of international collaborative research. Over the past year, high school students from around the world came together to engage in joint scientific inquiry—formulating research questions, conducting experiments or investigations, analyzing data, and presenting their findings. We sincerely hope that this experience was not only intellectually rewarding, but also personally meaningful for all participants.

Today's world faces an array of pressing global challenges. Environmental issues, the need for sustainable energy solutions, disaster resilience, and emerging technological risks are just a few of the complex issues that require urgent attention. These problems are inherently scientific, but they are also deeply international. No single nation, discipline, or perspective can resolve them alone. In this context, the ability to work collaboratively across borders in the pursuit of scientific understanding is not just a valuable skill—it is an essential one. Throughout this program, students tackled issues that demand critical thinking, scientific literacy, and effective teamwork. Beyond the research itself, students also navigated the challenges of communicating across different time zones, cultures, and languages. They learned how to negotiate differing viewpoints, assign roles and responsibilities, and build consensus within their teams. These are the very things needed for meaningful collaboration on the global stage.

At Ritsumeikan High School, we have long believed in the power of education to open minds and foster international cooperation. For nearly 20 years, we have promoted international collaborative research at the high school level. In the early days, such efforts were limited by the practical barriers of international communication. But thanks to the advancement of ICT tools, it is now possible for students to interact regularly and meaningfully with peers around the world, making sustained collaboration a reality. This year, we were delighted to welcome the participation of many schools from a diverse range of countries and regions. Over the course of the year, student teams engaged in thoughtful dialogue, rigorous inquiry, and mutual support as they worked toward shared research goals. The final presentations delivered at the International Collaborative Research Fair were a testament to the depth of their engagement and the quality of their work. We have compiled the research reports into this booklet in the hope that they will inspire others and serve as a record of the students' achievements.

We would like to express our heartfelt appreciation to all the students and teachers who contributed to this project, as well as to the administrators, guardians, and institutions who supported their efforts throughout the year. In particular, we are deeply grateful to the Japanese Ministry of Education, Culture, Sports, Science and Technology for their generous support of the International Collaborative Research Fair as part of its international exchange initiatives.

To all participating students: as you move forward in your academic and personal journeys, we hope that the lessons you learned during this project will continue to guide and empower you. The experience of working with others to solve scientific problems—across borders, cultures, and disciplines—will remain a source of strength as you face the uncertainties and opportunities of the future. Continue to pursue knowledge, build bridges across differences, and use science as a tool for understanding and improving our world. We look forward to seeing the remarkable things you will achieve in the years ahead.

March 2025
Ritsumeikan High School
SSH Department

Table of Contents

Participating Schools	3
Year Schedule	4
Research Topics	5
International Collaborative Research Fair	6
Research Reports	7
Group 1 (QASMT - Ritsumori)	8
Group 2 (QASMT - Tokai)	13
Group 3 (NGS PSSW - HatsuR)	18
Group 4 (NGS PSSW - Seishin)	22
Group 5 (NGS, YK - Ikunishi)	26
Group 6 (NGS, YK - Matsusho)	30
Group 7 (GT - MWU)	34
Group 8 (BMD - Sensan)	38
Group 9 (MP - TGUSHS)	41
Group 10 (PSHS EV - MWU)	45
Group 11 (PSHS-SRC - KFNHS)	51
Group 12 (SST - Ryuichi)	55
Group 13 (SST - Futen)	61
Group 14 (KGHS - Rits)	66
Group 15 (KGHS - SGHS)	73
Group 16 (KSHS - HatsuR)	79
Group 17 (KSHS - STHS)	83
Group 18 (KSHS - WUHS)	88
Group 19 (CD - Fukuko)	92
Group 20 (CD - Rits)	97
Group 21 (CUD - Nara Seisho)	103
Group 22 (KVIS - IG)	107
Group 23 (PDS - Tokai)	113
Group 24 (PDS - STHS)	116
Group 25 (PCSHSM - Fukuko)	120
Group 26 (PCSHSM - KHS)	125
Group 27 (PCSHS PT - EPMm)	129
Group 28 (PCSHSTRG - Akashi-Kita)	133
Group 29 (PCSHSTRG - Tokko)	136
Post Survey Results	138

Participating Schools

Total 41 Schools

Australia	Queensland Academy for Science Mathematics and Technology
Cambodia	New Generation School, Preah Sisowath High School New Generation School, Preah Yukunthor High School
Hong Kong	GT College
Indonesia	Budi Mulia Dua High School Mutiara Persada High School
The Philippines	Philippine Science High School - Eastern Visayas Campus Philippine Science High School - SOCCSKSARGEN Region Campus
Singapore	School of Science and Technology, Singapore
Taiwan	Kaohsiung Municipal Kaohsiung Girls' Senior High School Kaohsiung Municipal Kaohsiung Senior High School
Thailand	Chitralada School Chulalongkorn University Demonstration Secondary School Kamnoetvidya Science Academy Patumwan Demonstration School, Srinakharinwirot University Princess Chulabhorn Science High School Mukdahan Princess Chulabhorn Science High School Pathum Thani Princess Chulabhorn Science High School Trang
Japan	Chiba Prefectural Funabashi High School Ehime Prefectural Matsuyamaminami High School Fukushima Prefectural Fukushima High School Hatsushiba Ritsumeikan Junior & Senior High School Hyogo Prefectural Akashi-Kita High School Hyogo Prefectural KOBE High School Ichikawa High School Ikueinishi High School Institute of Science Tokyo High School Matsushogakuen High School Mukogawa Women's University Senior High School Nara Prefectural Seisho High School Ritsumeikan Moriyama High School Ryugasaki Daiichi Senior High School Seishin Girls' High School Seishingakuen High School Sendai Daisan High School Tennoji Senior High School Attached to OsakaKyoikuUniversity Tokai University Takanawadai Senior High School Tokyo Gakugei University Senior High School Waseda University Honjo Senior High School Yamaguchi Prefectural Tokuyama Senior High School Ritsumeikan High School

Year Schedule

On May 10, we held the first learning session for Japanese students, introducing the project's objectives, significance, and annual schedule, along with guidance for international collaborative research. A week later, on May 17, we hosted an orientation for overseas teachers, explaining the project's purpose and key considerations. Schools then registered their available research fields—math, physics, chemistry, biology, earth science, and information science—and were matched into collaborative research groups.

The first plenary meeting between Japanese and overseas schools was held online on May 31. It included an overview of the project, exchange activities, schedule confirmation, and introductions of the research groups. At the second plenary meeting on June 7, Ritsumeikan High School led cultural exchange activities, such as school and language introductions, to help build rapport within groups. Native English-speaking staff from Ritsumeikan supported the first group meetings to facilitate initial research topic discussions.

From that point on, each group held regular meetings to advance their research. After each meeting, activity reports were submitted via Google Forms and automatically published on the project homepage to visualize each group's progress.

On July 19, we held a teachers' meeting for Japanese schools to share updates and confirm that all groups had finalized their research themes and summer plans. Ritsumeikan offered additional support to groups that needed it. After the summer break, on September 6, the second learning session for Japanese students was held. Students presented their research progress and plans, organized by subject, and received feedback from partner school teachers.

On September 13, overseas teachers gathered online to share updates. Then, on October 4, we held the third plenary meeting with both domestic and international schools. The session began with a lecture on data analysis titled "More than Average" by Mr. Leo Hsieh of Kaohsiung Municipal Kaohsiung Senior High School in Taiwan. Students then gave interim presentations in breakout rooms, with feedback provided by international graduate students from Ritsumeikan University.

The fourth plenary meeting took place on December 20, covering research report writing, final presentation preparation, and a mini-lecture on effective slide design. Groups then met in breakout rooms to plan for the International Collaborative Research Fair (ICRF).

The ICRF was held on January 11, 2025. After a keynote lecture, students gave presentations in four breakout sessions organized by research field. A post-activity questionnaire was conducted, followed by random breakout sessions for participants to reflect on the year's experience through informal discussions. Each group submitted an English-language report summarizing their research.

All project activities were conducted online. Ritsumeikan organized all sessions and meetings via Zoom. Slack was used for communication, with dedicated group channels. Activity reports were submitted using Google Forms, and content was automatically published to the project homepage using Google Sites and Google Apps Script.

Research Topics

Group	Research Topic
Group 1	Researching the Effectiveness of Using Bioethanol Generated from Invasive Plants as Fuel
Group 2	Investigating the Protein Content and its Respective Allergens of Common Milk in Australia and Japan
Group 3	Mathematics of Sudoku Puzzles
Group 4	Water Quality Tests Using Bivalve
Group 5	Comparison of Physical Properties of Roofing Materials in Japan and Cambodia
Group 6	Mold Found in Different Environment.
Group 7	Use Food Waste to Absorb Heavy Metal Ions
Group 8	Environmental Problems as Seen through Pine Leaves
Group 9	Utilization of Soybean Extract as an Alternative Nitrogen Source in Making Nata De Coco
Group 10	Development of an Interactive Game on Environmental Awareness Titled: "Oh, Crab! Echoes Of The Shore"
Group 11	Lactic Acid Synthesis from Starch-Based Biomass Materials
Group 12	Investigation on the Correlation Between a Runner's Finger Angle and Their Speed
Group 13	Determining the Most Suitable Dam Type to Instigate Anti-Phase Waves and Reduce Seawater Overtopping at Coastal Areas
Group 14	Scientific Analysis of the Taste And Texture of Rice
Group 15	Pumping Straw
Group 16	Learning Behavior of Fruit Flies (<i>Drosophila melanogaster</i>)
Group 17	The Relationship Between Surface Shape and Airflow
Group 18	Drop and Rebound
Group 19	The Study of Microplastics in Marine Animals in the Seas of Thailand and Japan
Group 20	Comparative Analysis of Extract Alone Versus Extract with Blood
Group 21	Developing Hemostatic Agents Using Different Plants
Group 22	The Study of Cellulose Fiber Water Filter from Bamboo and Teas
Group 23	Measuring Sugar in the Fruits
Group 24	Comparative Assessment of Doxorubicin and Ethanol Production Using Japanese and Thai Fruit Waste
Group 25	The Study of Moon's Orbit by Kepler's Second Law
Group 26	Producing Bio-Ethanol From Food Waste Utilizing Yeast Fermentation
Group 27	Comparison and Consideration of Damage by Lantana Camara in Japan and Thailand
Group 28	A Study Comparing Water Quality Between Thailand and Japan.
Group 29	The Difference Between Japanese Rice and Thai Rice in Making Rice Resin

International Collaborative Research Fair

Date/Time	January 11th, 2025, 12:00~17:00 (JST)
Format	Online (Zoom)
Language	English
Scale	32 Research Topics / Approximately 250 participants 43 Schools (20 overseas schools, 23 Japanese schools)
Schedule	<p><u>12:00-12:10 Opening Ceremony</u></p> <p>Opening Address</p> <p><u>12:10-12:50 Special Lecture</u></p> <p>Through the science lecture, participating students gained a deeper understanding of global-scale research activities and the importance of collaboration with researchers around the world. The lecture helped make these ideas more concrete and relatable.</p> <p><u>13:00-15:30 Science Project Presentation</u></p> <p>Presentations were held in four breakout sessions. Each group gave a joint presentation using the slides they had prepared collaboratively. Each presentation lasted 10 minutes, followed by a 5-minute Q&A session. Teachers from participating schools acted as commentators and provided advice.</p> <p><u>15:30-16:00 Feedback Session</u></p> <p>All participants completed a post-event questionnaire. Japanese students also completed an AAR survey</p> <p><u>16:00-16:45 Group Discussion and Reflection</u></p> <p>Students from both domestic and overseas schools were randomly assigned to groups to reflect on their collaborative research experience and share advice for future participants.</p> <p><u>16:30-17:00 Closing Ceremony</u></p> <p>Instructions were given regarding the submission of final reports, followed by closing remarks.</p>

Research Reports

Sustainability of Producing Biofuel from Invasive Plant Species

Ashwanth Duraipandian¹, Bhavy Garg¹, Prabha Thakur¹, Miura Kazuho², Yusei Shimazu², Hana Suese²

¹Queensland Academy for Science Mathematics and Technology (Australia)

²Ritsumeikan Moriyama High School (Japan)

Abstract:

In this experiment, bioethanol was extracted from Japanese and Australian invasive weed species and compared. The general procedure was to harvest Japanese and Australian plants, crush them, and then treat them with a 3% sulfuric acid solution to enable cellulose accessibility, followed by high-temperature treatment to break down and neutralize the cell walls. Cellulase was then used to facilitate saccharification at 40-50°C, followed by fermentation for several days. Japanese weeds yielded 453L-686L, whilst Australian weeds yielded 48.3-154L of ethanol per tonne of biomass. The results from both countries were then compared to each other and accepted literature from first and second-generation biofuels sources to evaluate their environmental and economic efficiency.

Keywords: Bioethanol ; Invasive-plant-species; Saccharification ; weed-management ; lignocellulosic feedstocks ;

Background:

Since biofuels first gained attention in the 19th century, they have been explored as a renewable replacement for fossil fuels targeted toward transportation fuel needs (IEA, 2023). Bioethanol is one category distinguished by the fermentation process in its production and is blended with petrol to make E10. Second-generation bioethanol utilises inedible biomass, including lignocellulosic feedstocks found in weeds. Both Australia and Japan suffer from invasive weed species that displace native flora and present toxicity to pasture animals, generally harming both ecosystem and agricultural productivity (Hunter Regional Weeds, 2024). For example, in 2016 *Vachellia Farnesiana* covered more than 30-40 million ha's of grazing land in Australia (Invasive Weeds and Animals Committee, 2016). As of 2015, Japan identified 200 invasive weed species infesting fields of crops (Tominaga & Kurokawa, 2018). Current post-removal management methods involve composting, solarisation, and processing into mulch. However, with large-scale removal of invasive weeds, they present an opportunity as a biofuel feedstock. As of now, Australia's bioethanol is dominated by first-generation fuels such as wheat starch and molasses from sugarcane (Australian Government, 2022), whilst Japan's industry is seeking to grow toward 2030 alongside sustainable goals. Thus, this report aims to evaluate whether managing specific invasive weeds by producing bioethanol from them is more environmentally and economically viable. Two invasive species were assessed from Australia and four from Japan (*Ageratum Houstonianum* (A.H.), *Solanum Mauritium* (S.M.), *Pueraria Montana* (P.M.), *Reynoutria Japonica* (R.J), *Miscanthus Sinensis* (M.S.), *Solidago* (S.)) respectively.

1. Method

Australian Method: Leaves and flowers were discarded from weed stems and stems were placed in a drying oven at 60°C for at least 18 hours to remove moisture. It was then grounded into a fine grain using a blender, then distributed equally among 4 500mL Erlenmeyer flasks plugged with corks, and pre-treated with 50mL of 3% H₂SO₄ at 50°C for 20 minutes. The mixture was then placed onto a strainer, and washed with distilled water until clear water ran through. It was then distributed into two Erlenmeyer flasks and filled with distilled water until the mixture met the 400mL line. Sodium Bicarbonate was added and stirred in, until a pH between 5.0-7.0 was reached, measured by a pH probe. 1mL/100mL of CMCase was added to the flask along with approximately a teaspoon of Sodium Metabisulphite, and placed into a 50°C water bath for at least 24 hours. 3mL of the solution was mixed with 3mL Benedict's solution into a test tube, and heated over a Bunsen burner at blue flame, until the mixture turned orange, indicating the presence of glucose. These were put aside. The glassware for fermentation such as Erlenmeyer flasks and air traps were sterilised using a solution of distilled water and sodium meta-bisulphate. The remaining glucose solution was poured into 2 sterilised flasks through filter paper, and the remaining biomass was discarded. The flasks were heated until 37°C and approximately a teaspoon of baker's yeast was added with 0.5g ammonium sulphate, and then filled with distilled water until the neck of the flask. They were plugged using air-traps that were half-filled with a sodium metabisulphite solution, and left to ferment for at least 5 days. The solution was then separated into 4 flasks equally, and an ethanol probe was used to obtain the percentage of ethanol in solution from each flask.

Japanese Method: Leaves, flowers and stems from four types of plants—Japanese knotweed (*R.J.*), pampas grass (*M.S.*), kudzu (*P.M.*), and goldenrod (*S.*)—were collected. They were dried for a few days and then ground into fine particles using a blender, with 100 g of each plant being processed. To make cellulose and hemicellulose easier to break down, a 3% sulfuric acid solution was used for chemical treatment. Next, the cell walls were destroyed using high temperature and pressure (120–160°C). After that, baking soda was added to neutralize the solution until the pH test paper turned green. This process was considered the pretreatment stage. To convert cellulose into simple sugars (glucose), cellulase enzymes were used. One gram of cellulase was added to each of the four solutions. The solutions were kept at 40°C for 24–72 hours using a circulator. In the fermentation stage, yeast was added to the saccharified solution to induce fermentation. The solutions were kept at 30–35°C for 24–48 hours to produce ethanol. Finally, an refractometer was used to measure the ethanol concentration and determine the amount of ethanol produced from each plant.

Variables

Table 1: IV and DV

Independent Variable	Invasive Weed Species
Dependent Variable	Quantity of Ethanol Produced in mL/100g biomass

Table 2: List of controlled variables and relevance in affecting data in different processes throughout method

Controlled Variable	Impact on Data	Method of Control
Temp (°C)	1) If the temperature during the acid pre-treatment was too low or high, it would reduce its effectiveness in degrading the cell walls and preparing the cellulose to be available for digestion, reducing the total mLs of ethanol produced 2) Temperature being too high/low during the digestion of cellulose could cause enzyme inactivity, or the enzyme to denature; reducing the DV 3) Temperature being too high/low during fermentation can lead to inefficient fermentation, and higher risks for bacterial growth, reducing the DV 4) Through all parts of the method, inconsistent temperatures would cause imprecision in the DV data	All processes involving temperature were conducted in a water bath or circulator with a controllable temperature, as measured in °C. All flasks for each trial were put into the water bath at the same time at the same temperature to ensure consistency and high precision.
pH	If the pH of the biomass was not properly controlled it would decrease enzyme activity which would result in a smaller quantity of bioethanol being produced. It may also result in denaturation of the enzyme which would further decrease enzyme activity and the quantity of ethanol produced.	While neutralizing the H ₂ SO ₄ a calibrated pH probe was utilized to ensure that the pH of the biomass reached the optimal level for the enzyme; between 5-7, to promote efficient enzyme activity.

Raw Data

Table 3a: Raw measurements for dry mass, final beaker volume and final ethanol yielded in mL/quantity of biomass - Australian plants

	<i>Ageratum houstonianum</i>				<i>Solanum mauritianum</i>			
	Trial 1	Trial 2	Trial 3	Trial 4	Trial 1	Trial 2	Trial 3	Trial 4
Dry Mass (g) ± 0.01	22.50	22.50	22.50	22.50	20.00	20.00	20.00	20.00
Volume of Final Beaker (mL) ± 0.5	150	153	150	154	202	225	205	230
Ethanol v/v Percentage (%) ± 20%	0.39	0.63	0.87	0.97	1.47	1.41	1.46	1.37

Table 3b: Raw measurements for dry mass, final beaker volume and final ethanol yielded in mL/quantity of biomass - Japanese plants

	<i>R.J.</i>	<i>M.S.A</i>	<i>P.M</i>	<i>S.</i>
Dry Mass (g) ± 0.01	100.00	100.00	100.00	100.00
Volume of Final Beaker (mL) ± 0.5	206	177	232	245
Ethanol v/v Percentage (%) ± 0.5	21.00	30.00	25.00	28.00

Data Processing Steps:

Ethanol yield equation, averaged from four trials for the Australian species (Litres/tonne):

$$\frac{\text{Ethanol Percentage} \times \text{Volume of Final Beaker (ml)}}{\text{Dry Biomass (g)}} \times 1000$$

The bioethanol produced will be used to create E10 (10% ethanol and 90% gasoline) for fuel. Equation for the producible Volume of E10 per Tonne of Dry Biomass (Litres/tonne):

$$\text{Ethanol Yield (L/tn)} \times 1 \text{ (tn)} \times 10$$

Bioethanol production costs on average US\$1 per litre (Martins, 2022), compared to 2024 unleaded petrol prices of US\$1.21 in Australia (ACCC, 2024) and US\$1.15 in Japan (Trading Economics, 2019). This information was used to calculate the savings created per tonne of dry biomass (US\$/tn):

$$(\text{Price of gas (\$/L)} - \text{Price of Ethanol Production (\$/L)}) \times \text{Ethanol Yield (L/tn)}$$

Furthermore, 1 litre of petrol emits 2.3 kg of emissions (National Transport Commission, 2019). This is reduced by 2.7% when using E10 after taking into consideration the emissions due to ethanol production (NSW Fair Trading, 2021). This information was used to calculate the amount of CO2 emissions saved (kg/tn):

$$2.3 \text{ (kg/L)} \times \text{Ethanol Yield (L/tn)} \times 0.027$$

Processed Data



Figure 1: Comparing the average ethanol yield (L/tn), money saved (US\$/tn), and CO₂ emissions saved (tn/tn) from the biomass sources.

Discussion

Upon review, many sources of error in this experiment impacted the data and the following data analysis. Discrepancies in the method between each country such as the varying temperature, time for enzymatic digestion and specific feedstocks utilised reduced the accuracy of the experiment. Firstly, the higher temperature of 120°C during the Japanese pre-treatment compared to 50°C for Australian pre-treatment likely resulted in a more efficient cell wall break down, resulting in a greater availability of fermentable sugars in the Japanese trials (Corredor et al., 2006). Additionally, Japanese trials spent more time in the digestion process, up to 3 days as opposed to 1, resulting in enhanced enzyme activity and thus greater yields. Lastly, Japan additionally utilised leaves and flowers, which for certain plants outputted substantial ethanol. For example, Solidago had dense yellow flowers which have been proven to contain high quantities of fermentable sugars, as supported by Figure 1. All of these things result in a systematic error where trials with shorter digestion periods and lower temperature had a reduced ethanol yield, as shown by the significantly lower yield from Australian plants. A possible solution to this error is to standardize the methods in order to minimize variability across the trials. Alternatively, multiple trials of the weed could be conducted with adjustments to temperature in pre-treatment along with varying time spent in the digestion phase in order to find the best treatment that maximizes ethanol yield prior to official trials.

Traditional first generation feedstocks such as corn yields 433L/tonne of biomass (Kumar & Singh, 2016), whilst other lignocellulosic feedstocks such as forest thinnings have yielded 306L/tonne of biomass (Nalley & Hudson, 2004). In regards to this, the Japanese yield is highly efficient as shown in Figure 1 with values of 453L, 531L, 580L and 686L/tonne. However, Australian ethanol outputs were deficient with values of 48L and 154L, thus requiring further investigation with efficient methodologies as discussed above, as well as a wider range and better choice of invasive weed species such as *Lantana Camera* and *Mimosa Pigra*.

Conclusion

Overall, Japanese invasive plant species produced 453-686 L of ethanol per ton of biomass, while Australian species yielded only 48.3-154L. The significant disparity in ethanol production is likely due to variations in the methods employed by each country. Japanese weeds present a promising feedstock for their biofuel industry with highly efficient ethanol yields, whilst Australian weeds require further investigation for a more accurate decision on their use in the biofuel industry.

References

- ACCC. (2024, September 24). *Lower recent petrol prices welcome after prices moved higher in the June quarter*. Australian Competition and Consumer Commission. <https://www.accc.gov.au/media-release/lower-recent-petrol-prices-welcome-after-prices-moved-higher-in-the-june-quarter>
- Australian Government. (2022). *Snapshot - World biofuels trade*. DAWE. <https://www.agriculture.gov.au/about/news/snapshot-world-biofuels-dec-22>
- Hunter Regional Weeds. (2024). *Why are weeds a problem?* Hunterregionalweeds.net.au. <https://www.hunterregionalweeds.net.au/index.php/about-weeds/132-why-are-weeds-a-problem>
- IEA. (2023). *Biofuels - Energy System*. IEA. <https://www.iea.org/energy-system/low-emission-fuels/biofuels>
- Invasive Weeds and Animals Committee. (2016). *Australian Weeds Strategy 2017-2027*. Australian Government Department of Agriculture and Water Resources, Canberra. <https://www.agriculture.gov.au/sites/default/files/sitecollectiondocuments/pests-diseases-weeds/consultation/aws-final.pdf>
- Kumar, D., & Singh, V. (2016). Dry-grind processing using amylase corn and superior yeast to reduce the exogenous enzyme requirements in bioethanol production. *Biotechnology for Biofuels*, 9(1). <https://doi.org/10.1186/s13068-016-0648-1>
- Martins, O. C. (2022). OPTIMAL COST OF PRODUCTION OF BIOETHANOL: A REVIEW. *SSRN Electronic Journal*. https://www.researchgate.net/publication/363121544_OPTIMAL_COST_OF_PRODUCTION_OF_BIOETHANOL_A_REVIEW
- Nagler, A., & Gerace, S. (n.d.). *FIRST and SECOND GENERATION Biofuels WHAT'S THE DIFFERENCE?* https://waferx.montana.edu/documents/fact_sheets/1st%20v%202nd.pdf
- Nalley, L. L., & Hudson, darren. (2004). The Potential Viability of Biomass Ethanol as a Renewable Fuel. *ResearchGate*, 0412002. https://www.researchgate.net/publication/23748558_The_Potential_Viability_of_Biomass_Ethanol_as_a_Renewable_Fuel
- National Transport Commission. (2019). Carbon Dioxide Emissions Intensity for New Australian Light Vehicles 2018. In *National Transport Commission*. <https://www.ntc.gov.au/sites/default/files/assets/files/Carbon%20dioxide%20emissions%20intensity%20for%20new%20Australian%20light%20vehicles%202018.pdf>
- NSW Fair Trading. (2021, January 19). *E10 and the environment*. NSW Government. <https://www.nsw.gov.au/driving-boating-and-transport/e10-fuel/e10-and-environment>
- Tominaga, T., & Kurokawa, S. (2018). Research issues, challenges, and opportunities for weed management in Japan. *Crop Protection*. <https://doi.org/10.1016/j.cropro.2018.02.002>
- Trading Economics. (2019, December 7). *Japan Gasoline Prices*. Tradingeconomics.com; TRADING ECONOMICS. <https://tradingeconomics.com/japan/gasoline-prices>

Investigating the Protein Contents and their Respective Allergens of Common Milk in Australia and Japan

Tina Kwon¹, Hannah Ryu¹, Fiona Tijo¹, Eishal Qamar², Rinka Yagi²

¹Queensland Academy for Science Mathematics and Technology (Australia)

²Tokai University Takanawadai High School (Japan)

Abstract:

This report aimed to measure and compare the protein content in different types of milk (Soy, Full Cream, Almond, A2, Oat and Goat Milk) using the Bradford assay and SDS page electrophoresis. This is significant as alternative milk types are becoming more widely consumed, and they may not provide the same protein content levels, which could inhibit growth and development, particularly in children. The results show that A2 and Full Cream had the highest protein content, while Almond and Oat had significantly lower levels. These findings highlight that not all milk alternatives are nutritionally equivalent in terms of protein, which could affect dietary choices.

Keywords: Milk, Food Allergies, Plant-based Alternative, Bradford Assay, Electrophoresis

1. Introduction

Milk is a commonly enjoyed beverage in both Australia and Japan, but it is also often the cause of allergies. Milk allergy is primarily caused by the malfunction of the immune system, as they identify certain proteins to be harmful and release immunoglobulin antibodies to neutralise these proteins. This process is what leads to irritating and puffy symptoms of the allergy (Milk Allergy - Symptoms & Causes - Mayo Clinic, 2022). This allergic response is mostly found in dairy milk as their casein (made of α s1- and α s2) and whey proteins trigger the immune system malfunction (Caffarelli et al., 2010). Milk allergy is common in Australia, especially during childhood, affecting more than 2% of children aged 6-12 months (Allergies and Anaphylaxis Australia, 2024). As this allergic response carries on into adulthood, Australians have a variety of plant-based milk such as almond, soy and oat in replacement of animal milk, with almond milk being the most popular alternative. Meanwhile, there is less variation of milk types in Japan with low production of almond and oat milk. This may be due to their relatively lower prevalence to milk allergy with only 0.23% showing allergic reactions at 6 months and 1.03% at 12 months (Tezuka et al., 2020).

This investigation aims to explore the reason behind the differing prevalence to milk allergy, comparing the quantity of protein and the protein types within the different milk in Japan and Australia. The proteins found in each type of milk tested are provided in the table below.

Table 1: types of milk investigated and their respective proteins

	Milk Type					
	Cow	Soybean	Oat	Almond	Goat	A2 milk
Types of Protein	A1 Casein	B-conglycinin, Glycinin, Soy protein (globulins, albumins)	Globulin, Prolamins (avenins), Albumin, Glutelin	(low protein)	A2 Casein, Whey	Beta-CaseinWhey

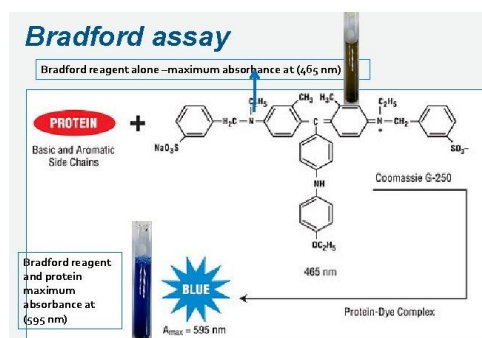
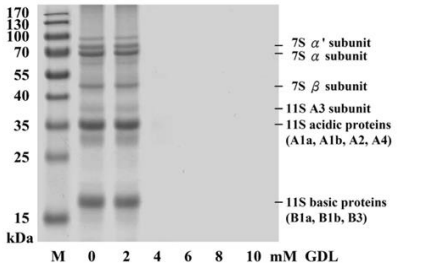
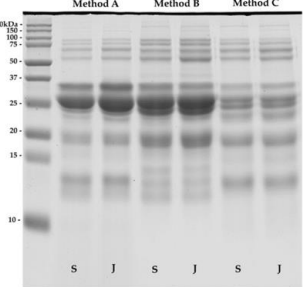
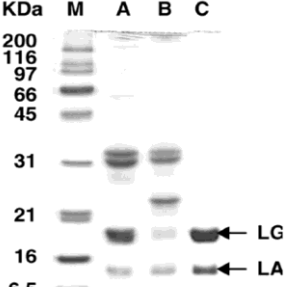


Figure 1: process of how Bradford Assay works in identifying protein

The Bradford protein assay is used to determine protein concentration in the sample. This assay uses Coomassie Brilliant Blue dye, which binds to proteins, resulting in a colour change from brown to blue, as shown in Figure 1. The intensity of the blue colour correlates with the protein concentration and can be measured spectrophotometrically at 595 nm (Bio-rad, 2024). Protein concentration of the sample (milk) is determined by comparing the absorbance to a known standard (typically bovine serum albumin). Protein electrophoresis is also used to separate proteins based on their size and charge (Khan Academy, 2023). This method involves applying an electric field to a protein sample, causing the proteins to migrate through a gel.

Below is the pre-existing electrophoresis of different milk types in Australia. This will be used to identify various types of protein in the experiment result.

Table 2:: analysis of SDS-Pages gel electrophoresis of common milk type and its proteins

<p>a</p>  <p>Figure 2: Electrophoresis of soy milk</p>	 <p>Figure 3: Electrophoresis of goat's milk</p>	 <p>Figure 4: Electrophoresis on whey (cow)</p>
<p>Consist of a globulin family of proteins called legumin (11S globulin fraction) and vicilin (7S globulin) (Patel, Cudney and McPherson, 1994)</p> <p>11S globulin are found within 28-52 kDa</p> <p>7S globulins are around 156 kDa (Abdel-Shafi et al., 2019)</p>	<p>The most abundant casein is αs2-casein. (Runthala et al., 2023)</p> <p>Molecular weight: 25.2–25.4 kDa (ROMJ, 2024).</p> <p>Also contains whey proteins α-lactalbumin, which is around 15kDa (ROMJ, 2024).</p>	<p>Whey proteins contain β-lactoglobulin (LG) and α-lactalbumin (LA) (Ulluwishewa et al., 2022)</p> <p>α-Lactalbumin (α-La) is the second major protein of whey with molecular weight of 14 kDa (Sánchez, Pérez and Parrón, 2020)</p>

2. Methodology

Part 1: Preparation of the standard curve

The Bradford Assay was used to determine protein concentration in the different milks.

1. The egg-albumin sample was diluted to 0.02/100mL (there was a mistake and the sample was diluted to 0.2g/100mL, making the final concentration in g/10L).
2. The egg albumin stock solution was prepared using the ratios stated in the table below:

Table 3:Measurements for BSA stock solution

Concentration g/10L	Water (mL)	Cuvette	Amount of diluted egg albumin 0.02g/100mL
0	10	1	0
0.01	9.5	2	0.5
0.02	9	3	1
0.04	8	4	2
0.06	7	5	3
0.08	6	6	4
0.1	5	7	5
0.12	4	8	6
0.14	3	9	7

3. 5 mL of the diluted solution was pipetted into a new test tube for each concentration.
4. 1 mL of Bradford Reagent was pipetted into each 5 mL of stock solution.
5. After 10 minutes, the stock solution with Bradford reagent was pipetted into a cuvette.
6. After wiping the cuvette clean, the absorbance of each concentration was measured using a spectrometer.
7. The absorbance was calculated and placed as a graph as shown in figure 5 and 6

Part 2: Determination of milk protein content

1. All milk samples were diluted to 1: 99ml, milk and water respectively
2. 5 ml of each diluted solution was placed into a tube
3. 1ml of Bradford reagent was added into the 5 ml of diluted solution
4. After 10 minutes, the solution was pipetted into a cuvette and its absorbance was measured
5. Steps 3-5 were repeated for each milk type
6. The actual protein content was calculated

Part 3: Gel electrophoresis

1. 50 uL of 1:249 ml diluted milk samples were added to tubes
2. 50 uL of treatment buffer was added to each tube
3. Two sets of the six milk types were made and were placed in a boiling water bath
4. After heating for 5 minutes, each sample was pipetted into the gel to conduct the electrophoresis
5. Electrophoresis was conducted.

3. Results

1. Standard curve:

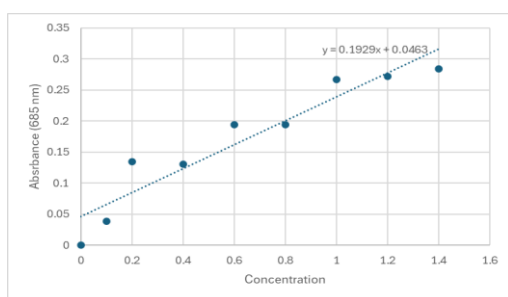


Figure 5: Standard curve from QASMT measured at 685 nm

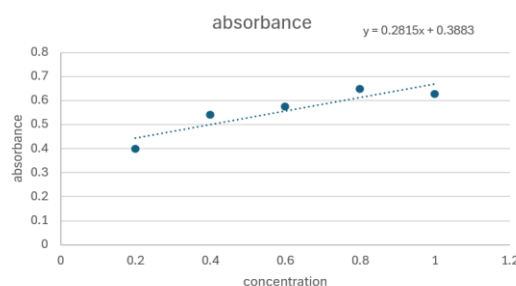


Figure 6: Standard curve from Tokai

A standard curve was prepared using egg albumin as described in methodology part 1. The absorbance of 685 nm (A₆₈₅) for each solution was plotted against the known protein concentration. Linear regression was used to determine the line of best fit for the data to show the relationship between protein concentration and the A₆₈₅ value of the solution.

The increasing absorbance was also evident in the darkening colour of the cuvettes after adding the Bradford Reagent:

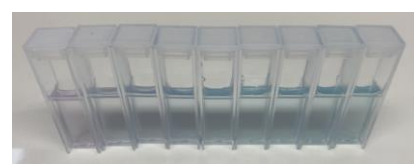


Figure 7: cuvette of different concentrations going low to high from left to right

2. Determination of milk protein:

The Bradford Assay was used to determine the protein concentration of the milk samples. The milk was diluted 100 times so that the absorbance value fell within the range of the standard curve.

Table 4: protein calculation from QASMT

Milk type	Soy	Full	Almond	A2	Oat	Goat
Actual protein (g/100ml)	3.3	3.3	0.6	3.2	0.8	3.5
Calculated protein (g/100ml)	3.054692	5.231985	0.721877	5.491187	1.045879	4.052618

Table 5: Protein calculation from Tokai

Milk type	Cow	Soy	Almond	Oat
Actual protein (g/100ml)	3.4	4.15	0.55	0.5
Calculated protein (g/100ml)	1.52	1.5	0.84	0.04

Gel electrophoresis

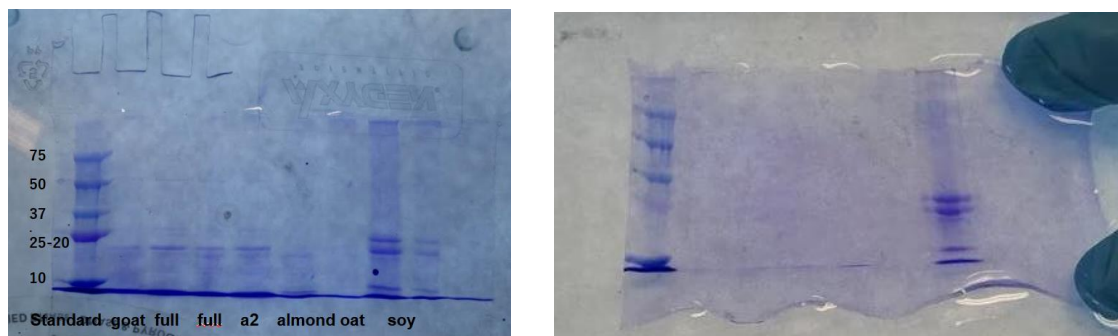


Figure 8: Gel electrophoresis results from QASMT

4. Discussion

As evident in figure 8, the standard curve of QASMT and Tokai are different. This may be due to a miscommunication of the methodological process. Another reason may have been due to the different number of trials that each school conducted.

As seen in figure 4, protein detection for almond and oat milk remains mostly clear, indicating lack of protein content. This supports the reason for the common use of almond and oat milk as an alternative to others that often cause allergic reactions. Meanwhile, goat, full, and A2 milk show some levels of protein. In figure 4, there is a clear detection at approximately 20 kDa, indicating the presence of whey proteins containing β -lactoglobulin (LG). This protein is prone to causing allergic reactions based on inflammation.

The results show soybean milks to contain the most protein around 20 and 35 kDa, like the detection of 11S acidic proteins in figure 4. These proteins are also one of the main contributors to allergic reactions, suggesting why soybean milks are not commonly used amongst those prone to allergic reactions.

However, these results show a significant difference to the literature results as proteins over 20 kDa are not identified. This may be due to over-diluting the solution or it could be a cause of a malfunctioning electrophoresis.

5. Conclusion

The purpose of this experiment was to investigate the protein contents in various common types of milk in Australia and Japan in response to their allergenic potentials. The results of the Bradford assay agree with the researched protein profiles, which are vital for understanding dietary requirements for individuals with milk allergies, especially children who require adequate protein intake for growth and development. Further, the results highlight the need for careful selection of alternatives in case of allergies, considering not only the allergenic properties but also the nutritional adequacy of protein to maintain a healthy diet. This experiment emphasises the need for further studies regarding establishing healthy milk alternatives.

7. References

- Abdel-Shafi, S., Al-Mohammadi, A.-R., Osman, A., Enan, G., Abdel-Hameid, S. and Sitohy, M. (2019). Characterization and Antibacterial Activity of 7S and 11S Globulins Isolated from Cowpea Seed Protein. *Molecules*, 24(6), p.1082. doi:<https://doi.org/10.3390/molecules24061082>.
- Allergies and Anaphylaxis Australia (2024). Milk/Dairy - Allergy & Anaphylaxis Australia. [online] Allergy & Anaphylaxis Australia - Your trusted charity for allergy support. Available at: <https://allergyfacts.org.au/allergy/milk-dairy/> [Accessed 9 Jan. 2025].
- Bio-rad (2024). Bradford Protein Assay. [online] Bio-Rad Laboratories. Available at: <https://www.bio-rad.com/en-au/feature/bradford-protein-assay.html> [Accessed 3 Jan. 2025].
- Caffarelli, C., Baldi, F., Bendandi, B., Calzone, L., Marani, M. and Pasquinelli, P. (2010). Cow's milk protein allergy in children: a practical guide. *Italian Journal of Pediatrics*, [online] 36(5), p.5. doi:<https://doi.org/10.1186/1824-7288-36-5>.
- Khan Academy (2023). Khan Academy. [online] Khanacademy.org. Available at: <https://www.khanacademy.org/test-prep/mcat/biomolecules/x04f6bc56:protein-analysis-techniques/a/protein-electrophoresis-and-sds-page>.
- Patel, S., Cudney, R. and McPherson, A. (1994). Crystallographic characterization and molecular symmetry of edestin, a legumin from hemp. *Journal of Molecular Biology*, 235(1), pp.361–363. doi:[https://doi.org/10.1016/s0022-2836\(05\)80040-3](https://doi.org/10.1016/s0022-2836(05)80040-3).
- ROMJ (2024). Structure and biological functions of milk caseins | Russian Open Medical Journal. [online] Romj.org. Available at: <https://www.romj.org/2022-0209>.
- Runthala, A., Mbye, M., Ayyash, M., Xu, Y. and Kamal-Eldin, A. (2023). Caseins: Versatility of Their Micellar Organization in Relation to the Functional and Nutritional Properties of Milk. *Molecules*, 28(5), p.2023. doi:<https://doi.org/10.3390/molecules28052023>.
- Sánchez, L., Pérez, M.D. and Parrón, J.A. (2020). Chapter 11 - HPP in dairy products: Impact on quality and applications. [online] ScienceDirect. Available at: <https://www.sciencedirect.com/science/article/abs/pii/B978012816405100011X>.
- Ulluwishewa, D., Mullaney, J., Adam, K., Claycomb, R. and Anderson, R.C. (2022). A bioactive bovine whey protein extract improves intestinal barrier function in vitro. *JDS Communications*, 3(6), pp.387–392. doi:<https://doi.org/10.3168/jdsc.2022-0245>.
- Williams, J. (2018). Protein's Important Role in Child Growth and Development. [online] Nutritionnews.abbott. Available at: <https://www.nutritionnews.abbott/pregnancy-childhood/kids-growth/why-is-protein-important-for-kids-growth/>.

Mathematics of Sudoku puzzle

Kim Keo Sokunpidor¹, Chhin Seangeng¹, Tang Hangbu¹, Akari Nakamura², Chihiro Kamiie²

¹New Generation School Preah Sisowath High School (Cambodia)

²Hatsushiba Ritsumeikan Junior & Senior High School (Japan)

Abstract:

The 3D Sudoku puzzle expands the traditional game into a 4x4x4 cube, adding a new layer of complexity. Each layer operates as a 4x4 grid where every row, column, and 2x2 sub-grid must contain the symbols 1, 2, 3, 4, A, B, C, and D exactly once. Additionally, vertical stacks spanning all layers must maintain unique symbols, introducing a challenging three-dimensional aspect. To solve these puzzles, foundational strategies like unique missing candidate, naked single, and hidden single are highly effective. The unique missing candidate identifies cells where only one symbol can fit due to exclusions. The naked single highlights cells with only one possible option after accounting for all constraints, while the hidden single pinpoints symbols that appear as valid candidates in only one cell of a specific row, column, sub-grid, or stack. These methods simplify the puzzle-solving process, offering a structured approach to navigating the added complexity and testing spatial reasoning and problem-solving skills.

Keywords: 3D Sudoku, 4x4x4 cube, Spatial reasoning, Problem-solving, Unique missing candidate, Naked single, Hidden single, Three-dimensional puzzle, Vertical stacks, Multi-dimensional logic

1. Introduction

The 3D Sudoku puzzle follows standard Sudoku rules with an added dimension of complexity. The puzzle consists of a 4x4x4 cube, where each layer (front, middle, back) represents a 4x4 Sudoku grid. Within each layer, the regular Sudoku rules apply: every row, column, and 2x2 sub-grid must contain all the given symbols or numbers exactly once. Additionally, vertical consistency across the layers must be maintained. This means that within a vertical stack of cells spanning from the front to the back layer, the digits or letters must also be unique, adhering to the same rules applied within the planes. In this 3D version of Sudoku, the symbols used are a combination of numbers and letters: the numbers 1, 2, 3, 4, and the letters A, B, C, D. These symbols must be placed strategically to satisfy the rules across all dimensions of the cube, adding a unique twist to the classic puzzle format.

2. Methodology

We will start with a few strategies that are relatively straightforward, though identifying them in a puzzle can sometimes be challenging due to the many factors to consider. Most puzzles come with a difficulty rating, and the techniques in this section are sufficient to solve almost all easy puzzles and many intermediate ones. We'll begin with the simplest observations and gradually move on to slightly more complex ones. The methods are organized roughly by their increasing difficulty for a human to apply, whereas computers often use entirely different and simpler approaches.

Step 1: Unique Missing Candidate:

- Check each row, column, and **2x4** or **1x8** block in every layer.
- If a row, column, or block already contains all but one number/letter (**A, B, C, D** or **1, 2, 3, 4**), fill in the missing value.

For example:

- In a row that already has the values **1, 2, 3, 4, A, C, D** the missing value must be **B**, because it's the only one not yet placed.
- This same rule applies to columns, layers, and 3D blocks.

This strategy is most effective when many cells are already filled, as it's easy to spot what's missing.

Step 2: Naked Singles:

- **Naked Singles** is a key strategy used to solve Sudoku puzzles when a cell has only one possible value based on the constraints of the rows, columns, and grids. This technique simplifies the puzzle by identifying cells that can have no other option, making it an essential method for

progressing.

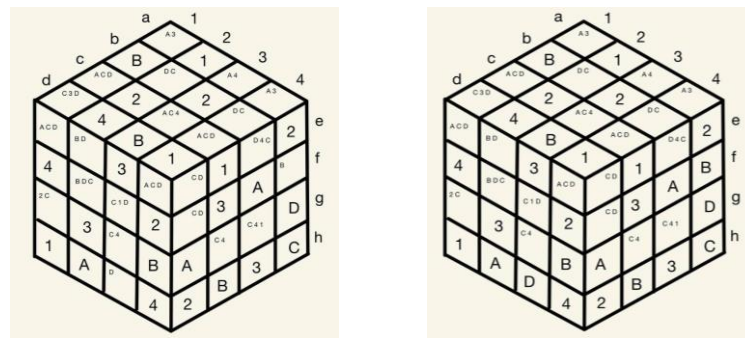


Figure1: Candidate Elimination and Naked Singles

- For example, in the 3D Sudoku puzzle, consider **row h, column 3**. Looking at the constraints of **row h** (what is already placed in that row), **column 3** (what is already placed in that column), and the grid it belongs to, the only possible value for this cell is **D**. No other number or letter fits due to the constraints. Similarly, in **row a, column f**, the constraints from the row, column, and grid indicate that the only possible value is **B**. This is because all other numbers or letters that could be placed in this cell are already present in the relevant row, column, or grid.
- By identifying these “naked singles,” we can confidently fill in those cells and eliminate the corresponding values from consideration in the other cells in the same row, column, and grid. This method helps to gradually reduce the puzzle’s complexity and is especially useful in the early stages when many cells have only one viable candidate. By continuing to apply this strategy across all rows, columns, and grids, the puzzle gradually becomes easier to solve.

Step 3: Hidden Singles:

- A **hidden single** refers to a number that must occupy a specific square, even though this might not be immediately obvious because other possibilities seem valid at first glance. Without carefully examining all restrictions, the square may appear to have multiple potential candidates (e.g., **1, 2, 5, 8, or 9**). However, by analyzing all options and constraints, it becomes clear that only one number can fit, making it “hidden.”
- For example, let’s analyze **row 1** to determine where the number “**2**” must be placed. In **row g, column 1**, there is a possibility for both “**2**” and “**C**” to fit in this block. However, when considering the constraints imposed by other rows, columns, and blocks, the square at **g1** emerges as the only valid position for the number “**2**” in this block. As a result, “**2**” is a hidden single for square **g1**, as no other square in **row 1** can accommodate it.
- For example, let’s analyze **row 2** to determine where the letter “**B**” must be placed. In block **e2**, there is a possibility for both “**B**” and “**D**” to fit in this block. However, when considering the constraints imposed by other rows, columns, and blocks, the square at **e2** emerges as the only valid position for the letter “**B**” in this block. As a result, “**B**” is a hidden single for square **e2**, as no other square in **row 2** can accommodate it.

Applying Strategies to the 3D Cube:

Each method involves using different perspectives to ensure all numbers (1-4) and letters (A-D) are placed correctly while avoiding repetition in their respective regions:

1. Horizontal Rows (a-d)

- Look at rows **a, b, c, d**. Each row must contain all numbers (**1-4**) and letters (**A-D**) without repetition.
- Example: In **row a**, we already have **1, 2, D, C**, so the missing values are **A, 3, 4, B**. Repeat this process for rows **b, c** and **d**

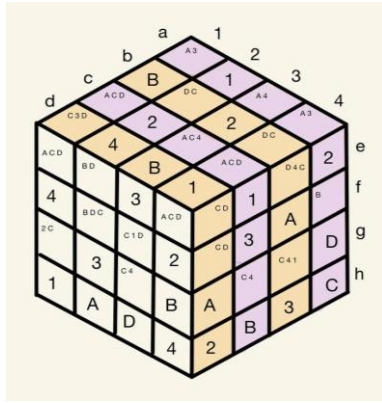


Figure2: Horizontal Rows (a-d)

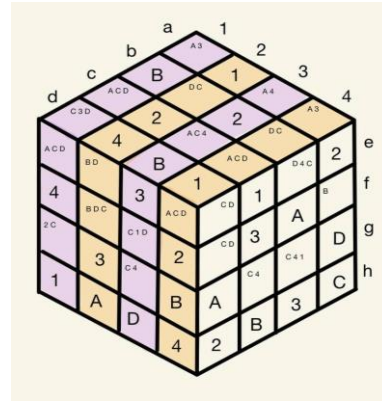


Figure3: Vertical Columns (1-4)

2. Vertical Columns (1-4)

- Look at columns **1 through 8**. Each column must also have all numbers (**1-4**) and letters (**A-D**) without repetition.

- Example:

In column **1**, we already have **B, 4, 1**, so the missing values are **A, 3, C, D, 2**. Repeat this process for columns **2 to 8**.

3. Horizontal Rows (e-h)

- Now examine rows **e, f, g, h**, which also follow the same rule: each must contain all numbers (**1-4**) and letters (**A-D**).

- Example:

In row **e**, we already have **2, 1, 3**, so the missing values are **A, D, C, 4, B**.

Repeat this for rows **f, g, and h**.

4. 2x4 Blocks

- Finally, look at **2x4 blocks** (two rows and four columns, such as rows **a & b** across columns **1-4**). Each block must also contain all numbers (**1-4**) and letters (**A-D**).

- Example:

In the block formed by rows **a & b**, columns **1-4**, the values already present are **1, 2, B**, so the missing values are **A, 3, C, D, 4**.

Repeat this for other 2x4 blocks (e.g., rows c & d, columns 1-4, etc.).

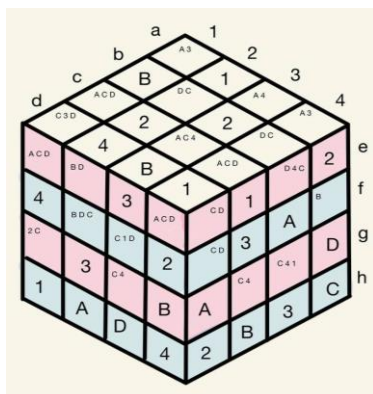


Figure4: Horizontal Rows (e-h)

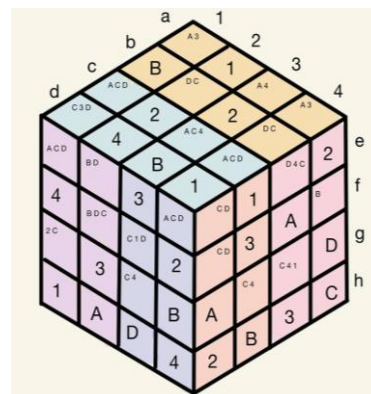


Figure5: 2 x 5 blocks

These methods ensure that all constraints are satisfied across rows, columns, and blocks. Each approach focuses on a different perspective of the puzzle to systematically deduce the missing values.

3. Results

The solved 3D Sudoku cube adheres to all constraints, demonstrating the effectiveness of the methodology. The backtracking algorithm was implemented, requiring a total of 15 iterations to complete the puzzle. Through our journey of researching, we have discovered 3 fundamental steps in common and 4 specific strategies to enhance the skill in solving sudoku puzzles way faster and smarter.

4. Discussion

In this discussion, we examined different techniques for solving Sudoku puzzles, such as naked singles, hidden singles, and unique missing candidates. These strategies proved useful in simplifying the solving process, particularly in the case of 3D Sudoku, where the puzzle's complexity increases with an added dimension. A key challenge identified was the difficulty of determining valid placements due to the expanded constraints across rows, columns, sub-grids, and vertical stacks. This variation of Sudoku required a more thoughtful approach compared to standard puzzles. The methods applied relate to broader mathematical ideas like set theory, demonstrating how the puzzle helps develop spatial reasoning and logical thinking. When compared to traditional Sudoku, the 3D version introduced additional layers of complexity, demanding a more advanced understanding of multi-dimensional logic. Furthermore, Sudoku puzzles have practical benefits, such as improving cognitive abilities and contributing to fields like artificial intelligence, where similar problem-solving techniques are applied. However, the limitations of the current methods and the challenges of solving larger or more complex Sudoku puzzles suggest a need for further investigation into more advanced solving techniques or alternative puzzle designs.

5. Conclusion

In conclusion, the aim of this research is to explore solving Sudoku puzzles in unique shapes and dimensions. As demonstrated, there are various methods to solve Sudoku puzzles that's different from the traditional format we are familiar with. The strategies outlined above provide valuable guidance to effectively approach and solve these challenging puzzles.

7. References

- Tom Davis. (September 13, 2012). The Mathematics of Sudoku <http://www.geometer.org/mathcircles>
- Kyle Oddson, Under the direction of Dr. John Caughman (Winter2016) Math and Sudoku. <https://web.pdx.edu/~caughman/Oddson-Math%20and%20Sudoku.pdf>
- All site contents ©Any Puzzle Media Ltd and ©Dr Gareth Moore 2005-2024 <https://www.anypuzzle.com/3D%20Sudoku>
- My Joomla CMS (2015, February 09). Rules of Sudoku 3D. <https://innoludic.com/sudoku-rule/2015-02-08-20-11-14/3d-simple/13-rule-of-sudoku-3d.html>
- Atlanta, Georgia (2012, March 08). G4G10 Exchange Book. Math, Puzzle, & Science. <https://www.gathering4gardeners.org/g4g10gift/G4G10-Book-Volume2-ForWeb.pdf>
- Hideki Tsuike & Yohei Yokota (2011, September 01). Enumerating 3D-Sudoku Solutions over Cubic Pre Fractal Objects https://www.jstage.jst.go.jp/article/ipsjjip/20/3/20_667/_pdf

Water Quality Tests Using Bivalve

Keahak Heang¹, Bidaliya Ngor¹, Setthireach Sun¹, Azusa Ogata², Kaede Obata², Naoko Hashimoto²

¹New Generation School Preah Sisowath High School (Cambodia)

²Seishin Girls' High School (Japan)

Abstract:

Sinanodonta lauta, *Pronodularia japonensis*, and *Unio douglasiae* are all species of freshwater mussels with distinctive shell shapes in the family of *Unionidae*, which are distributed in East Asia. In the following experiment, the feasibility of three species of bivalves would be investigated as bioindicators of water contamination. To address this, soap would serve as a non-lethal model contaminant; the clams will be stored in a 30L tank for storage, while the test will take place in a 1L tank. The data is collected and analyzed using Excel. We calculate the average time for all the bivalves, and we used ANOVA to calculate the p-score. The shell closure as a behavioral response to contamination was measured, and the average response time in all species was 20.99 seconds. The reaction to this stimulus was slowest in *Sinanodonta lauta*; the response time recorded was 32.02 seconds, and *Pronodularia japonensis* and *Unio douglasiae* reacted in 12.34 and 18.65 seconds, correspondingly. During the control tests, no shell closure was observed in bivalves within 30 min. The observed results define bivalves as sensitive to contaminants and could serve in low-cost, sustainable environmental monitoring.

Keywords: Bivalves, Anova, Shell closure, Bioindicator, Environmental monitoring

1. Introduction

Water is essential to life, yet many regions continue to face water scarcity and suffer the harmful effects of unsafe water on human health. In fact, 2.2 billion people in the world lack access to safe water (Arney, 2024). Despite this, many people remain unaware of the quality of the water they use daily. This study explores an innovative method, inspired by practice in Poland, that uses bivalves, such as clam, as biological indicators to control the quality of water (Harris, 2020).

Bivalves, particularly clams, exhibit a notable behavioral response to environmental conditions. In clean environments, clams typically keep their shells widely open for filter-feeding. Conversely, in contaminated environments, particularly those with chemical pollutants, they tend to close their shells as a protective mechanism. This readily observable behavior makes them valuable bioindicators of water quality. By observing bivalve reactions to varying water conditions, this study aims to develop sustainable strategies for utilizing them in coastal water quality management, promoting a cost-effective alternative to expensive sensor-based monitoring.

2. Methodology

To achieve this, Specimens of three bivalve species—*Sinanodonta lauta*, *Pronodularia japonensis*, and *Unio douglasiae*—were collected from rivers and ponds in Okayama, Japan. These species were selected due to their phylogenetic relatedness to clam species that are used in Poland to manage the quality of water. Initially, all three clams were placed in a 33-liter holding tank and allowed to acclimate to the new environment. Following this acclimation period, individual bivalves were transferred to a 1-liter experimental tank and allowed a 10-minute acclimation period within this smaller tank. Soap was chosen as a model contaminant for this experiment since it does not harm bivalves. After adding the chemical in, the time required for complete shell closure was recorded using a timer. This procedure was replicated nine times for each individual bivalve to ensure data reliability and account for individual variation. As for the control test, clams were placed in the experimental tanks for 30 minutes, during which time no shell closure was observed. The resulting data were then compiled and analyzed using a one-way ANOVA (Single Factor) test in Microsoft Excel to determine statistical significance (p-value).

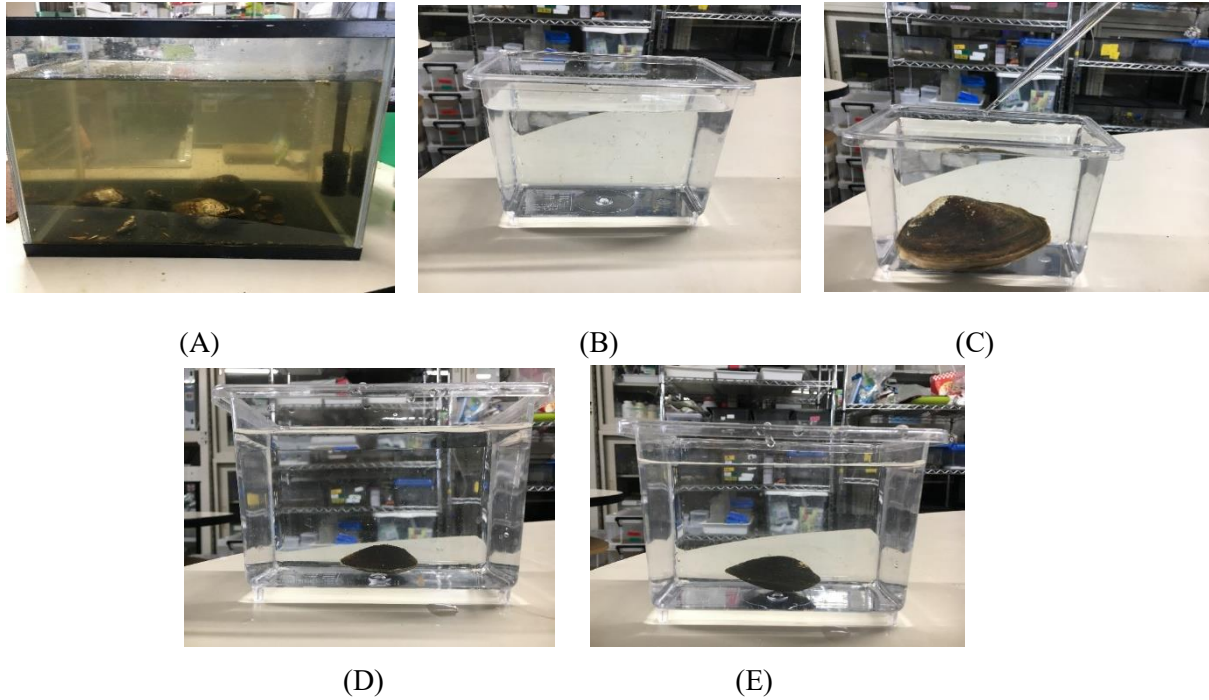


Figure 1. (A) The breeding tank (B) The experiment tank (C) *Sinanodonta lauta* (D) *Pronodularia japonensis* (E) *Unio douglasiae*

3. Results

The study revealed that among the three shell species examined, *Sinanodonta lauta* exhibited the longest average shell-closing time, taking 32.02 seconds, while *Pronodularia japonensis* demonstrated the shortest average closing time at 12.34 seconds. Notably, none of the shell species exhibited shell-closing behavior when placed in their natural environment for a period of 30 minutes. This observation suggests a potential relationship between the length of the gap and the environmental conditions. After collecting the data and performing a p-test by using Excel, we determined that the p-value was less than 0.05, indicating a statistically significant relationship between the two variables.

<i>Sinanodonta lauta</i> (Dish Soap)	<i>Pronodularia japonensis</i> (Dish Soap)	<i>Unio douglasiae</i> (Dish Soap)	<i>Sinanodonta lauta</i> (Control)	<i>Pronodularia japonensis</i> (Control)	<i>Unio douglasiae</i> (Control)
7.1	4.74	17.12	1800	1800	1800
16	25.18	16.4	1800	1800	1800
5.62	11.39	4.34	1800	1800	1800
8.68	6.82	7.38	1800	1800	1800
91.43	17.32	80.08	1800	1800	1800
42.29	13.26	7.61	1800	1800	1800
52.04	12.85	9.99	1800	1800	1800
38.93	7.99	12.01	1800	1800	1800
26.12	11.53	12.96	1800	1800	1800

Table 1. The duration required for shells to close their gap

SUMMARY STATISTICS						
Groups	Count	Sum	Average	Variance		
<i>Sinanodonta lauta</i> (Dish soap)	9	288.21	32.02333333	779.717725		
<i>Pronodularia japonensis</i> (Dish soap)	9	111.08	12.34222222	37.43549444		
<i>Unio douglasiae</i> (Dish soap)	9	167.89	18.65444444	548.2725028		
<i>Sinanodonta lauta</i> (Control)	9	16200	1800	0		
<i>Pronodularia japonensis</i> (Control)	9	16200	1800	0		
<i>Unio douglasiae</i> (Control)	9	16200	1800	0		
ANOVA RESULTS						
Source of Variation	SS	df	MS	F	P-value	F crit
Between Groups	42726851.03	5	8545370.207	37550.35547	5.76303E-85	2.4085141
Within Groups	10923.40578	48	227.5709537			
Total	42737774.44	53				

Figure 2. Analysis of Variance (ANOVA) - Single Factor

4. Discussion

The results indicate that bivalves are good bioindicators of water pollution. One can determine the sensitivity to pollutants from how the bivalves behave towards soap. Among these, *Pronodularia japonensis* was the fastest, followed by *Unio douglasiae* and *Sinanodonta lauta*. This behavior saves them from ingesting or exposing their soft tissues to toxic chemicals or pollutants.

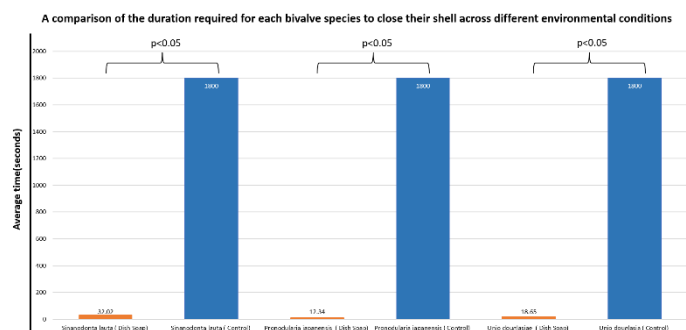


Figure 3. The p-score between the experiment and control test

Figure 3 shows no abnormalities from the experimental runs were observed. Without soap, there was no shell closure from control tests. The reason for different response times might be because of the size and age of any contaminant that might have infected the clams before the experiment or sensitivity developed through natural selection.

The response of bivalves to environmental change can be seen today in society. Response times are fine-tuned for monitoring, a species-specific phenomenon. According to Scott (2022), bivalves are already being used in Poland for monitoring water quality, and according to Check out these mussels: Today Minneapolis: Fishing for Clean Water: Using Mollusks to Monitor Water Quality (2019); "Minneapolis Water Treatment and Distribution Services, 12 mussels are the muscle behind clean and safe water."

The results indicate that aquatic organisms' biological sensitivity can act as an early warning system. Variations in response time can be used to detect a variety of chemicals. Bivalves are a cheap, low-maintenance method of water quality monitoring and can alert to a variety of chemicals.

It illustrated that bivalves are sensitive to contaminants and could be acceptable as bioindicators.

Pronodularia japonensis allows for real-time monitoring with a very short response time. Besides, the use of bivalves can increase awareness of water pollution and its endangerment. The result helps monitor ecologically and helps conserve the bivalve population for biodiversity and ecosystem health.

5. Conclusion

In conclusion, this research aimed to show the effectiveness of using bivalves as biological indicators to test water quality. According to the data shown above, provided with a statistical analysis calculation performed by p-test, the study revealed that the *Sinanodonta Lauta* shell exhibited the longest average closing time. At the same time, the *Pronodularia Japonensis* exhibited the shortest time for their gaps to close. It can be concluded that chemical substances and environmental conditions played a significant role in defining the duration for the bivalve shells to close their gaps. The p-test analysis showed the p-value was less than 0.05 which means the two variables are statistically significant. By using the p-test calculation tables, it is confirmed that the experiment was accurate according to the existing theory. Overall, this study conveys the effectiveness of using bivalves as a helpful tool to utilize the water system. Their responses provide valuable insights into the chemical, enabling more efficient management and utilization of water resources in a specific region or country.

6. Acknowledgements

We would like to express our deepest gratitude towards Mr. Pin Kakada, who is a PhD student majoring in biology at the Royal University of Phnom Penh, for guiding, lecturing, and giving constructive feedback to us throughout this research process; In addition, this would not have been possible without his collaboration and dedication with us.

7. References

- Heather Arney. (2024, February 22). How many people are affected by the global water crisis. *water.org*. <https://water.org/about-us/news-press/how-many-people-are-affected-by-the-global-water-crisis-2024/>
- Cecilia Harris. (2020, December 10). This Polish city is using mussels to monitor water quality. *AUSTRALIAN WATER ASSOCIATION*. <https://www.awa.asn.au/resources/latest-news/technology/innovation/polish-city-using-mussels-monitor-water-quality#:~:text=The%20D%C4%99biec%20Water%20Treatment%20Plant,when%20water%20quality%20is%20poor.>
- Check Out These Mussels: Minneapolis Using Mollusks To Monitor Water Quality. (2019, May 14). <https://www.cbsnews.com/minnesota/news/mussels-helping-monitor-water-quality-in-minneapolis/>
- Scott, T. (2022, October 31). Is Poland's tap water really protected by clams? <https://www.youtube.com/watch?v=i0RkEs3Xwf0>
- Nazology (2020, May 29). Poland's "water-testing clams" provides water for 8 million people <https://nazology.kusuguru.co.jp/archives/61166>
- Aichi prefecture (2024, September 30) What is domestic wastewater (pollution of rivers and seas in Aichi Prefecture)? <https://www.pref.aichi.jp/soshiki/mizutaiki/0000049169.html>

Comparison of Physical Properties of Roofing Materials in Cambodia and Japan

Chhean Chao¹, Zana Ro¹, Sidianna Thay¹

Mitsuki Chujo², Mizuki Ibata², Rioko Ito², Mio Yamamoto²

¹New Generation School, Preah Yukunthor High School (Cambodia)

²Ikuei-nishi High school (Japan)

Abstract:

The physical properties of Cambodian and Japanese clay roof tiles were compared. Size and density are larger in Japanese, freezing resistance was greater in Japanese, and thermal shielding properties were stronger in Cambodian. This result was consistent with our expectations and could be considered to reflect differences between the climate of two countries.

Keywords: Durability of roof tiles; Freezing resistance; Thermal shielding; Water absorption

1.Introduction

The climates of Japan and Cambodia are very different, with Japan experiencing temperate conditions characterized by four distinct seasons and significant annual temperature variations, while Cambodia's tropical climate near the equator exhibits less temperature fluctuation. Focusing on clay tiles, a common roofing material in both countries, we hypothesized that the physical properties of these tiles reflect their respective climates. In Cambodia, where temperatures are high and sunlight is intense, clay roof tiles are likely designed to reflect infrared rays effectively, have a low radiant heat absorption rate, high specific heat capacity, and low thermal conductivity to mitigate the effects of extreme heat. Conversely, in Japan, where winters can be harsh, roof tiles likely exhibit high freeze resistance due to low water absorption, achieved through high-density manufacturing, which prevents water from freezing and expanding within the tiles, thus reducing the risk of cracking. This hypothesis would be tested through freezing experiments, heat shielding experiments, and measurements of tile density and specific heat, as shown in Table 1.

Table.1 Hypothesis comparing tiles in different countries relative to each other

	Freezing resistance	Heat shielding	Density	Specific heat
C (for tile of Cambodia)	×	○	×	○
J (for tile of Japan)	○	×	○	×

(○ is strong or larger, × is weak or smaller)



Fig.1 Clay roof tiles
Left: Cambodian, Right: Japanese

2. Methodology

The experiments were conducted in the following method.

1.Measurement of size and density

Size was measured with a tape measure in length, width, and thickness. Volume was obtained by converting from buoyancy. Weight was measured with a digital scale.

2.Measurement of water absorption

For water absorbency, the tiles measured in 1, were soaked in water for 20 hours and then weighed on a digital scale. Water absorption was determined by comparing the weight after soaking with the weight before soaking.

3.Investigation of freezing resistance

1. A container with sufficient water to submerge the tiles was prepared, and two tiles were soaked for 16 hours.
- 2.The soaked tiles were wrapped in plastic bags and frozen at -18°C for 8 hours.
- 3.Steps 2 and 3 were repeated 10 times, with a 64-hour soaking period during the fourth cycle.
- 4.After freezing and soaking, the tiles were observed for damage.
- 5.A 200-g sand-filled "bullet" was created using a PET bottle with a cap nut and sand.
- 6.A device (Fig. 2) was constructed to drop the bullet onto the same spot on a tile.
- 7.Tiles frozen and soaked 10 times were placed face-up on 5 piece of newspapers over concrete. A bullet was dropped from 1 meter to observe the number of drops and the crack patterns.
- 8.Results were compared with tiles that had not undergone freezing.



Fig.2 dropping device

4. Measurement of Thermal Conductivity

- 1.A house model was constructed using 30 mm thick Styrofoam boards for the floor and walls (200 mm each for length, width, and height) with a single roof tile as the roof (Fig. 3).
- 2.The model was placed in a drying constant-temperature apparatus set at 50°C .
- 3.A temperature logger inside the model measured the time and temperature change from 26°C to near 50°C .
- 4.The time required for the temperature difference between the inside and outside of the model to reach less than 1°C was recorded.



Fig.3 the house model

5. Measurement of Radiant Heat Absorption

1. A 100W incandescent lamp, positioned 15 cm above the tile, was used as a sunlight substitute (Fig. 4).
2. A thermocouple sensor measured the temperature change on the back of the tile every 5 minutes for 50 minutes.



Fig.4 measuring of radiant heat absorption

3. Results

1. Size and density

The results are shown in the following table (Table.2).

Table.2 Size and density

	Length(cm)	Width(cm)	Thickness(cm)	Weight(g)	Volume(cm^3)	Density(g/cm^3)
C	27	16	1	870	432	1.88
J	27	25	2	2,787	1,482	2.01

2. Water absorption

The results are shown in the following Table.3.

Table.3 Compare of water absorption

	Weight before soaking(g)	Weight after soaking(g)	Water absorption (%)
C	870	900	8.5
J	2,751	3,103	12.8

3. Freezing resistance

The results are shown in Table.4 below.

Table.4 Freezing resistance

	Number of dropping until a tile crack	
	Unfrozen tiles (Ave of 2)	Frozen tiles (Ave of 2)
C	07	05
J	19	14

One of Frozen Japanese tiles was partially chipped by 2cm from the center after 10 times freezing. (Fig.5)

Japanese tiles had some black spots and dents around the beginning of dropping, but finally, they were not crack completely.

Cambodian tiles cracked open by a dropping bullet.



Fig.5 After freezing 10 times, part of the surface of the tiles chipped off.

4. Thermal conductivity

The results are shown Table.5 below.

Table.5 Time until the temperature difference between the inside and outside of the house model was less than 1°C

	Time (min.)
C	120
J	105

5. Radiant heat absorption

Radiant heat absorption was measured in Japan only. Fig.6 shows the temperature rise on the back side of the Japanese tile after incandescent lamp irradiation started, compared with the air temperature.

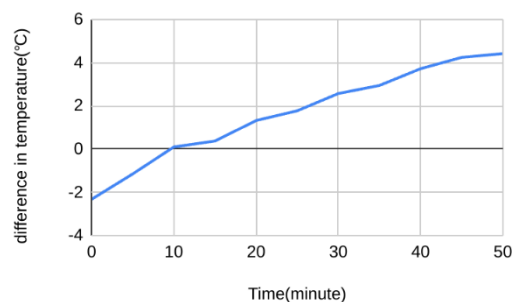


Fig.6 Temperature change due to incandescent lamp irradiation

4. Discussion

Size: Both had the same length, but the Japanese tile was about 10 cm wider. The thickness of the Japanese tile was about twice that of the Cambodian, and it was about three times heavier. The volume of the Japanese tile was about three times larger. Overall, we could conclude that Japanese tiles were larger compared to Cambodian. And Japanese had larger density compared to Cambodian.

Color: The Japanese tile was grey, while the Cambodian tile was terracotta (smoked tile vs. unglazed tile). The bright color of the Cambodian tile indicates that it was fired at a lower temperature, resulting in a relatively lower density. In contrast, the Japanese tile was fired at a higher temperature, resulting in a relatively higher density.

Water absorbency: Hypothetically, we thought Cambodian tile would be higher than Japanese, and in fact it was lower than Japanese. Water absorption in Cambodian was lower than in Japanese, probably due to the shorter water supply time. Japanese had 20 hours of water supply, while Cambodian had 6 hours. Therefore, this result is not accurate.

Freezing Resistance: The number of times a bullet had to be dropped on a frozen tile before it cracked was smaller than the number of times it had to be dropped on a non-frozen tile, in both Cambodian and

Japanese. This is thought to be due to the fact that when the roof tiles freeze, their durability decreases. Cambodian tiles broke faster than Japanese, probably because they were thinner. Cambodian tiles had a large rate of decline in the number of drops after freezing. This suggests that Cambodian tiles were more severely damaged by freezing. This indicates that Cambodian tiles were less resistant to freezing. This supports the hypothesis.

Thermal shielding: The hypothesis that Cambodian tiles have better heat shielding properties than Japanese tiles was confirmed. Even though the Cambodian tiles are only half as thick as the Japanese tiles, it took time to equalize the temperature difference between the inside and outside of the model. This suggests that thickness has little effect on thermal conductivity. Additionally, the bright orange color of Cambodian tiles is thought to have the effect of suppressing the absorption of radiant heat, but no experiments have been conducted to prove this. The excellent heat shielding properties of Cambodian tiles can be attributed to their material and microstructure. Further research is needed on how these contribute to thermal shielding.

Specific Heat: We found out that there is an experiment in which a heated metal ball or something object is placed in water and the temperature at which the water and object reach thermal equilibrium is used to determine the specific heat, but due to time constraints, we were unable to perform the measurement. So, we are thinking of doing this as an extension of the experiment in the future.

5. Conclusion

This study compared the physical properties of roof tiles from Japan and Cambodia, revealing differences that reflect the climatic conditions of each country. The results supported the hypothesis that Cambodian tiles exhibit low thermal conductivity, while Japanese tiles have higher density and greater freeze resistance. This study suggests that the selection of roof tiles plays a critical role in the choice of building materials. However, specific heat and radiant heat absorption rates were not compared in this study, and further research is needed to fully validate the hypothesis.

6. Acknowledgements

We would like to extend our heartfelt appreciation to Mr. Kenji Ota and Mr. Kenji Yamamoto of Yamamoto Tile Industry Co., Ltd., and the skilled tile production technicians for their generous provision of numerous resources and valuable insights, which greatly supported the progress of this research.

Furthermore, we are deeply grateful to Mr. Khun Kimleang, President of the Physics Department at the Royal University of Phnom Penh, for his expert guidance and unwavering support throughout this project. His contributions, particularly in providing access to critical resources and sharing his expertise, were invaluable in ensuring the success of this study.

7. References

General Incorporated Association: All Japan Federation of Tile Contractors

The Professional Group for Roof Construction

Official Website of the General Incorporated Association: All Japan Federation of Tile Contractors

January 3, 2024

<https://www.yane.or.jp/kawara/seinou07.shtml>

Takenaka Carpentry Tools Museum, "The Thousand-Year Roof: Restoring Ancient Roof Tiles," Public Interest Incorporated Foundation, October 14, 2017, January 4, 2024

Class 2-3: Kotomi Ishimaru, Nagomi Takahira, Haruka Furuishi; Class 2-4: Chika Arima, "Study on Reducing the Firing Temperature of Oyster Shell Tiles," SSH Student Research Paper, Uwajima Higashi High School, p.4, January 4, 2024

<https://uwajimahigashi-h.esnet.ed.jp/uploads/r12nen05.pdf>

Mold found in different environments

Azusa Miwa¹, Yuki Chin¹, Yuri Yoshimura¹, Heng Sopha², Lay Soryta², Thy Thea Yanuth²

¹*Matsusho Gakuen High School(Japan)*

²*NGS,Preah Yukunthor High School(Cambodia)*

Theme:

Molds are a natural part of the environment and can be found almost anywhere that moisture and oxygen are present and it belongs to the kingdom Fungi. Mold has drawn significant attention from researchers due to its wide-spread effects on both human health and the environment. Mold produces allergens (substances that can cause allergic reactions), irritants, in some cases potentially toxic substances (mycotoxins). Inhaling or touching mold or mold spores may cause allergic reactions in sensitive individuals with symptoms like hay-fever, runny nose, and skin rashes. Mold thrives in environments with excess moisture and poor ventilation making buildings with poor ventilation a hazard for people to live in.

The important of understanding mold is crucial, as its presence not only presents substantial health risks but also environmental concerns.

Abstract:

We investigated to compare the types of mold present in two different school environments. Our findings revealed significant differences in the abundance and variety of mold spores at Preah Yukunthor High School and Matsusho Gakuen High School.

At Preah Yukunthor High School, located in a region with consistently warm temperatures throughout the year, we observed that a wide variety of mold spores are present in the air. These spores float year-round, indicating that the warm and humid climate provides favorable conditions for mold growth and dispersal. Mold thrives in environments with minimal seasonal changes, and Preah Yukunthor's climate perfectly matches these criteria.

In contrast, Matsusho Gakuen High School experiences colder temperatures, particularly in the winter months when temperatures drop significantly. This cooler climate appears to limit the variety and quantity of mold spores in the air. During our study, we found far fewer types of spores floating at Matsusho Gakuen compared to Preah Yukunthor. The seasonal variations, especially the harsh winter cold, likely inhibit the growth and spread of molds, resulting in a more restricted spore presence overall.

Our investigation highlights how environmental factors, particularly temperature, play a crucial role in influencing mold growth and spore distribution. Warmer climates foster more diversity and activity in mold populations, while colder climates suppress them.

Keywords: Mold spores; Environmental factors; Temperature

1. Introduction

Cambodia is a country in Southeast Asia, its capital is classified as a tropical wet and dry climate where temperatures don't vary greatly, but the city is subject to tropical monsoons in the wet season. In December, Cambodia is characterized by dry, sunny weather, low humidity, and relatively cool temperatures (average temp: 26 °C) throughout the country. This research is conducted during December in Preah Yukunthor New Generation High School located in Phnom Penh city, the heart of Cambodia.

On the other hand, Japan has a mostly temperate climate. There are four distinct seasons and each is approximately three months long. Matsusho Gakuen High School is located in Nagano, Japan. Their research was conducted in September which is a notable month of the summer season that generally includes high temperatures and heavy rainfall. You can expect daytime temperatures to reach around 24°C.

We picked these two months to conduct our research because it was when temperatures were most

similar to each other. The weather in both countries is favorable for mold growth, however, what type of mold growth there is where varies. There are many types of molds and they all grow because of different factors. This research would give you a solid foundation to compare both environments, analyzing the environmental properties in both locations, and understanding factors like pollution levels, climate, and soil properties could offer valuable insights into each location.

2. Background

The purpose of this research is to identify molds in two different areas from different environments, Japan and Cambodia. From past research, they discovered that the development of molds depended on environmental factors. We know that the Earth can be broadly divided into three regions, the tropical zone, the subtropical zone, and lastly, the temperate zone. Most regions of Japan belong to the temperate zone with subtropical climate and Cambodia is in the tropical zone.

Does it necessarily mean that different environments in different regions have different mold development? In this research we will examine the mold growth in Japan and Cambodia, and make a comparison to see if there are any features that separates them and if there is anything that connects them.

3. Methodology

1. Prepare a culture medium and place it in three selected locations: the stairs, bathroom, and locker. Allow mold spores to adhere to the medium.
2. Seal the culture medium by closing the lid to prevent the spread of mold spores. Incubate under controlled conditions to promote mold growth.
3. Identify the types of molds based on color, shape, and microscopic characteristics.
4. After completing the observations, sterilize the culture medium and all materials using an autoclave to ensure safe disposal.

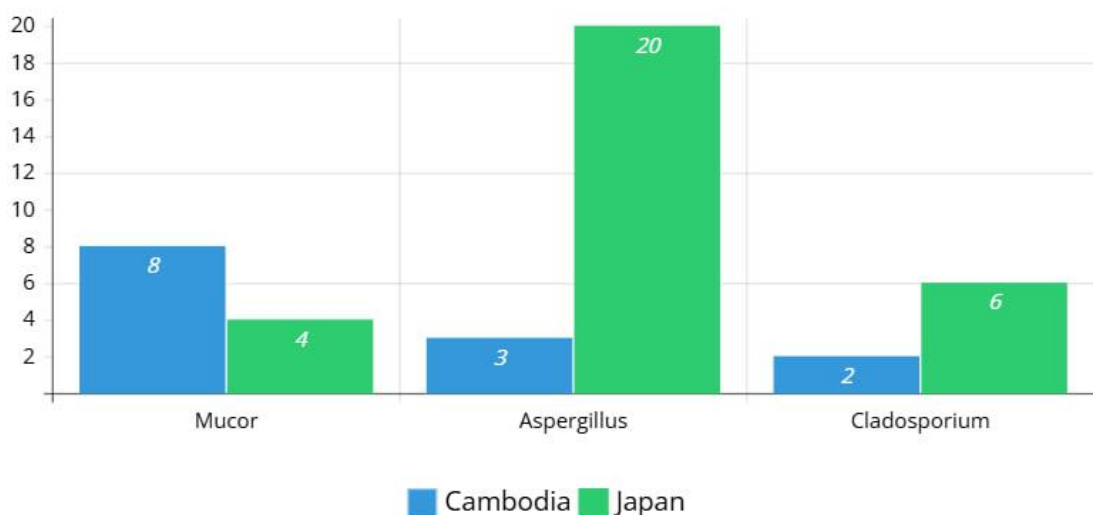
4. Results

Mold name	Preah Yukunthor high school			MatsushoGakuen high school		
	Stairs	Bathroom	Locker	Stairs	Bathroom	Locker
Aspergillus	0	2	1	4	15	1
Mucor spp	4	4	0	1	3	0
Cladosporium	3	0	4	0	5	1
Botrytis blight	0	2	2	0	0	0
Monascus spp	2	0	0	0	0	0
Penicillium spp	1	0	0	0	0	0
Rhizopus	0	0	0	0	0	2

※The numbers in the table indicate the number of colonies formed.

- We were able to identify several types of mold found in both Nagano, Japan, and Phnom Penh, Cambodia, despite the significant differences in climate and ecological conditions between these regions, including Aspergillus, Mucor, Cladosporium,
- Six types of mold were found in Cambodia compared to four in Japan.

5. Discussion



This figure: shows the numbers of colonies from mold found in both school.

6. Conclusion

In conclusion, this study revealed differences in the types of mold spores floating in the air between Matsusho Gakuen High School in Japan and Preah Yukunthor New Generation High School (NGS) in Cambodia. At NGS, the warm, humid climate allows for a greater variety and abundance of mold spores year-round. In contrast, Matsusho Gakuen experiences colder temperatures, particularly during winter, which limits the presence and diversity of mold spores. Despite these differences, mold spores are present in both locations, demonstrating that mold can thrive in diverse environmental conditions.

This study highlights that, although we live in two very different parts of the world with distinct climates and lifestyles, mold is a common element. Regardless of temperature or geographical location, mold spores are always present in the air, adapting to the environment around them. The findings emphasize the importance of understanding how different environmental factors, like temperature and humidity, influence mold growth. It also serves as a reminder that, no matter where we are, certain biological factors, like mold, are universal and affect us all.

Further research could explore how other environmental factors, such as air quality, pollution, and human activity, impact mold growth in various regions. This study provides a foundation for understanding mold ecology in different climates, shedding light on the global nature of mold spores.

7. Acknowledgements

First and foremost, we would like to express our deepest gratitude for the invaluable guidance, support, and care we have received throughout the program from our respective advisors. We are also thankful to both schools for granting permission to use the biology lab and for providing resources and scientific equipment that allowed us to initiate and conduct these experiments.

We sincerely thank the faculty at both schools for allowing us to carry out this research. Special thanks to our research colleagues, who patiently collaborated with us despite the challenges posed by language barriers and the time required to explain ideas. Coordinating schedules was often difficult, but their dedication made this research possible.

Finally, we are deeply grateful to our parents for their unwavering encouragement and support, which inspired us to persevere and complete this program successfully.

8. References

1. Description about Cambodia's weather: <https://www.intrepidtravel.com/en/cambodia/weather-in-cambodia#:~:text=Just%20like%20Siem%20Reap%2C%20Cambodia's,the%20driest%20month%20is%20February.>
2. Description of Japan's weather: <https://weather-and-climate.com/nagano-nagano-jp-September->

averages

3. Mold causes health risks and environmental concerns: <https://www.epa.gov/mold/can-mold-cause-health-problems#:~:text=Molds%20have%20the%20potential%20to,allergic%20reactions%20in%20sensitive%20individuals.>
4. Regions of the Earth divided into 3 regions: https://www.researchgate.net/figure/The-Earth-can-be-broadly-divided-into-three-major-regions-the-temperate-subtropical-and_fig1_268274685
5. Mold Identification: <https://rainbowrestores.com/blog/mold-identification>
6. Mold Introduction: <https://www.epa.gov/mold/mold-course-chapter-1>
7. Aspergillus: https://en.wikipedia.org/wiki/Aspergillus#Commercial_importance
8. Cladosporium: <https://en.wikipedia.org/wiki/Cladosporium>
9. Penicillium: <https://en.wikipedia.org/wiki/Penicillium>
10. Monascus: https://www.researchgate.net/figure/Plate-colonies-of-Monascus-purpureus-above-left-Monascus-pilosus-above-right-and_fig1_307583382
11. Influence of environmental factors on Mold development: <https://www.sciencedirect.com/science/article/abs/pii/S0360132319306316>

Using Food Waste to Reduce Heavy Metal Ions

Law Yui Lam¹, Yip Hei Hoo¹ and Wang Yuhan¹

Yuzuki Ohta², Sari Asada², Kahori Minami², Ririka Tada², Satoe Nagahara²

¹*G.T.(Ellen Yeung) College (China, HK),*

²*Mukogawa woman's University Senior Highschool (Japan)*

Abstract

Heavy metal ions, a significant pollutant, presents in the environment such as wastewater. They are considered as pollutants due to their toxic impacts on ecosystem and human health as they can enter the food chain. Heavy metal ions mainly come from industrial activities, waste disposal and agricultural runoff. This research focus on reducing the concentration of health metal ions by using food waste. In HK, nearly half of all food produced are fruit and vegetables. In this research, orange and lemon peels are used as they are readily available, simple, and low-cost material to tackle the issue of heavy metal ions. To detect the amount of heavy metal ions, the conventional detection methods are atomic absorption spectroscopy or inductively couple plasma mass spectrometry. However, those methods require complex pre-treatment procedure and expensive equipment. In this research, colorimetry is used to detect the colored heavy metal ions. It aims to prove that fruit peels can remove the coloured species in sample in which the absorbance decreases significantly.

Keywords: Fruit peel, removing heavy metal ions, colorimetry

1 Introduction

Heavy metals usually refer to transition metals in which with a high density of 5g/cm^3 . At a trace level, some of them are highly poisonous and hazardous to human, for example, mercury, chromium, cadmium and lead. In general, the heavy metal ions are also considered as carcinogens and toxic to both human and environment. The use of cosmetic products, fertilizer and industrial discharge waste are the common source of heavy metal ions. They are considered as non-biodegradable. They are unable to decompose and hence tends to accumulate in the environments once they are leaked out. For human, those carcinogens can lead to gastrointestinal, reproductive, nervous, and immune health problem. Human will be exposed to those toxic heavy metal ions mainly through air, water and seafood as they can accumulate in the aquatic animals (Bansod et al., 2017).

Bio-sorption, an alternative method to remove heavy metal ions by using natural biomass. Food waste can be one of the biomasses, they are eco-friendly, readily available, simple, and low-cost material. Nearly 50% of the food waste in HK are fruit peels. The specific functional groups (carboxyl, carbonyl and hydroxyl group) have been proven to absorb and trap heavy metal ions in solution. The fruit peel wastes have been proven that they are able to the heavy metal ions (Afolabi et al., 2021).

The conventional method to detect the presence of heavy metal ions are usually atomic absorption spectroscopy or inductively couple plasma mass spectrometry. Those methods are atomic absorption spectroscopy or inductively couple plasma mass spectrometry. However, they need expensive equipment and need complex pre-treatment. In this research, colorimetry is used as the detection method. However, there is a limitation in which only colored heavy metal ion species can be detected. We aim to prove that if the fruit peels can absorb the heavy metal ions in solution, the absorbance of the solution should be lowered.

2 Methodology

Orange and lemon peels were collected and rinsed with distilled water. The fruit peels were dried, and water were removed by filter paper. 3.0g fruit peels were obtained and cut into small pieces and then immersed into 0.05M hydrated copper (II) sulphate solution for several days. The solution was wrapped with paraffin wrap to prevent the evaporation of solution. The absorbance was recorded for day 0,1,2,3,6 days. The absorbance was measured by using wireless colorimeter and turbidity sensor with model number PS-3215. Red filter was used for measurement.



Figure 1 Wireless colorimeter and turbidity sensor with model number PS-3215



Figure 2 Orange peel in 0.05M CuSO_4 after 1 day



Figure 2 Lemon peel in 0.05M CuSO_4 after 1 day

3 Results

	Absorbance			
	Trial 1	Trial 2	Trial 3	Average
Day 1	1.218	1.246	1.233	1.232
Day 2	1.028	1.049	1.059	1.045
Day 3	1.163	1.074	1.118	1.118
Day 6	1.136	1.182	1.125	1.147

Table 1 Absorbance of solution when orange peel is immersed in 0.05 M CuSO_4 solution.



Figure 3 and 4 The appearance of orange peel after 6 days

	Absorbance			
	Trial 1	Trial 2	Trial 3	Average
Day 1	1.086	1.087	1.068	1.080
Day 2	1.093	1.104	1.156	1.117
Day 3	1.082	1.044	1.062	1.049
Day 6	1.061	1.066	1.064	1.063

Table 2 Absorbance of solution when orange peel is immersed in 0.05 M CuSO₄ solution.



Figure 5 and 6 The appearance of lemon peel after 6 days

From both table 1 and 2, they showed the average absorbance of solution when the fruit peels were immersed into the metal ion solution after six days.

For orange peel, the initial absorbance was 1.232. It can prove that it can be used as a bio absorbent as the absorbance dropped from 1.232 to 1.045 which decreased by 0.187. After 6 days' immersion, the average absorbance decreased by 0.085M.

For lemon peel, the initial absorbance was 1.080. It showed a slight drop of absorbance after 6 days. The absorbance fell from 1.080 at day 1 to 1.063 at day 6. The absorbance only dropped by 0.017.

Discussion

In this research, orange peel is a better bio-absorbent to absorb the heavy metal ions and hence lower the concentration and absorbance. For colored species, the colour intensity increases with the concentration of species. The absorbance is directly proportional to the concentration of solution. Orange peel showed the absorbance of copper (II) sulphate solution decreased by 0.187 in the first two days. When the absorbance decreases, it indicates that the immersed material can successfully absorb some heavy metal ions and hence lead to a lower absorbance value.

However, although this method is fast and easy, it still has some limitations.

Firstly, the color of copper (II) sulphate solution initially was pale blue. However, after 1 day, the solution color change to pale green. Therefore, the absorbance was recorded after it turned colour and when the absorbance value become stable.

Secondly, for colorimetry, in this research method, only the absorbance of colored species can be detected. However, some of heavy metal ions, they are colorless for example lead (II) ions.

References

- Afolabi, F. O., Musonge, P., & Bakare, B. F. (2021). Application of the response surface methodology in the removal of Cu^{2+} and Pb^{2+} from aqueous solutions using orange peels. *Scientific African*, 13, e00931.
- Bansod, B., Kumar, T., Thakur, R., Rana, S., & Singh, I. (2017). A review on various electrochemical techniques for heavy metal ions detection with different sensing platforms. *Biosensors and Bioelectronics*, 94, 443-455.

Measuring Air Pollution Using Pine Leaves

Ryoya Minakawa¹, Kazuma Sato¹,

Julian Unggul Wisnu², Salsabila Novita Putri², Maheswara Rafa Rinaldi Putra²

¹*Sendai Daisan High School (Japan)*

²*Budi Mulia Dua High School (Indonesia)*

Abstract:

It is known that we can observe some dirt on the stomata of pine leaves. They have many stomata which are sunken and accumulate pine resin. Therefore, stomata of such leaves tend to be gotten in by dirt. The dirt is made from different materials, such as Particulate matter (PM), sand, microplastics and so on. In this research, we collected them around Sendai-city in Miyagi-prefecture in Japan and a forest located in the southern part of Yogyakarta special region in Indonesia. Also, we could measure atmospheric pollution regarding volumes of vehicles and microplastics, using pine leaves. In addition, we could compare the Japanese data and that of Indonesia.

Keywords: pine; stomata; vehicle; PM2.5; microplastic

1. Introduction

Air pollution is a significant environmental issue impacting ecosystems, human health, and climate. Among the common pollutants, particulate matter (PM) such as PM_{2.5} and microplastics pose severe risk due to their microscopic size and can cause significant harm when inhaled or ingested. Monitoring air quality is crucial, but modern methods, such as using specialized sensors or advanced sampling tools can be costly and often require expert handling. Pine trees have a unique capability to capture air pollutants on their needle-like leaves. Pine leaves possess many stomata that can trap particulate microscopic particles. Pine needles are passive biomonitors of air pollution (Romanic & Krauthacker, 2007). Effective monitoring and mitigation of these pollutants are essential for ensuring health and a sustainable environment management.

PM is a heterogeneous mixture of liquid and solid components consisting of both primary and secondary particles (Freer-Smith et al., 2005). (PM) is classified into different sizes. According to (aerodynamic) diameter, namely ultrafine PM_{0.1} (<0.1 μm), fine PM_{2.5} (<2.5 μm), coarse PM₁₀ (<10 μm), and large PM_{>10} (10–100 μm) particles (Popek et al., 2013; Schraufnagel, 2020). However, most studies do not adhere to the conventional definitions of PM classes, but instead utilize size intervals from the commonly used filtration process (Steinparzer et al., 2023). Based on the filters used, the cut-off for ultrafine particles is < 0.2 μm (PM_{0.2}), for PM_{2.5} particles range from 0.2 μm to 2.5 μm , and for PM₁₀ between 2.5 μm and 10 μm (Corada et al., 2021; Sæbø et al., 2012; Sgrigna et al., 2020).

Pine needles, due to their unique morphological and biochemical characteristics, are effective bioindicators for measuring particulate matter (PM), including PM_{2.5} and microplastics, across different environmental settings. It is hypothesized that pine needles collected from urban areas in Japan will exhibit higher concentrations of PM compared to those from rural areas in Indonesia, primarily due to differences in urbanization levels and pollution sources (Steinparzer et al., 2023; Freer-Smith et al., 2005). Additionally, the retention of smaller particles such as PM_{2.5} and ultrafine

particles ($<0.2 \mu\text{m}$) on pine needles may vary based on climatic conditions and deposition velocities of pollutants in each region (Popek et al., 2013; Schraufnagel, 2020).

Despite the advancements in air quality monitoring technology, current methods often rely on this expensive equipment, air quality monitoring stations are usually of large sizes and high costs for installation and maintenance (Zheng et al., 2016). Which may not be accessible for many places. We noticed that there is limited comparative research on using pine leaves as bioindicators across different geographical locations, especially by contrasting urban areas in developed country settings in Japan and rural regions in developing countries such as Indonesia. This research highlight the need of potential exploration of pine peages as a tool for crossing-regional air pollutant assessment.

This research aims to evaluate the use of pine leaves as a bioindicator for monitoring air pollution, particulate matter and microplastics. By comparing samples collected from Sendai-city in Miyagi-prefecture Japan and a forest in the southern part of Yogyakarta, we're seeking to address the gap in comparative biomonitor using microscope to provide insights into the applicability of pine needles for air quality monitor across diverse area.

2. Methodology

As mentioned above, we collected pine leaves around Sendai-city in Miyagi-prefecture in Japan and a forest located in the southern part of Yogyakarta special region in Indonesia. In Japan, the main species of pine are Japanese black pine, Japanese red pine, and Japanese Larch. As for Indonesia is Sumatran pine. We observed them by using a microscope directly and counted all stomata and stomata with dirt. Also, for Japanese data, we referred to the Ministry of Land, Infrastructure, Transport and Tourism.

3. Results

Group Statistics					
	Country	N	Mean	Std. Deviation	Std. Error Mean
PercentageOfPores	Indonesia	15	1.7847	.91640	.23661
	Japan	60	2.2559	1.99048	.25697

Independent Samples Test						
		Levene's Test for Equality of Variances		t-test for Equality of Means		
		F	Sig.	t	df	Sig. (2-tailed)
PercentageOfPores	Equal variances assumed	4.004	.049	-.890	73	.376
	Equal variances not assumed			-1.349	49.997	.183

Based on the "Independent Samples Test" output table in the "Equal Variances Assumed" section, the Sig value is known. (2-tailed) is $0.376 > 0.05$, so as the basis for decision making in the independent sample t test, it can be concluded that there is no significant (real) difference or homogen between the average results of checking stomata on pine trees between Japan and Indonesia.

4. Discussion

This study aimed to evaluate the effectiveness of pine leaves as biomonitors for measuring air pollution levels, with a focus on comparing pollution levels between Indonesia and Japan. The result indicates no significant difference in the average stomatal contamination between two countries, suggesting that both regions experience comparable pollution levels despite differing urbanization. This finding challenges the initial hypothesis that urban areas in Japan would show higher PM concentrations. Further research is necessary to explore local environmental factors influencing pollutant retention, enhancing the use of pine needles as bioindicators across diverse ecosystems.

5. Conclusion

We successfully measured air pollution using pine leaves. A comparison of Japan and Indonesia found that both areas have similar levels of contamination. However, The results are not yet sufficient for practical application in society and further research is needed. As a future outlook, we want to conduct research that takes into account climatic conditions such as wind and humidity.

6. References

Draft:

- Chen L, Liu C, Zhang L, Zou R, Zhang Z. Variation in Tree Species Ability to Capture and Retain Airborne Fine Particulate Matter (PM_{2.5}). *Sci Rep*. 2017 Jun 9;7(1):3206. doi: 10.1038/s41598-017-03360-1. PMID: 28600533; PMCID: PMC5466687.
- Freer-Smith, P. H., Beckett, K. P., & Taylor, G. (2005). Deposition velocities to *Sorbus aria*, *Acer campestre*, *Populus deltoides* × *trichocarpa* 'Beaupre', *Pinus nigra*, and × *Cupressocyparis leylandii* for coarse, fine, and ultra-fine particles in the urban environment. *Environmental Pollution*, 133(1), 157–167. <https://doi.org/10.1016/j.envpol.2004.03.031>
- K. Zheng, S. Zhao, Z. Yang, X. Xiong and W. Xiang, "Design and Implementation of LPWA-Based Air Quality Monitoring System," in *IEEE Access*, vol. 4, pp. 3238-3245, 2016, doi: 10.1109/ACCESS.2016.2582153.
- Romanic SH, Krauthacker B. Are pine needles bioindicators of air pollution? Comparison of organochlorine compound levels in pine needles and ambient air. *Arh Hig Rada Toksikol*. 2007 Jun;58(2):195-9. doi: 10.2478/v10004-007-0012-8. PMID: 17562603.
- Sæbø, A., Popek, R., Nawrot, B., Hanslin, H. M., Gawronska, H., & Gawronski, S. W. (2012). Plant species differences in particulate matter accumulation on leaf surfaces. *Science of the Total Environment*, 427–428, 347–354. <https://doi.org/10.1016/j.scitotenv.2012.03.084>
- Sgrigna, G., Baldacchini, C., Dreveck, S., & Calfapietra, C. (2020). Characterization of leaf-level particulate matter for an industrial city using electron microscopy and X-ray microanalysis. *Environmental Science and Pollution Research*, 27, 12368–12378. <https://doi.org/10.1007/s11356-020-07812-3>
- Steinparzer, M., Schaumbryr, J., Godbold, D. L., & Rewald, B. (2023). Particulate matter accumulation by tree foliage is driven by leaf habit types, urbanization, and pollution levels. *Environmental Pollution*, 335, 122289. <https://doi.org/10.1016/j.envpol.2023.122289>

Utilization of Soybean Extract as an Alternative Nitrogen Source in Making *Nata de Coco*

Aldona Pangestu¹, Andhita Aprilliane¹, Arda Sahita¹, HORITA Ema², NODA Momoka²

¹Mutiara Persada High School (Indonesia)

²Tokyo Gakugei University Senior High School (Japan)

Abstract:

Nata de coco is a food product made from the fermentation of coconut water using the bacteria *Acetobacter xylinum* which takes the form of jelly and is popular among Southeast Asian countries. The nitrogen source of nata de coco is usually urea, commonly used in other food ingredients if urea is food grade. However, there are often controversies over the use of urea due to its high metal content. The soybean plants contain nitrogen (N) by the fertilizer and fixation of Nitrogen from the air by the bacteria *Rhizobium* which absorbs nitrogen from the soil. In this research, we evaluated the use of soybeans as nitrogen sources other than urea by comparing the results based on the texture, flavor, and thickness of each nata de coco. Also, we compared nata de coco made with three forms of soybeans, ungerminated, ground-ungerminated, and germinated. It is concluded that each nata de coco differs in taste, texture and color depending on whether the nitrogen source is urea, or soybeans. Also, it is shown that nata de coco differs in water content depending on the form of soybeans, ungerminated, ground-ungerminated, and germinated.

Keywords: *Nata de coco*; Soybean; Urea; Nitrogen source; Eco-Friendly

1. Introduction

Nata de Coco is a food product made through the fermentation of coconut water using the bacteria *Acetobacter xylinum*. During fermentation, nata de coco is combined with nitrogen source urea or sulfuric ammonia. Coconut water are substances that are not very well known and usually cause problems from the scent they emit. Meanwhile, aged coconut water is an important ingredient in making nata de coco because it contains bacteria that can activate the substances (Lubis and Dian, 2018 in Fitri *et al.*, 2022).

The nitrogen source is usually urea. However, there are controversies over the use of urea due to its high metal content which is not recommended for use in food (Widyaningrum *et al.*, 2014, Noviyanti, 2019). According to Korobko, *et al.* (2024), *Rhizobium* bacteria provide a significant increase in the nitrogen-fixing capacity of soybean plants and serve as an important source of nitrogen supply. Using soybean as a natural nitrogen source can serve as an alternative in the production of nata de coco, providing a safer option for consumption.

The purpose of this research (Indonesia side) is to investigate the effect of soybean extract addition in the production of nata de coco. The evaluation is conducted by testing the physicochemical properties and the organoleptic properties to determine the optimal conditions for nata de coco production. The purpose of this research (Japan side) is to compare nata de coco made with three forms of soybeans, ungerminated, ground-ungerminated, and germinated.

2. Methodology

<Methods from Indonesia side>

The methodology used in this research is organoleptic testing, namely testing a product involving the human senses (Erdi Surya *et al.*, 2020). The texture, color, and taste were tested and assessed by 10 panelists. This research also identified differences in the thickness and wet weight of each nata de coco with a nitrogen source in the form of 2 grams of urea and different soybean extracts, namely 38 grams and 50 grams. The organoleptic testing was performed by assessing food quality based on the value scale from 1 to 5. For the texture, 1 is not chewy, 2 is less chewy, 3 is chewy, 4 is chewier, and 5 is very chewy. For the taste, 1 is not sweet, 2 is less sweet, 3 is sweet, 4 is sweeter, and 5 is very sweet. For the color, 1 is yellowish-white, 2 is white, 3 is clear white, 4 is clear, and 5 is very clear (Surya *et al.*, 2020).

In this experiment of making nata de coco with soybean extract and urea, the ingredients needed in one experiment are 500 mL of mature coconut water, 50 grams of granulated sugar, 30 mL of vinegar and 50 mL of starter in the form of *Acetobacter xylinum*, a source of nitrogen (soybean extract 38 g and

50 g, and urea 2 g). Procedure: Grind the 38g or 50g of soybeans and pour the coconut water into a blender (as for urea, just boil them along with the coconut water). Boil them and add 50g sugar. After boiling, pour the mixture into a tray and wait until they are cooled. Pour 30mL vinegar and Acetobacter xylinum. Close it tight with a lid or newspaper. Make sure the paper isn't dirty. Wait for 7-10 days and put nata de coco in soak water for another 3 days. Cook the nata de coco with 500mL water and 75g sugar, and once the water has reduced, it is finished.

<Methods from Japan side>

We made three kinds of nata de coco using ungerminated soybeans, ground-ungerminated soybeans, and germinated soybeans and compared them from the perspective of their water content to see which form of soybeans is best for making nata de coco.

The ingredients are as follows.

Ingredients

• 25g of fructose • 10g of monosodium glutamate • 6.25g of 80% glycerol • 30g of 15% acid
• 100g of coconut water • 318.75g of 40°C water • Soybeans(ungerminated/ ground- ungerminated/ germinated)

Each nata de coco was measured first, then cut each nata de coco into a 2cm square on each side. We measured the dice-shaped nata de coco by weight before and after taking out its water inside. To take out the water, we put each nata de coco into small plastic bags, and put each bag into hot water(°C) for minutes. After that, each block of nata de coco was squeezed and measured again.

3. Results

<Results from Indonesia side>

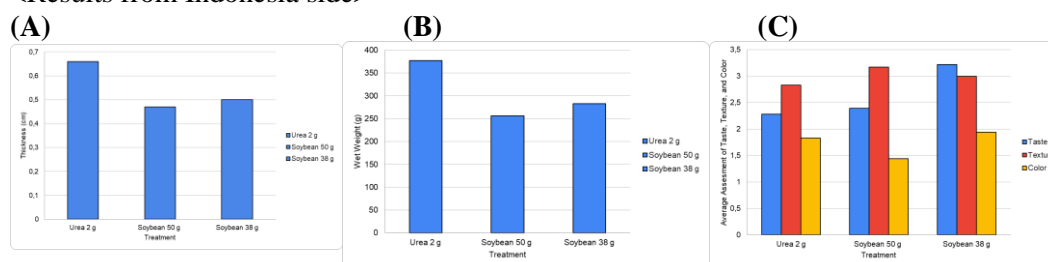


Figure 1. A) Thickness of the nata. Nata de coco with 38 g soybean extract has a thicker thickness than nata de coco with 50 g soybean extract. B) Wet weight of the nata. Nata de coco with 38 g soybean extract has a wet weight that contains more water than nata de coco with 50 g soybean extract. C) Organoleptic Properties. In taste, nata de coco with 38 g soy extract is sweeter than nata de coco with 50 g soy extract, in texture, nata de coco with 38 g soy extract is more chewy than nata de coco with 50 g soy extract, in color, nata de coco with 38 g soy extract is whiter than nata de coco with 50 g soy extract.

<Results from Japan side>

We used the formula below to calculate the water contained in each nata de coco.

$$R = \frac{W - W'}{W} \times 100$$

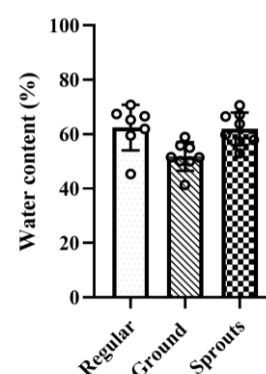
- R = The water content in nata de coco (%)
- W = Original weight of nata de coco (g)
- W' = Weight of nata de coco after taking out water contain (g)

The result is as follows.

Table 1. Water Contain of Nata de Coco Using Soybeans as Nitrogen Source

Type of Soybeans	Original Weight (g)	Weight after squeezing (g)	Water content (g)	Water content (%)
ungerminated	18.49	6.95	11.53	62.42
ground- ungerminated	27.65	13.42	14.23	51.80
germinated	25.20	9.40	15.80	62.00

Nata de coco made with germinated soybeans had the largest amount of the water contained, and nata de coco with ground-ungerminated soybeans had the least amount of the water contained.

Figure 2. Water Content of Nata de Coco

4. Discussion

In the process, the carbon and nitrogen content in the coconut water is not enough to be converted into glucose/sucrose into cellulose by the *Acetobacter xylinum*. Which is why in this experiment, the addition of sugar is used as the main carbon source, and the use of soybean for the nitrogen. The result of the fermentation trials using *Acetobacter xylinum* shows that the process is affected by additional nutrients and how long they ferment for. The process shows that the more the *Acetobacter xylinum* is active and the higher the concentration of soybean, the thicker the nata de coco becomes. Though this also affects the moisture level which decreases when the nitrogen concentration gets higher (Surya *et al.*, 2020). This will result in a dense texture of the nata de coco due to how low the moisture value is. The wet weight and thickness is most valued when using urea as a nitrogen source, as for using a natural alternative it is preferred to use soybeans as much as 38g rather than 50g (figure 1. A and B). One of the key factors of the wet weight is the concentration level the nitrogen source has, which causes different weights to the results with the addition of soybeans for about 256.5 g to 282.5 g and urea of 377 g. The thickness for the nata de coco is one of the key aspects to the quality of the final result. The cellulose is produced by the high water absorption capacity of the *Acetobacter xylinum*, in which the outer layer of the nata de coco contains the most moisture in which the cellulose tissue is far from the others. The addition of nutrients can increase the quality of the nata de coco. The soybeans vary along 0.47 cm to 0.5 cm, while the urea on 0.66 cm. The cellulose is produced by the high water absorption capacity of the *Acetobacter xylinum*, in which the outer layer of the nata de coco contains the most moisture in which the cellulose tissue is far from the others. A nitrogen source is added when the condition is optimal, producing more cellulose. Hence the more cellulose formed, the more nata de coco is produced (Surya *et al.*, 2020). As for the organoleptic test was conducted on the texture, taste, and color of nata de coco. Based on the results of the organoleptic evaluation (Figure 1.C), the chewiest texture was found in the treatment with 38 g of soybean extract, with a score of 3.17 (chewy). For taste, the highest score was observed in the nata de coco with 50 g of soybean extract, scoring 3.22 (sweet). As for the color test, all treatments exhibited a similar color, which was predominantly white.

5. Conclusion

<Conclusion from Indonesia side>

In the conclusion of the nata de coco experiment, it can be concluded with the different sizes in their results. The thickness of nata de coco was made with 38 g soybean extract with a thickness of 0.5 cm and a wet weight of 282.5g. The nata with the highest quality in taste, meaning the highest sweetness level was made with 38g soybeans with an average of 3.22 (sweet). While for the best texture was made with 50g soybeans of nata de coco with an average of 3.17 (chewy). As for the colors, nata de coco with the whitest color was made with 38g soybeans with an average of 1.94 (white). It is concluded that each nata de coco experiment differs depending on the nitrogen source and its measurements.

<Conclusion from Japan side>

Nata de coco can be made with soybeans as an alternative nitrogen source. By changing the form of soybeans, the rate of water content of each nata de coco changes. For example, nata de coco made with

germinated soybeans had the largest amount of water contained, and nata de coco with ground-ungermated soybeans had the least amount of water contained. This means that it is possible to control the water content of nata de coco by grinding or letting them sprout rather than using ungerminated soybeans.

6. Acknowledgements

The *Acetobacter xylinum* Japan side students used was cultured by Hokkaido Sarabetsu Agricultural High School, and the cultivation techniques were developed by Mr. OTA Yuichi of the Okhotsk Food Concerto.

We would like to thank Mr. Otani for useful discussions and for carefully proofreading the thesis.

Thus as for the Indonesia side, we are all grateful for the help we have gotten including in research and experimentation from our teacher Miss. Meri and Miss. Restu. As well for the lab facilities from Miss. Hindun, and for our principal Mr. Wahyudi for giving us this opportunity.

7. References

- Fitri, A. I., Annisa, A., Amini, D. S., Rahma, D., & Advinda, L. (2022). Pembuatan Nata De Coco dengan Penambahan Kecambah Kacang Hijau (*Vigna radiata*) sebagai Sumber Nitrogen. In Prosiding Seminar Nasional Biologi (Vol. 2, No. 2, pp. 243-249).
- Korobko, A., Kravets, R., Mazur, O., Mazur, O., Shevchenko, N. (2024). Nitrogen-Fixing Capacity of Soybean Varieties Depending on Seed Inoculation and Foliar Fertilization with Biopreparations. *Journal of Ecological Engineering*, 25(4), 23-37. <https://doi.org/10.12911/22998993/183497>.
- Surya, E., Ridhwan, M., Rasool, A., Noviyanti, A., Sudewi, S., & Zulfajri, M. (2020). The utilization of peanut sprout extract as a green nitrogen source for the physicochemical and organoleptic properties of Nata de coco. *Biocatalysis and Agricultural Biotechnology*, 29, 101781. <https://doi.org/10.1016/j.bcab.2020.101781>
- Utama, Y. P. (2024). Pengaruh Perbedaan Konsentrasi Ekstrak Kecambah Kacang Kedelai (Glycine max) Terhadap Hasil Nata de Coco. *Jurnal Pendidikan Tambusai*, 8(2), 18974-18981.
- Widiyaningrum., P., Mustikaningtyas, D., & Priyono, B. (2017). Evaluasi Sifat Fisik Nata de Coco Dengan Ekstrak Kecambah Sebagai Sumber Nitrogen. In PROSIDING SEMINAR NASIONAL & INTERNASIONAL.

Development of an Interactive Game on Environmental Awareness Titled: “Oh, Crab! Echoes of the Shore”

Hina Eguchi¹, Miku Eguchi¹, Narumi Motoura¹, Saki Shindo¹, Ashkinaz Canonoy², Leila Sabando², Jezrel Saño²

¹*Mukogawa Women's University Senior High School (Japan)*

²*Philippine Science High School - Eastern Visayas Campus (Philippines)*

Abstract:

This study presents the development of “Oh, Crab! Echoes of the Shore,” an interactive game designed to promote awareness of Sustainable Development Goal 14 (SDG 14), which emphasizes the conservation and sustainable use of marine resources. The game’s narrative follows a young boy from a coastal town who, after polluting the ocean, is transformed into a crab and must navigate an underwater journey to return home. Through engaging gameplay mechanics, such as collecting trash for power-ups and assisting marine animals affected by pollution, players experience the direct consequences of improper waste management and climate change on marine ecosystems. The game aims to foster empathy and understanding of these issues while encouraging actionable behavior. The story concludes with the protagonist inspiring his community to adopt eco-friendly practices, emphasizing the potential for individual and collective efforts to address environmental challenges. This game aims to inspire players to care for the environment and take environmental action in real life.

Keywords: marine conservation; SDG 14; environmental sustainability; climate change; interactive game

I. Introduction

Environmental conservation has become an urgent global priority as the adverse effects of climate change and pollution continue to threaten ecosystems and human communities. Among these, ocean pollution is a particularly pressing issue as it endangers marine life and threatens the livelihoods of those who rely on the sea for survival. This growing issue increasingly burdens the world’s oceans, jeopardizing marine biodiversity, coastal ecosystems, and human well-being. (Fava, 2022). According to Ritchie et al. (2023), coastal communities, particularly those in middle-class economies, often experience the consequences of improper waste management firsthand which include environmental degradation and health issues linked to contaminated water. Furthermore, it is estimated that around 11 million metric tons of plastic pollution enter the ocean each year, which equates to more than a garbage truck’s worth of plastics every minute (Ocean Conservancy, 2021). Despite numerous global initiatives to address ocean pollution, many individuals remain unaware of their role in contributing to these problems.

Interactive digital games have shown potential as a medium for education, offering an engaging way to communicate complex issues and encourage active learning (Gui et al., 2023). Studies by Janakiraman (2020) and Adipat et al. (2021) have demonstrated the effectiveness of game-based learning tools in enhancing knowledge retention and influencing behavior, particularly on social and environmental topics. While some existing games have successfully addressed various important themes, there is a lack of games that tackle the critical issues of ocean conservation and sustainable practices. Current educational initiatives often fail to bridge the gap between gameplay and real-world actions, thus hindering active engagement with environmental issues. Notably, there is a scarcity of games that explicitly target Sustainable Development Goal 14 (SDG 14): Life Below Water, which aims to conserve and sustainably use oceans, seas, and marine resources. This underscores the need for innovative approaches that integrate interactive gameplay with education on marine conservation.

Through interactive and immersive gameplay, the project aims to educate participants on the importance of ocean conservation while empowering them to take proactive measures to protect and

preserve the environment. The project focuses on developing an interactive single-player adventure game titled "Oh, Crab! Echoes of the Shore." In the game's narrative, players assume the role of a boy transformed into a crab, directly experiencing the consequences of pollution and learning about sustainable practices. By bridging the gap between education and entertainment, this project offers an innovative approach to engaging and informing individuals about the SDG 14 in a meaningful and impactful way.

II. Methodology

The study employed a developmental research design to create "*Oh, Crab! Echoes of the Shore*," an interactive game aimed at promoting marine conservation and environmental awareness. The game development process was structured into five phases: conceptualization and planning, asset creation, game development, testing and iteration, and finalization and deployment.

1. Conceptualization and planning phase

The research team identified the project's objectives, aligning them with Sustainable Development Goal 14 (SDG 14). A comprehensive game design document (GDD) was drafted to outline the storyline, gameplay mechanics, level designs, and educational elements. The Godot Engine, an open-source game development platform, was selected for its flexibility and efficiency.

2. Asset creation and collection phase

The visual assets, including characters, environments, and animations, were developed using digital illustration tools or were collected from third-party resources. Audio assets, such as background music and sound effects, were sourced from royalty-free libraries or composed specifically for the game. All assets were optimized to ensure compatibility with the Godot Engine.

3. Game development phase

The game development phase involved programming the framework using GDScript, with features including character movement, object interaction, and level transitions. Realistic underwater ecosystems and pollution scenarios were designed to mirror real-world issues, while interactive elements, such as collecting trash and assisting marine animals, were integrated to enhance player engagement.

4. Evaluation

Testing and iteration were conducted to refine the game's functionality and educational impact. Internal testers provided feedback on gameplay mechanics, narrative flow, and overall experience. This feedback addressed bugs, improved user engagement, and enhanced the game's performance.

III. Results

The results of this study were evaluated through three primary metrics: gameplay functionality, educational content, and user engagement.

a. Gameplay Functionality

The game integrated various features to enhance interactivity and realism. Key functionalities included character movement, object interaction, and level transitions. Various underwater environments were created to depict marine ecosystems affected by pollution. Gameplay mechanics such as collecting trash and assisting marine animals were also implemented.

b. Educational Content

The game effectively incorporated Sustainable Development Goal 14 (SDG 14) themes into its narrative and gameplay. Educational elements included tasks that highlighted the consequences of pollution, aimed at reinforcing learning objectives.

c. User Engagement Potential

The game's narrative and visual elements were crafted to maximize engagement. Inspirations from popular games such as *Stardew Valley* and *Spiritfarer* influenced the design, aiming to create a similarly enjoyable experience.



Figure 1. Screenshot of Scene 2: Outside the house



Figure 2. Screenshot of ‘Scene 4: Nugu chases the garbage truck’



Figure 3. Screenshot of beach environment



Figure 4. Screenshot of underwater environment

IV. Discussion

The development of “Oh, Crab! Echoes of the Shore” demonstrates the potential of interactive games as tools for addressing environmental issues while providing engaging educational experiences. By integrating realistic underwater ecosystems and gameplay tasks, the game can create awareness of marine conservation and the consequences of pollution. Its narrative aligns with Sustainable Development Goal 14 (SDG 14), offering players a structured understanding of ocean sustainability. It also inspires empathy through relatable storytelling by drawing inspiration from established game design practices.

V. Conclusion

“Oh, Crab! Echoes of the Shore” can be a promising example of how interactive games can merge education and entertainment to raise awareness about critical environmental issues. By tackling themes from Sustainable Development Goal 14 (SDG 14), the game highlights the consequences of marine pollution while encouraging players to adopt eco-friendly behaviors. Future related studies could explore expanding the game's scope, incorporating multiplayer modes, or integrating real-world environmental data to enhance its educational impact. Further research could also investigate the game's effectiveness in influencing players' attitudes and actions toward marine conservation.

References

- Adipat, S., Laksana, K., Busayanon, K., Asawasowan, A., & Adipat, B. (2021). Engaging students in the learning process with game-based learning: The fundamental concepts. *International Journal of Technology in Education (IJTE)*, 4(3), 542-552. <https://doi.org/10.46328/ijte.169>
- Fava, M. (2022, May 9). *Ocean plastic pollution an overview: data and statistics*. UNESCO. <https://oceanliteracy.unesco.org/plastic-pollution-ocean/>
- Gui, Y., Cai, Z., Yang, Y., Kong, L., Fan, X., & Tai, R. H. (2023). Effectiveness of digital educational game and game design in STEM learning: a meta-analytic review. *International Journal of STEM Education*, 10(1). <https://doi.org/10.1186/s40594-023-00424-9>
- Janakiraman, S. (2020). Digital Games for Environmental Sustainability Education: Implications for Educators. In *TEEM'20: Eighth International Conference on Technological Ecosystems for Enhancing Multiculturality* (pp. 542–545). 2020 Association for Computing Machinery. <https://doi.org/10.1145/3434780.3436649>
- Ocean Conservancy. (2021). General Ocean Plastic. Retrieved from https://oceanconservancy.org/wp-content/uploads/2022/03/General-Ocean-Plastic_Oct-2021.pdf
- Ritchie, H., Samborska, V., & Roser, M. (2023, December 28). *Plastic pollution*. Our World in Data. <https://ourworldindata.org/plastic-pollution>

Lactic Acid Synthesis From Starch-Based Biomass Materials

Yuma Fukumuto¹, Sara Umezono¹, Viena Angela B. Muyco², Frenchie Mae L. Sembrano², Patrick Quinn R. Yan²

¹Chiba Prefectural Funabashi High School (Japan)

²Philippine Science High School SOCCSKSARGEN Region Campus (Philippines)

Abstract

The key significance of lactic acid as a precursor in PLA production lies in the fact that PLA is a biodegradable polymer. This paper concerns the fermentation of starch-based biomass from three sources: *Artocarpus odoratissimus* (Marang) seeds and two rice varieties, Japonica and Indica, aiming at optimizing starch for lactic acid production. Fermentation with *Lactobacillus* species through hydrolysis of starch to simpler sugars was used in this fermentation process. All biomass sources supported lactic acid fermentation; however, considerable variations were seen in fermentation efficiencies between Japonica and Indica rice. These biomasses are starch-rich sources. This study confirms the direct relationship between starch content and the lactic acid yield; however, its significance rests in optimizing the biomass feedstock in industrial fermentation processes. The research finds that the choice of appropriate biomass along with optimized starch content may make fermentation more efficient, reduce waste, and lead to sustainable lactic acid and PLA production as part of crop development for an environmentally friendly transition toward material usage and production.

Keywords: lactic acid; enzymatic hydrolysis; starch; marang; rice

1. Introduction

Lactic acid (LA) is one of the most versatile organic acids with extensive industrial application. It can be used in food preservation or the production of biodegradable plastics. Fermentation is a very efficient technology for lactic acid production, using starch-based biomass materials as renewable feedstock. A polysaccharide of glucose units, starch is readily available and relatively cheap in comparison to other sources of feedstock used in biotechnological processes (Manandhar & Shah, 2023). Among the diverse starch-based biomass sources, by-products from agricultural sources like rice and fruit waste have been increasingly considered alternatives. Rice, one of the most abundantly produced starch-rich crops worldwide, has been used to produce lactic acid for quite some time now because of its high starch content and large quantities available (Fukushima et al., 2004). Besides rice, underutilized biomass sources such as marang (*Artocarpus odoratissimus*) offer a fascinating opportunity to produce lactic acid. Marang, a tropical fruit native to the Philippines and Southeast Asia, generates plenty of waste during its seeds and husk disposal (Alvarado, 2023). However, research has found that marang seed starch, with its high levels of fermentable sugars, can effectively be used for lactic acid production through Simultaneous Saccharification and Fermentation (SSF).

2. Experimental Methods 1 (Starch From Marang Seeds)

2.1 Starch Extraction

The marang seeds were cleaned using a brush and water before drying in an oven cabinet at 130°C for 2 hours. The oven-dried seeds were blended with added water. The resulting mixture was filtered to separate the dregs from the liquid filtrate (starch suspension). The obtained suspension was deposited in a beaker for 24-48 hours. Afterward, the starch-rich liquid was filtered through filter paper into a 500 mL Erlenmeyer flask to obtain wet starch. The precipitate was then dried in an oven at 70°C for 30 minutes. Finally, the dried starch powder was sieved using a 100-mesh sieve for further refinement.

2.2 Culture Medium Preparation

In this process, 7.5 grams of PCA powder and 13.03 grams of MRS broth powder were mixed and dissolved in 200 mL of distilled water in a 1000 mL Erlenmeyer flask. The mixture was stirred on a hot plate using a magnetic stirrer to dissolve the powders properly. Once fully dissolved, the flask containing the mixture was sealed with a cotton plug. Simultaneously, the petri dishes were wrapped in paper and housed in a transparent plastic bag in preparation for sterilization. After these preparations, the mixture and the petri dishes were sterilized in an autoclave at 121°C and 21 psi for 15 minutes.

(Mizuno et al., 2017). Once sterilization was complete, the materials were allowed to cool to room temperature to prevent heat damage to the *Lactobacillus casei* cells during inoculation.

2.3 Bacteria Inoculation

The researchers cultivated the bacteria from locally sourced fermented dairy milk with probiotic cultures (Yakult). The *L. casei* from the Yakult was streaked and isolated onto the prepared Petri dishes using an inoculating loop. The inoculated medium was then incubated at 30-37°C for 48 hours to promote optimal *Lactobacillus* growth before being used in the following process.

2.4 Simultaneous Saccharification and Fermentation

The SSF process was carried out in a 500-mL Erlenmeyer flask. The enzyme mixture was prepared for the saccharification process by adding 0.4% (v/w) of α -amylase to ground fresh material. This material was then mixed with water at a 1:3 ratio. To maintain a constant pH of 5.0, calcium carbonate (CaCO_3) was added at 50% of the dry mass weight. To initiate fermentation and complete the SSF process, the cultured bacteria were inoculated into the same medium. The flask containing the prepared medium was sealed with a fermentation airlock via a rubber stopper. The airlock was partially filled with water to create a protective barrier. The medium was then allowed to ferment at room temperature for approximately 72 hours.

2.5 Isolation and Characterization of Synthesized Lactic Acid

In this process, lactic acid was separated from the broth by heating the sample to 100°C for 10 minutes, followed by centrifugation at 3,500 rpm and 37°C for 40 minutes (Nguyen et al., 2013). The clarified solution was then decanted, leaving behind the separated debris layer. The synthesized lactic acid was analyzed using FTIR spectroscopy and compared to the FTIR results of commercial lactic acid to confirm the identity of the synthesized product.

3. Results

Lactic acid was confirmed through the Fourier Transform Infrared Spectroscopy (FTIR), where the present functional groups were identified using their standard frequency. Lactic Acid typically consists of an ester (carboxyl group and carbonyl group), methyl group, and hydroxyl group with varying standard frequencies in their absorption peaks.

Table 1. Lactic Acid FTIR Results Summary

Functional Groups	Standard Frequency cm^{-1}	LA wavenumber cm^{-1}
-OH (COOH)	3550 – 3200	3221.03
-CH ₃ (S)	3000 – 2840	1457.39
-C=O	1650 – 1750	1742.53
-C-O (COOH) -OH	1000-1300	1157.34
-CH ₃ (B)	1375-1475	1457.39

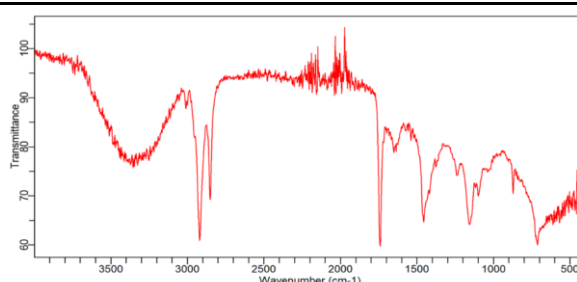


Figure 1. IR Chromatogram of LA Specimen.

IR Spectra of the Lactic Acid specimen revealed absorption peaks of ester and CH₃, along with other groups in Table 1. With the absorption peaks of -C=O (1742.53), -C-O (COOH) -OH (1157.34) within their standard frequency range, as long as the other functional groups reflected in Table 1, the tested specimen is confirmed to be lactic acid.

4. Experimental Methods 2 (Starch From Japonica or Indica Rice)

4.1 Rice Processing A (Cooking Then Kneading Rice)

One 500 mL beaker was filled with 100.0 g of Japonica rice, and another was filled with 100.0 g of Indica rice. Pure water (146.7 mL) was poured into each beaker. Two pieces of aluminum foil were placed over each beaker, and five small holes were made in the foil using a mechanical pencil. The beakers were heated for 10 minutes using gas burners and then steamed for 10 minutes (kept warm without gas burners). The contents were mixed with glass rods, transferred into plastic bags, and kneaded uniformly.

4.2 Rice Processing B (Grinding Then Cooking Rice)

Each 100.0 g of Japonica and Indica rice was ground using a coffee mill. Pure water (146.7 mL) was added, and the mixtures were poured into 500 mL beakers. Two pieces of aluminum foil were placed over each beaker, and five small holes were made in the foil using a mechanical pencil. The beakers were heated for 10 minutes with gas burners and then steamed for another 10 minutes (kept warm without gas burners). The contents were mixed with glass rods, transferred into plastic bags, and kneaded uniformly.

4.3 Enzymatic Hydrolysis by α -Amylase (Taka-diaxase)

Each 45 g of processed rice and 20 mL of pure water were placed into 50 mL beakers. Four to five samples were prepared for each type of processed rice. Two samples were mixed with 1.0 g of α -amylase (Taka-diaxase), while the others were left untreated.

4.4 Lactic Acid Fermentation by Lactobacillus LA-2

Yogurt (including probiotic lactic acid bacteria LA-2) was separated using a centrifuge at 3,000 rpm for 5 minutes. Two milliliters of the liquid from the upper layer of the separated yogurt (whey) was added to the samples. NaOH solution (0.1 mol/L) was added dropwise (2–3 drops) to adjust the pH to 7. The pH was measured using pH test paper. The samples were incubated at 40 °C for approximately one day. After incubation, the samples were removed, and their liquid layers were filtered. Due to the high viscosity of the Japonica rice samples with short enzymatic hydrolysis times, suction filtration was used.

4.5 Measuring Lactic Acid

The pH of the samples was measured using a pH meter. The relative amount of lactic acid was analyzed using Mass Spectrometry (MS) (Nexera X3-LCMS-9030) at Mitsui Link Lab.

5. Results

Table 2 shows the pH values of Japonica and Indica rice samples after fermentation, processed using different methods (A and B) and enzymatic hydrolysis durations (longer or shorter).

Table 2. pH values after the fermentation.

	Japonica Rice		Indica Rice	
	Processing A	Processing B	Processing A	Processing B
Longer enzymatic	4.8	4.5	5.4	5.3
hydrolysis	6.0	5.6	4.9	5.3
Shorter enzymatic	4.3	5.0	4.3	4.1
hydrolysis	4.5	5.0	4.9	4.3
	4.6	-	4.4	-

Table 3 presents the peak area data from mass spectrometry analysis for whey and rice-based samples processed under varying conditions.

Table 3. MS Results.

Sample Name	Whey (original)	Id-A-Long	Jp-B-Long	Id-A-Short
Peak Area	595757	319763	248566	37623

6. Discussion

The synthesis of lactic acid has various factors, from starch concentration and fermentation components. This includes the length of hydrolysis, where it was observed that the longer the enzymatic hydrolysis the specimen had, the more liquid LA was produced. Moreover, the controlled pH of the mixture was crucial for the experimentation process to produce lactic acid successfully. It was observed that the lower the pH, the more efficient the synthesis was; however, a pH content that is too high may prevent the formation of lactic acid due to too much enzymatic hydrolysis. Furthermore, the strain of bacteria is also significant in enzymatic hydrolysis; the most commonly utilized strain is *Lactobacillus*, which is the most effective. Different species of *Lactobacillus* can also lead to varying results. Additionally, the starch content of the biomass is one of the most crucial factors in the synthesis of lactic acid. Physical biomass processings give little to no differences in the lactic acid produced; however, the variance in the specific biomass type is considered a significant variable. Japonica rice might be able to generate more lactic acid than Indica rice; simultaneously, marang fruit would also produce a different amount of lactic acid. This is due to the differences in the initial starch concentration in the different biomasses. Therefore, it can be observed that the lactic acid amount is generally dependent on the initial starch amount.

7. Conclusion

The study investigated sustainable feedstocks for lactic acid production, focusing on marang seed starch and two rice varieties, Japonica and Indica. The method used for marang seed starch involved fermentation with *Lactobacillus casei*, successfully producing lactic acid similar to commercial lactic acid. For rice, the method used included enzymatic hydrolysis followed by fermentation, with Japonica rice showing a higher potential for lactic acid production than Indica. The results highlighted the importance of optimizing enzymatic hydrolysis time and starch content to enhance efficiency, reduce waste, and promote the use of renewable resources.

8. References

- Ashish Manandhar, & Shah, A. (2023). *Techno-Economic Analysis of the Production of Lactic Acid from Lignocellulosic Biomass*. 9(7), 641–641. <https://doi.org/10.3390/fermentation9070641>
- Alvarado, M. C. (2023). Marang fruit (*Artocarpus Odoratissimus*) waste: A promising resource for food and diverse applications: A review of its current status, research opportunities, and future prospects. *Food Bioengineering*, 2(4), 350–359. <https://doi.org/10.1002/fbe2.12065>
- Fukushima, K., Sogo, K., Miura, S., & Kimura, Y. (2004b). Production of D-lactic acid by bacterial fermentation of rice starch. *Macromolecular Bioscience*, 4(11), 1021–1027. <https://doi.org/10.1002/mabi.200400080>
- Mizuno, K., Mizuno, M., Yamauchi, M., Takemura, A., Romero, V., & Morikawa, K. (2017). Adjacent-possible ecological niche: growth of *Lactobacillus* species co-cultured with *Escherichia coli* in a synthetic minimal medium. *Scientific Reports*, 7(1). <https://doi.org/10.1038/s41598-017-12894-3>
- Nguyen, C. M., Choi, G. J., Choi, Y. H., Jang, K. S., & Kim, J. C. (2013). D-and L-lactic acid production from fresh sweet potato through simultaneous saccharification and fermentation. *Biochemical engineering journal*, 81, 40-46.

Investigation on the correlation between a runner's finger angle and their speed

Zavier Ong¹, Rissa Kwek¹, Ruki Honda², Miyamoto Shuichiro², Keita Fukuzawa², Eden Graves²,
Fujita Jin²

¹*School of Science and Technology (Singapore)*

²*Ryugasaki First High School (Japan)*

Abstract:

Much research has been done to understand the implications of how different angles of joints in the hand would affect the speed of the human body when running. This experiment was conducted with a wooden hand, rotating with the same force for different index and small finger joint angles. A wooden hand was attached to a servo motor and spun horizontally. The results revealed that the angle of the finger joints does not significantly affect the speed of the rotating hand.

Keywords: joints; speed; index; small; horizontally

1. Introduction

The human hand is an essential part of every human. It has many joints and bones allow humans to make different shapes for various tasks like holding a cup and more. The way these joints and bones work together for fine-motor work (i.e. knitting) has been deeply explored, while the impacts on gross-motor work (i.e. running) have not been investigated as much.

Running is one of the most practised sports worldwide. Competitive runners participate in competitions such as marathons and short races, while recreational runners run to keep fit. Studies have indicated how the arm swings would affect runners, however, there needs to be studies on hand shapes affecting runners.

Currently, there is little to no research on how the shape of hands can affect a runner. However, the hand's shape could help reduce the drag, making the runner more aerodynamic.

There is a close relationship between track and field and air resistance. For example, previous research on which this study is based has examined the effect that air resistance during running has on an athlete's performance. When running alone, the athlete is directly exposed to all air resistance. This has a particularly large effect when running at high speeds. Furthermore, when two or more people run together, the rear athlete is affected by the airflow created by the athlete in front, reducing air resistance. This is a factor that improves energy efficiency when running in a group. The findings of this previous research suggest the importance of air resistance in the arm swing motion of each athlete. This study further develops this concept, focusing on the finger joint angles.

2. Methodology

2.1 Data collection

The Singapore students surveyed their school's athletics club (running club), in which we inquired about their running hand shape and events.

The most common hand shape of SST's athletics club members when running was a fist shape, with all finger joint angles around 90 degrees.



Fig 1.1 Hand shape of SG runner

2.2 Procedure

For the Singapore experiment, the procedure is as follows:

1. Set both joint angles to 0 degrees of index finger
2. Spin set-up for 10 seconds
3. Increase joint angle (θ_1) by 10 degrees
4. Repeat steps 2-3 until 90 degrees
5. Set joint angle (θ_1) to 0
6. Repeat steps 2-4 for the second joint (θ_2)
7. Set all joints for the index finger back to 0
8. Repeat steps 1-6 for small finger

For the Japan experiment, the procedure is as follows:

1. All fingers joint angles set to 0 degrees
2. Spin set-up for 10 seconds
3. Increase joint angle (θ_1) of all fingers by 10 degrees
4. Repeat steps 2-3 until 90 degrees
5. Set joint angle (θ_1) to 0
6. Repeat steps 2-4 for the second joint (θ_2)

3. Results

3.1 Singapore Experiment

The following are the results of the Singapore set-up:

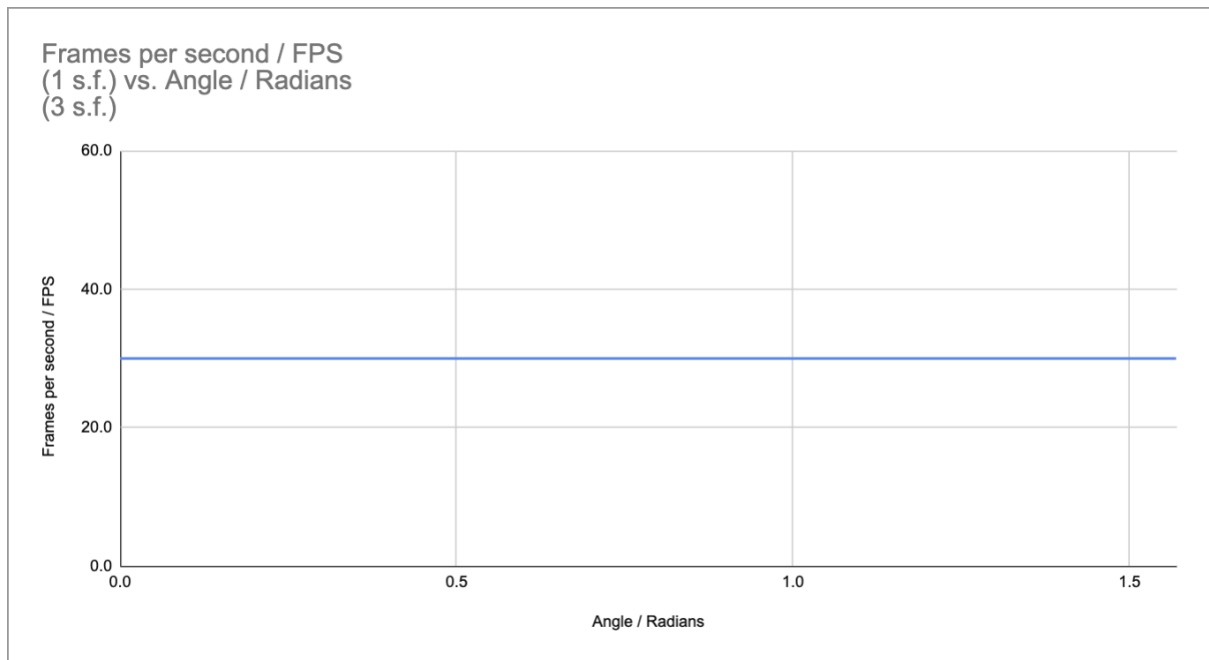


Fig 2.1 Index finger, PIP joint

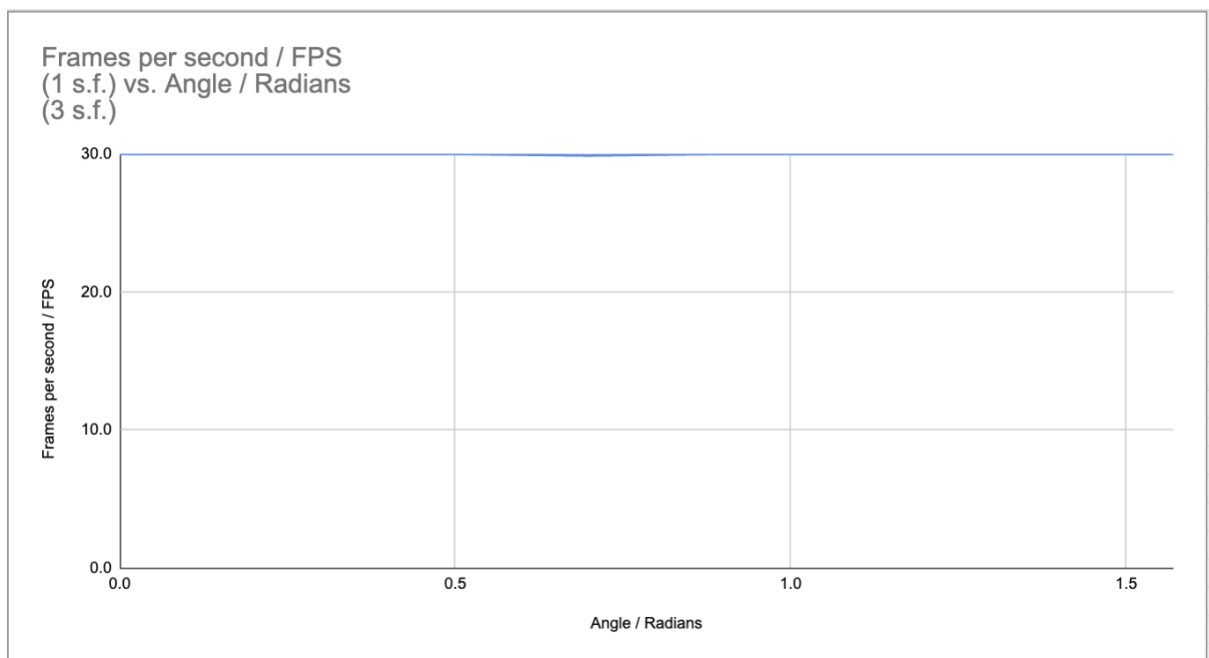


Fig 2.2 Index finger, MP joint

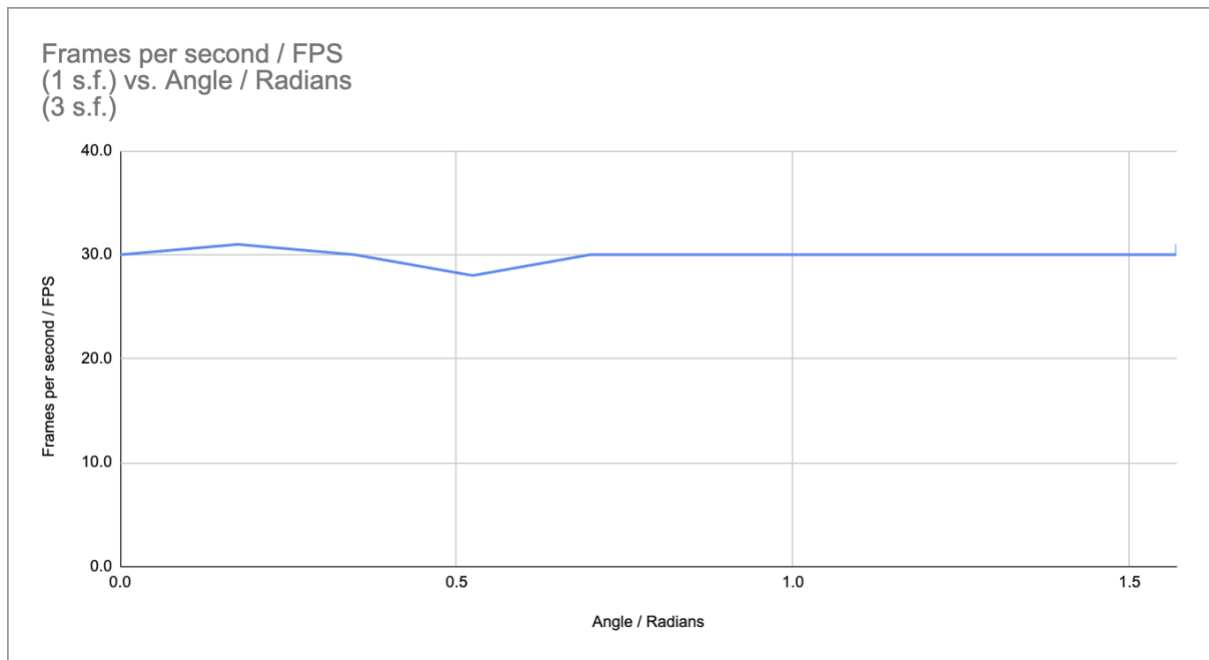


Fig 2.3 Small finger, PIP joint

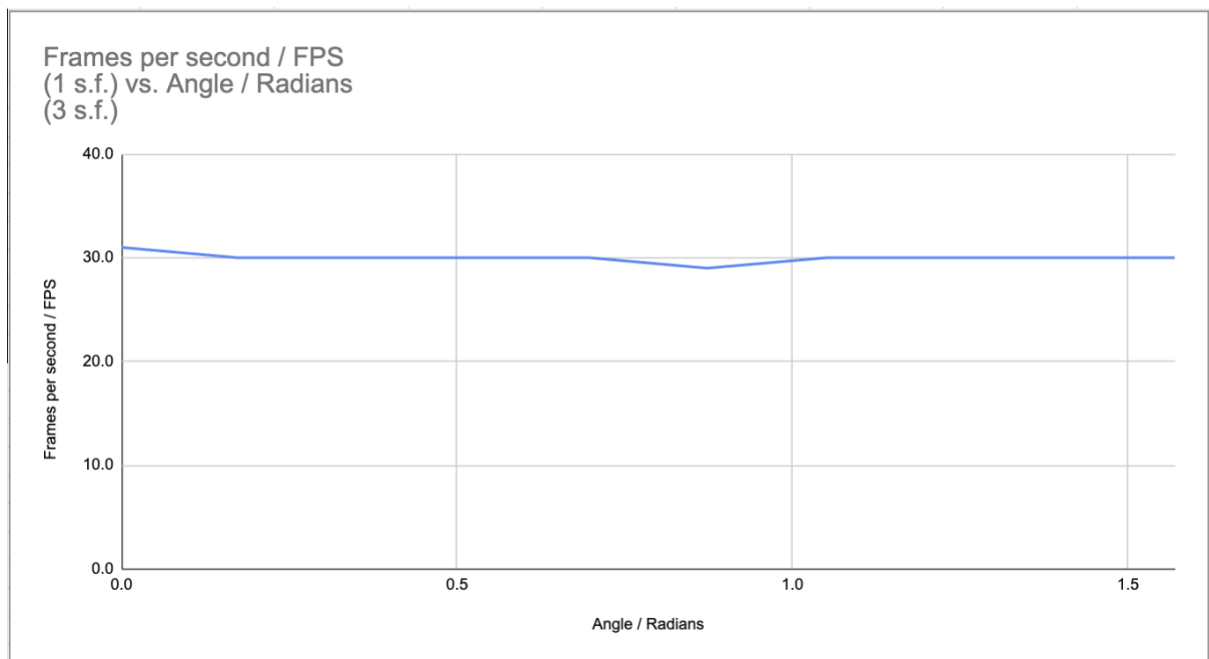


Fig 2.4 Small finger, MP joint

3.2 Japan Experiment

The following are the results of the Japan set-up:

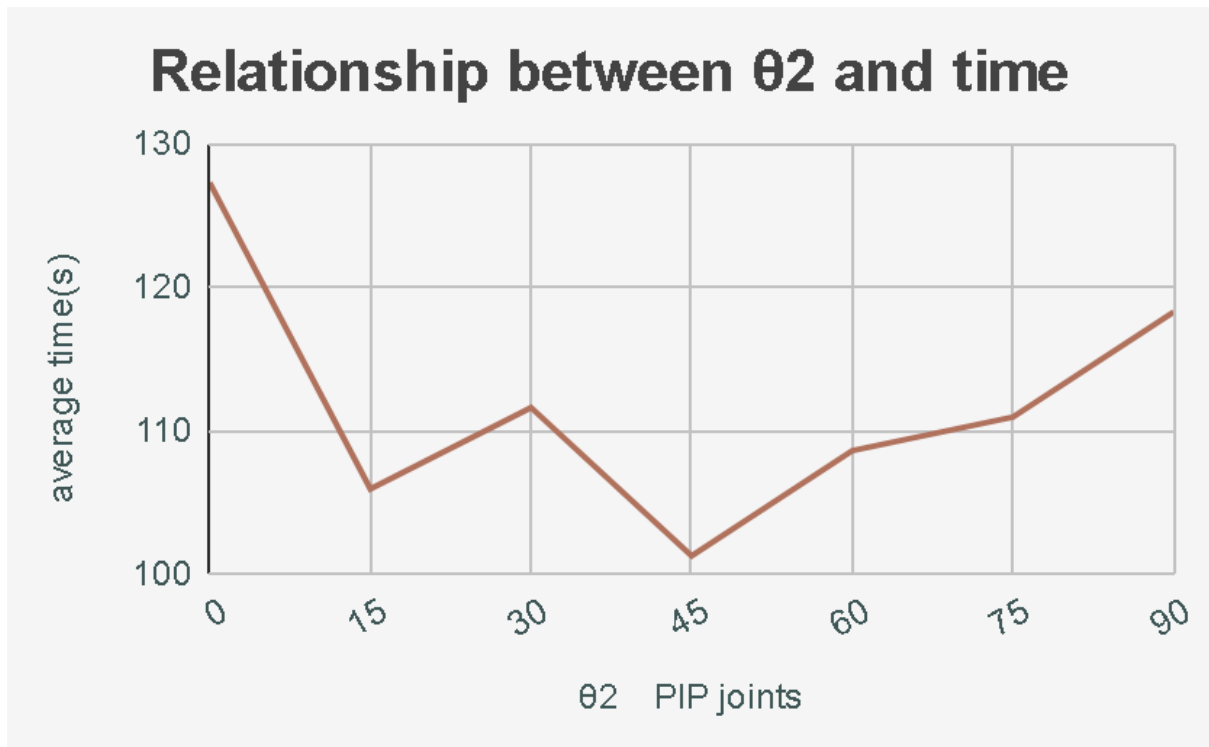


Fig 3.1 All fingers, PIP joint

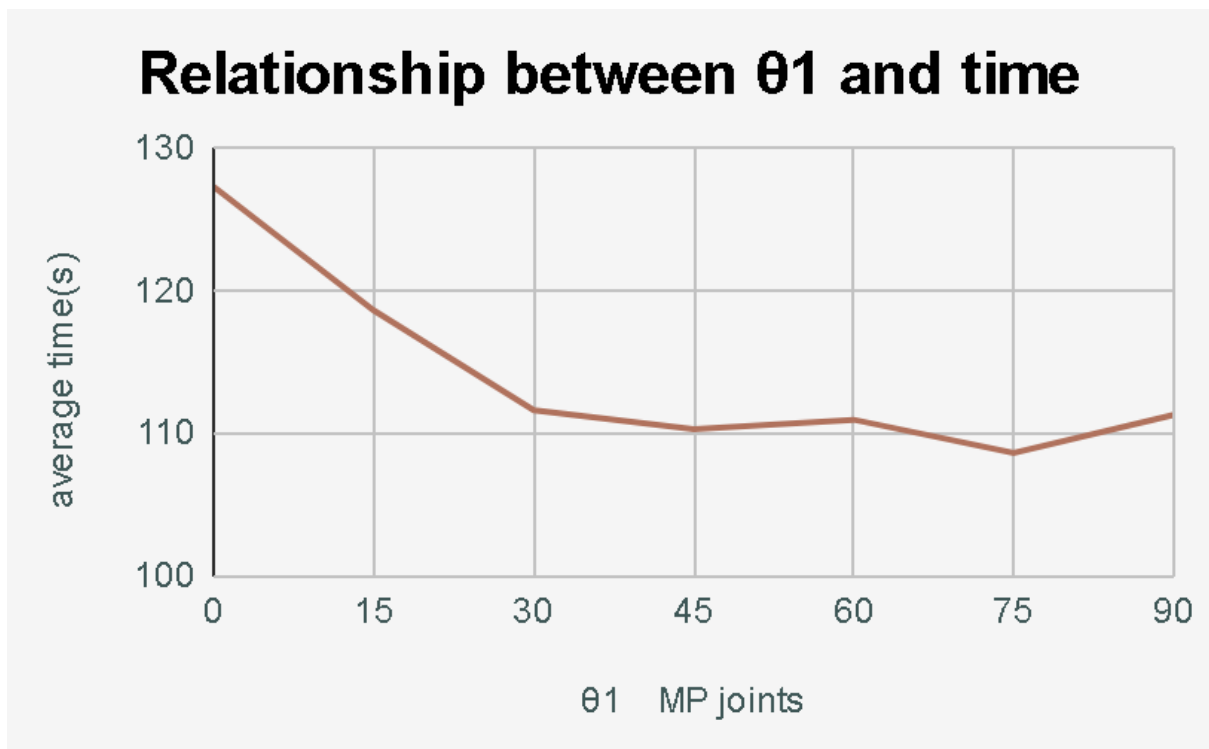


Fig 3.2 All fingers, MP joints

4. Discussion

As seen in Figures 3.1 to 3.4, the angles of the fingers do not significantly affect the speed of the hand movement. There is also no observable relationship between the speed of the hand moving and the angle of the fingers. This finding indicates that hand speed may be determined by factors besides finger articulation.

This can be seen in Figures 5.1 to 5.2, where the entire right upper extremity (that has a fixed position) was built to simulate a more realistic arm-swinging movement. This resulted in greater air resistance to the environment, potentially leading to a more significant reduction in speed. This supports the theory stated above.

5. Conclusion

5.1 Summary

The study investigated how the different hand shapes and finger joint angles affect running speed. The Singapore experiment results suggested that hand shapes and finger joint angles do not affect the running speed, with the fps of the different finger joint angles being at a constant of 30fps.

However, this does not prove that hypotheses H1 and H2 were incorrect. The setup of the Singapore setup is much smaller than the Japan setup. This means that the amount of air resistance in the Singapore setup is much lesser than the air resistance in the Japan setup. This is proven by the Japanese experiment showing that the hand shapes do significantly affect the speed of a runner.

5.2 Practical Applications

This experiment could be used to develop an analysis system on how hand and finger positioning affects the speed and accuracy of throwing a ball, hitting a racket, or swimming. This could be implemented in such systems to train future athletes to handle equipment, throw balls, etc, most efficiently.

This research could also extend to robotics and prosthetics. The research results could contribute to designing more efficient and simpler designs for robotic hands and prosthetic devices. This can help the physically impaired or allow remote control of artificial limbs.

6. References

- Interphalangeal joints of the hand. (n.d.). Physiopedia. Retrieved from [https://www.physio-pedia.com/Interphalangeal_Joints_of_the_Hand]
- Schweitzer, M. E., Mandel, S., Pathria, M. N., & Jacobson, J. A. (2014). High-resolution 3-T MRI of the fingers: Review of anatomy and common tendon and ligament injuries. *American Journal of Roentgenology*, 202(3), 552-562.
- Wu, J. F., Morris, R. P., & Hastings, H. II. (2011). Influence of index finger proximal interphalangeal joint arthrodesis on precision pinch kinematics. *The Journal of Hand Surgery*, 36(10), 1616-1622.
- Beginners aerodynamics. (n.d.). SkyNomad Paragliding School. Retrieved from <https://www.skynomad.com/articles/beginners-aerodynamics.html>
- 比留間 浩介「学校高学年児童における疾走中の腕振り動作の特徴」[Characteristics of arm swing movements during sprinting in upper-grade school children]、体育学研究、Vol.67、pp.79-90、2022
- 前田正登他「スプリント走における腕振りの役割」[The role of arm swing in sprint running]、陸上競技研究、Vol.1、pp.13-19、2010
- 平山修「腕の慣性モーメントと腕振り運動の周期を求めさせる課題」[A task to find the moment of inertia of the arm and the period of arm swing motion]、物理教育、Vol.59、pp.175-180、2011 2018 年度
- 神津慧、中野創洵「物体の形状による抵抗の変化一回転を用いて」[Change in resistance depending on the shape of an object - Using rotation -]、茨城県立竹園高校国際科活動報告書、pp.24-25、2019

Determining the most suitable dam type to instigate anti-phase waves and reduce seawater overtopping at coastal areas

Elavenil Anbarasu¹, Hau Yee Lee¹, Naoto Okazaki², Yuto Tsuji²

¹*School of Science and Technology, Singapore (Singapore)*

²*Tennoji Senior High School Attached to OsakaKyoikuUniversity (Japan)*

Abstract:

Coastal dams are crucial in preventing wave overtopping and mitigating coastal flooding. The three most commonly used coastal dam structures are vertical seawalls, curved seawalls, and riprap dams, each with unique characteristics. Using physical models, past papers have looked into how the overtopping of dam-break structures affects the inundation height behind the structures. Through this research, we used such physical models to understand how different types of dam shapes and textures affect overtopping, such as through constructive and destructive interference. The Japanese team used a blow dryer to create waves in a milk carton box and measured the volume of water overtopped while the Singapore team used a wave-generating tank and measured the maximum vertical displacement of water for 6 different wave frequencies. The Japanese team found that the vertical seawall results in a significantly higher volume of water overtopped than riprap and curved seawall dams. The Singapore team found that the relationship between the wave frequency and the maximum vertical displacement of water was linear for vertical seawalls and exponential for curved and riprap dams. We have concluded that curved seawall and riprap dams are similarly effective in reducing wave overtopping due to the curved shape directing waves downwards and the rocky texture of the riprap dam dispersing wave energy. However, for high-frequency waves, we have found that vertical seawalls are the most effective in reducing overtopping. We hope this research contributes to protecting the people living near coastlines, especially as climate change has exacerbated extreme weather conditions like ice cap melting, which increases sea levels across the globe and causes flooding and soil erosion.

Keywords: Coastal dams; overtopping; wave frequency; maximum amplitude; flooding

1. Introduction

Coastal erosion is an extremely significant problem. For example, in Hemsby, Norfolk in England, the coastal erosion has progressed to such an extent that residents had to be evacuated as the houses were about to collapse into the sea (Chikomba, 2023). Furthermore, although it occurs over long periods of time, it still results in extensive damage, especially to people or industries near the coast. According to (Coastal Erosion | U.S. Climate Resilience Toolkit, n.d.), erosion causes about USD 500 million annually in coastal property losses, damages and loss of land. Hence, coastal dams, such as vertical seawalls, curved seawalls, and ripraps, are crucial in preventing wave overtopping and mitigating coastal flooding, protecting inland areas from soil erosion, which can lead to disasters like landslides.

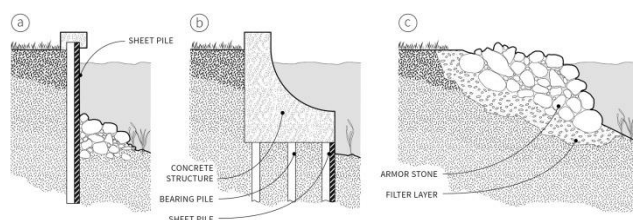


Fig. 1: From left to right: vertical seawall, curved seawall, and riprap dams (Hosseinzadeh, N., 2022)

Vertical seawalls are commonly employed in coastal defence due to their ability to withstand high-energy wave impacts. (Briganti, R., 2022). Curved seawalls are designed to redirect wave energy away from the structure and reduce overtopping. The curvature can help dissipate wave energy more effectively than vertical walls, potentially leading to lower overtopping rates.

Curved seawalls can reduce overtopping, but they may not be as effective as anticipated under certain conditions. (Briganti, R., 2022). Riprap dams, consisting of loose stones or boulders, serve as a flexible coastal defence mechanism. They are particularly effective in dissipating wave energy and reducing overtopping due to its rough surface and ability to absorb impact forces (Nils b., 2016). Studies have also highlighted that riprap can mitigate erosion and provide a more natural coastal appearance, which is increasingly valued in coastal management practices (Comfort, J. A, 1997).

A possible cause of overtopping is the constructive interference of coastal waves. When coastal waves hit the dam, the reflected wave may be in-phase with the coastal waves, causing the waves to be amplified and seawater to overtop the dams. The opposite is true for destructive interference. The coastal dams' shape and design largely influences the reflected wave's angle.

Research hypothesis: Curved seawall dams are the most effective in reducing the amount of seawater overtopping, followed by riprap dams and vertical seawall dams.

2. Methodology

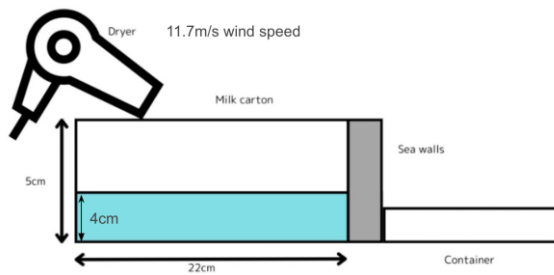


Fig. 2a: Experimental setup (Japan team), side view (not drawn to scale)

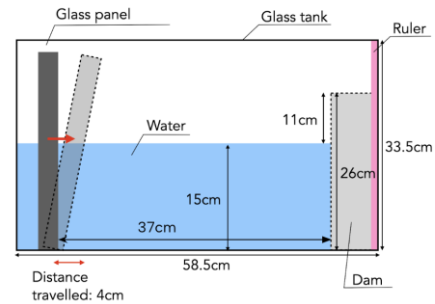


Fig. 2b: Experimental setup (Singapore team), side view (not drawn to scale)

3a. Results (Japan team)

Table 3. Volume of water overtopped for the 3 dam types

No. of experiments	Volume of water overtopped (ml)		
	Vertical seawall	Curved seawall	Riprap dam
1	2.03	0.01	0.38
2	2.62	0.11	0.15
3	2.20	0.00	0.41

3b. Results (Singapore team)

Table 4. Maximum vertical displacement of water for the 3 dam types across 6b different wave frequencies

Maximum vertical displacement of water (cm)				
Period of the wave, T (s)	Frequency of wave, f (Hz)	Vertical seawall	Curved seawall	Riprap dam
3.19	0.313	0.0	0.0	0.0
2.58	0.388	0.1	0.0	0.1
1.54	0.650	0.2	0.4	0.1
1.29	0.775	1.6	0.6	0.8
0.86	1.16	3.5	0.9	1.1
0.80	1.25	5.0	7.6	9.0

* $f = 1/T$

4a. Discussion (Japan team)

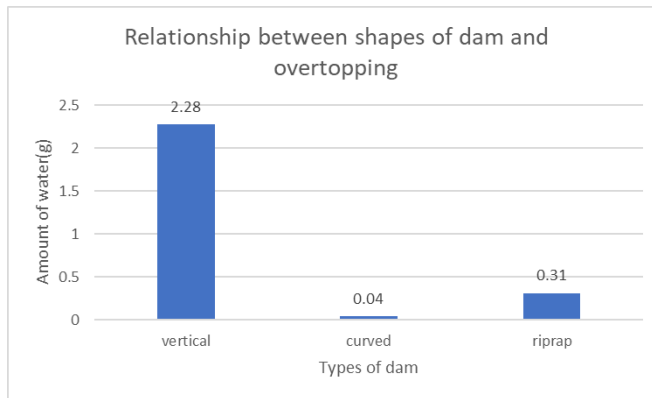


Fig. 5: Bar graphs of the amount of water collected for the three different dam types

From the graph, vertical seawall has the highest amount of overtopping. The amount of overtopped water for vertical seawater is significantly higher than that of the other dams, 57 times that of the curved seawall and 7.35 times that of the riprap dam. This corresponds with our hypothesis that the vertical seawall would be the least effective in reducing overtopping. Hence, suggesting that vertical seawall dams indeed are not effective in absorbing wave impact, causing constructive interference.

The riprap dam is the second most effective among the three different types of dams tested. This supports the hypothesis that the riprap dam would effectively reduce wave impact by reflecting the wave in many directions, causing turbulence. Additionally, the riprap dam is less effective than the curved seawall, with 7.75 times more overtopping than the curved seawall, indicating that the scattering of the wave impact in different directions due to the rough surface of the riprap dam is not as effective in reducing overtopping as the curved shape as the curved seawall in redirecting the wave energy downwards. However, compared with the vertical seawall, it is clear that riprap dams have better functionality in reducing wave amplitudes.

The curved seawall is the most effective among the three different types of dams tested, with 0.27g of water overtopped, thus supporting the hypothesis, suggesting that the curved shape of the dam indeed causes the wave to be reflected downwards, away from the top of the dam and reducing overtopping. This also may be due to the curved shape's ability to absorb wave impact as the water travels along the curved surface, reducing wave energy and overtopping. Furthermore, the protruding top section of the curved seawall blocks water from overtopping, proving the effectiveness of the curved seawall among the three dam types. The results for the three experiments were also consistent, indicating reliability.

4b. Discussion (Singapore team)

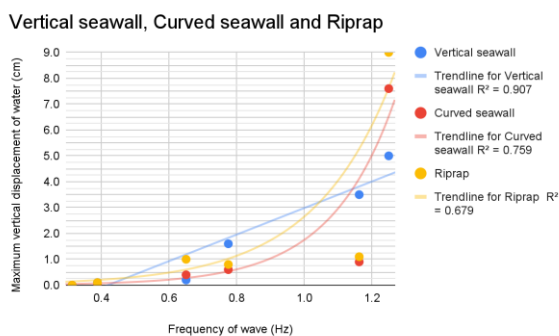


Fig. 6a: Graphs of the maximum vertical displacement of water against the frequency of wave with trend line

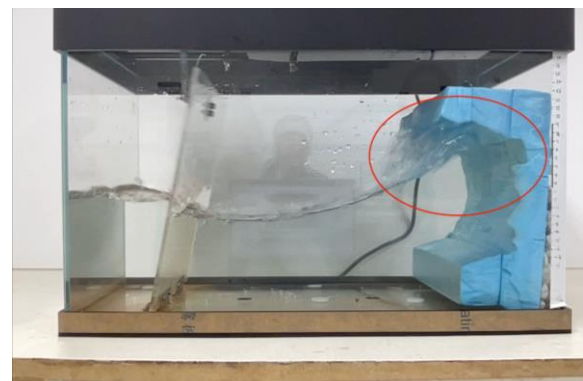


Fig. 6b: Side view of the tank for frequency 1.25Hz for curved seawall

From the data collected, vertical seawall seems to be the most consistent as the relationship between the maximum vertical displacement of water and the frequency of the wave, which is related to the speed of the glass panel motor, is linear, with an R^2 value of 0.907. This may be due to the vertical seawall not reflecting much wave impact, reducing the creation of in-phase waves that cause constructive interference. Therefore, the wave amplitude stays approximately the same due to the little constructive interference produced, suggesting that the vertical seawall absorbs wave impact more than it reflects wave impact.

For both the curved seawall and riprap dams, the trend is exponential, with an R^2 value of 0.759 and 0.679, respectively, showing that the trend fits an exponential trend line very well. The maximum vertical displacement of water stays relatively low until the wave frequency reaches 1.25 Hz, where the vertical displacement of water abruptly jumps to 8.4 and 8.1 times for curved seawall and riprap dams, respectively. For the curved seawall, at the highest wave frequency, the wave breaks, as shown in Fig. 6b. The water cannot reach a higher height because of the protruding curved shape directing the flow of the water downwards, showcasing the effectiveness of the curved seawall dam in stopping the overtopping of water. For the riprap dam, the significant increase in vertical displacement of water may be due to the dam reflecting the wave upwards. The wave impact may not have been dissipated enough by the rocks and the remaining wave energy would have been reflected upwards by the general shape of the dam. This may indicate a limit to the amount of energy the rocks can dissipate.

From the results obtained above, our hypothesis that the vertical seawall dam would be the least effective in reducing the amount of wave overtopping was proven wrong to a certain extent for high frequency waves. For the highest frequency of waves we tested, the vertical seawall was the most effective, followed by riprap dams and curved seawall dams. However, for lower wave frequencies, such as that of frequencies 0.775 Hz and 1.16 Hz the vertical seawall is the least effective, while riprap dams and curved seawall dams have similar effectiveness, with riprap being slightly less effective than curved seawall dams. This aligns with our hypothesis, hence indicating that our prediction may be true for waves of a lower frequency.

5. Conclusion

In conclusion, riprap and curved seawall dams effectively reduce wave overtopping, with both dam types showing very similar results, while vertical seawall dams may not be as effective. Although the Japan and Singapore teams' experiments were conducted in very different manners, both teams' experiments showed similar results, further reaffirming this conclusion. The outlier is the high-frequency wave causing a drastic change in results, as mentioned in section 4b, indicating that when the wave energy is high, vertical seawalls may be a better choice. However, for low-frequency waves that coastal areas would typically encounter, riprap and curved seawall dams are still the more effective options. For example, a hybrid of both curved and riprap dams can combine the benefits of both a curved surface and a rough texture, increasing the effectiveness of the dams. This can be applied to flood-prone areas, such as low-lying communities living near coastal areas or those prone to coastal erosion, to help improve public safety and reduce losses.

Through this research, we have contributed information on the relationship between the different dam shapes and designs in mitigating wave overtopping with varying wave frequencies, contributing to the development of better dam designs that can withstand the more volatile tidal conditions that climate change brings about globally. Therefore, this knowledge also contributes to the UN Sustainable Development Goal 13: Climate Action, by providing insights into effective coastal defence strategies and allowing us to build resilience to flooding and coastal erosion.

Further investigation into various dam types can be done, including different designs of riprap dams and our own dam model ideas incorporating various design and engineering factors. Furthermore, we can study more about how the gaps and surfaces of these structures can allow for aquatic ecosystems, such as crustaceans like barnacles to thrive, such as that of semi-permeable dams. Lastly, further study into how the different wave frequencies can impact the wave overtopping of the various dam types and its relation to high and low tides at different times of the day can be done.

6. References

1. Briganti, R., Musumeci, R. E., Van der Meer, J., Romano, A., Stancanelli, L. M., Kudella, M., ... & Schimmels, S. (2022). Wave overtopping at near-vertical seawalls: Influence of foreshore evolution during storms. *Ocean Engineering*, 261, 112024.
2. Chikomba, T. (2023, July). Coastal erosion causing homes in England to slide into the sea. GB News. <https://www.gbnews.com/news/coastal-erosion-homes-sea-norfolk>
3. Coastal erosion | U.S. Climate Resilience Toolkit. (n.d.). <https://toolkit.climate.gov/topics/coastal-flood-risk/coastal-erosion>
4. Comfort, J. A., & Single, M. B. (1997). Literature review on the effects of seawalls on beaches. Department of Conservation.
5. Hosseinzadeh, N., Ghiasian, M., Andiroglu, E., Lamere, J., Rhode-Barbarigos, L., Sobczak, J., ... & Suraneni, P. (2022). Concrete seawalls: A review of load considerations, ecological performance, durability, and recent innovations. *Ecological engineering*, 178, 106573.
6. SCHLURMANN, T., & KERPEN, N. B. (2016, May 13). STEPPED REVETMENTS – REVISITED. Proceedings of the 6th International Conference on the Application of Physical Modelling in Coastal and Port Engineering and Science (Coastlab16). https://www.lufi.uni-hannover.de/fileadmin/lufi/publications/Paper_CoastLab16_Kerpen_incl_Review.pdf
7. Esteban, M., Glasbergen, T., Takabatake, T., Hofland, B., Nishizaki, S., Nishida, Y., ... & Shibayama, T. (2017). Overtopping of coastal structures by tsunami waves. *Geosciences*, 7(4), 121.

7. Bibliography

1. Coastal protection. (n.d.). <https://www.nccs.gov.sg/singapores-climate-action/coastal-protection/>
2. Ghiasian, Mohammad & Andiroglu, Esber & Lamere, Joel & Rhode-Barbarigos, Landolf & Sobczak, James & Sealey, Kathleen & Suraneni, Prannoy. (2021). Concrete Seawalls: Load Considerations, Ecological Performance, Durability, and Recent Innovations. 10.31224/osf.io/h6zt8.
3. THE 17 GOALS | Sustainable Development. (n.d.). <https://sdgs.un.org/goals>

Scientific Analysis of The Taste and Texture of Rice

Uta Inoko¹, Nanako Imazato¹, Tian-Sin Chen², Yu-chi Chen²

¹*Ritsumeikan Junior and Senior High School (Japan)*

²*Kaohsiung Municipal Kaohsiung Girls' Senior High School (Taiwan)*

Abstract:

The inspiration for this research stems from the researchers wanting to discover the difference between Japanese rice and Taiwanese rice even though both of them are Japonica rice. This research focused on perceptions of the human senses to scientifically evaluate the taste and the texture experienced when eating either Japanese or Taiwanese rice. In addition, the grain size, water absorption, hardness were measured and general evaluations were made for each rice. Through this research, it was hoped that the factors that most affect taste can be determined in order to help improve various varieties of rice to become more tasteful.

Keywords: *Oryza sativa*; Hitomebore, Akitakomachi, Milky Queen; Huadong Yu Xiang, Huadong, Huadong Niunai Qingxiang, Chemical Assay

1. Introduction

We wanted to take advantage of having collaborative research in both Japan and Taiwan, so we decided to focus on the staple food of rice for both countries. One of the Japanese members has been to Taiwan many times. We thought there were differences between Japanese rice and Taiwanese rice. One of the differences observed is the size of the rice. We thought that Taiwanese rice is longer than Japanese rice. And another difference is the food texture. We felt that Japanese rice contains more moisture than Taiwanese rice. The food texture is related to the protein content. Those with less protein content have a softer texture. Because of that, we thought Japanese rice has more protein than Taiwanese rice.

2. Methodology

Size (Length) Measurement:

1. Raw rice, cooked rice and a vernier scale were prepared.
2. Each kind of rice was measured with a vernier scale ten times.
3. The averages were found for each rice. (accurate to two decimal places).

Hardness Experiment:

1. Raw rice, a ruler and weights of 50 g, 100 g, 250 g were prepared.
2. The weight was placed 8 cm above the ground.
3. The weight was dropped on the grain of rice repeatedly until it cracked.
4. The grain of rice was changed every time we smashed it .
5. The experiment was repeated three times for each result.

Starch Experiment (whole rice):

1. Cooked rice, a dropping pipette, and iodine solution were prepared
2. Iodine solution was pipetted onto each type of rice
3. The changes in the rice were observed

Cooking rice for tasting test:

1. 150 g of rice was measured out and placed in the container
2. The rice was rinsed in a microwave cooker three times.
3. 240 ml of water was added to the drained rice and it was soaked with the lid on for at least 30 minutes.
4. The rice was then heated in a microwave oven with the lid on for 7 minutes and 30 seconds at 600 watts.
5. It was covered and steamed for 10 minutes.
6. The rice was then mixed.
7. It was covered again and steamed for 10 minutes
8. The finished rice was then evaluated.

Tasting Test

1. Volunteers were asked to eat cooked rice.
2. Volunteers judged the cooked rice in three categories (texture, smell, and taste) and scored

them from 1 to 5 (1 is bad, 5 is good).

Water absorption

1. 50 ml of water was put into a 50 ml beaker.
2. The weight of 50 grains of each kind of rice was measured.
3. The 50 grains of rice were placed in a beaker.
4. The rice was kept in water and soaked for 30 minutes.
5. After 30 minutes passed, the 50 grains of rice were placed on filter paper, and left for 5 minutes.
6. The 50 grains of rice were measured and compared.
7. The above process was repeated 3 times for each type of rice each and averages were calculated.

Soluble starch

1. The rice was ground using a mill.
2. The ground rice was passed through a large mesh sieve, followed by a fine sieve.
3. Took 2 g and was removed from the resulting solution.
4. 50 ml of water was added.
5. The solution was then heated with a gas burner and boiled for two minutes.
6. After taking the solution off the heat, 1 ml was taken from the solution.
7. 50 μ l of iodine solution was added to the 1 ml.
8. Photos were taken and color differences were observed.

3.Results

Size (Length) Measurement:

As per the data of table 1, there are no big differences between Taiwanese rice and Japanese rice (raw), but overall Taiwanese rice is larger than Japanese rice. The difference between the maximum value of each rice was 0.184 (4.914-4.730 = 0.184), and the minimum value of each rice was 0.275 (4.705-4.430=0.275).

Table 1. Average size of different rice (Raw rice)

Rice	Huadong Yu Xiang	Huadong	Huadong Niunai Qinggxiang	Hitomebore	Milky Queen	Akitakom achi
Length (average)	4.886	4.705	4.914	4.720	4.430	4.600 (mm)

Table 2. Average size of different rice (Cooked rice)

Rice	Huadong Yu Xiang	Huadong	Huadong Niunai Qinggxiang	Hitomebore	Milky Queen	Akitakom achi
Length (average)	—	—	—	6.430	6.130	7.090 (mm)

Hardness Experiment:

According to the data, two kinds of Japanese rice (Hitomebore and Milky Queen) cracked when a 100 g weight was dropped from a height of 8 cm. Assuming the contact distance between the weight and the rice during impact is 1 centimeter, and using the free-fall formula and kinetic energy formula, it is estimated that these two types of rice can withstand a force of approximately 7.8125 Newtons. For Akitakomachi it is estimated that it can withstand a force of approximately 11.72 Newtons.

*Free fall formula $V=\sqrt{2gh}$, Kinetic energy formula $KE=\frac{1}{2}mv^2$

Table 3. Result of hardness experiment (O:cracked X:not cracked)						
Weight\Rice	Huadong Yu Xiang	Huadong	Huadong Niunai Qinggxiang	Hitomebore	Milky Queen	Akitakomachi
50 g	—	—	—	X	X	X
100 g	—	—	—	O	O	X
150 g	—	—	—	—	—	O

Starch Experiment (whole rice):

No differences between the various types of rice could be determined, as each kind of rice reacted with the iodine solution.



Figure 1. Hitomebore

Figure 2. Akitakomachi.

Figure 3. Milky Queen

Tasting Test:

The same microwave was used to cook each kind of rice in an attempt to reduce variance. However, this actually resulted in issues cooking the rice because the ambient temperature inside the microwave increased as each type of rice was cooked, affecting the internal heat sensor, which resulted in Hitomebore and Huadong Niunai Qinggxiang being undercooked. So the other 4 other types of rice were used to formulate general opinions.

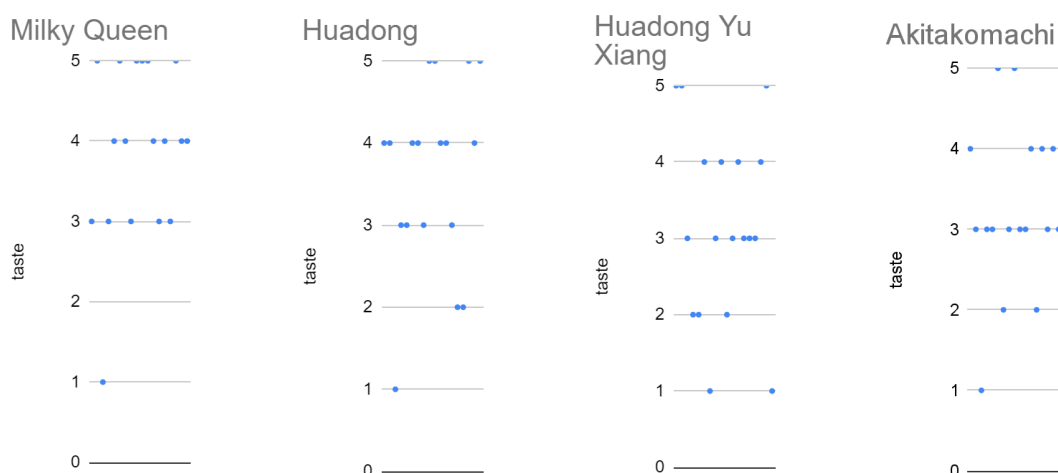


Fig.4 Result chart of taste

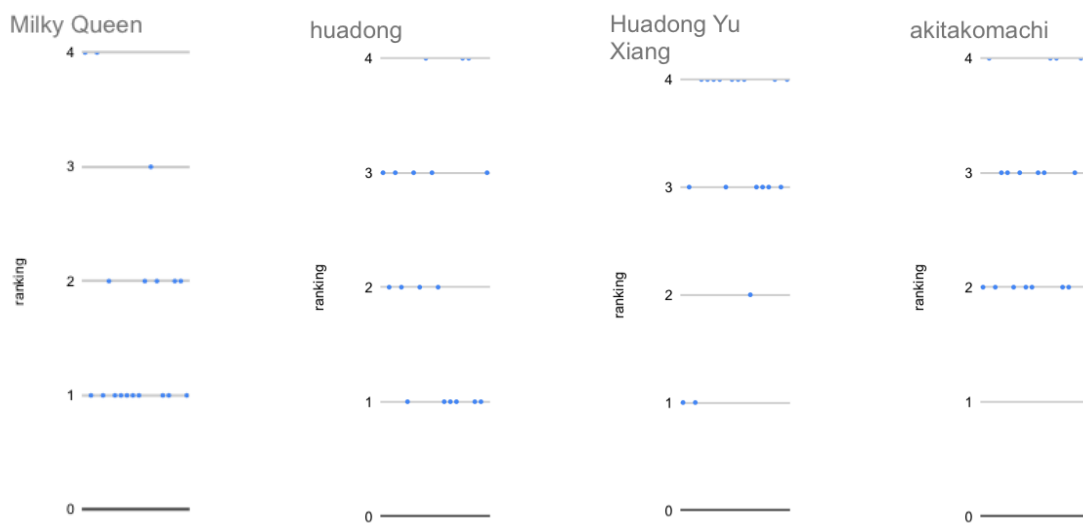


Fig.5 Result chart of ranking

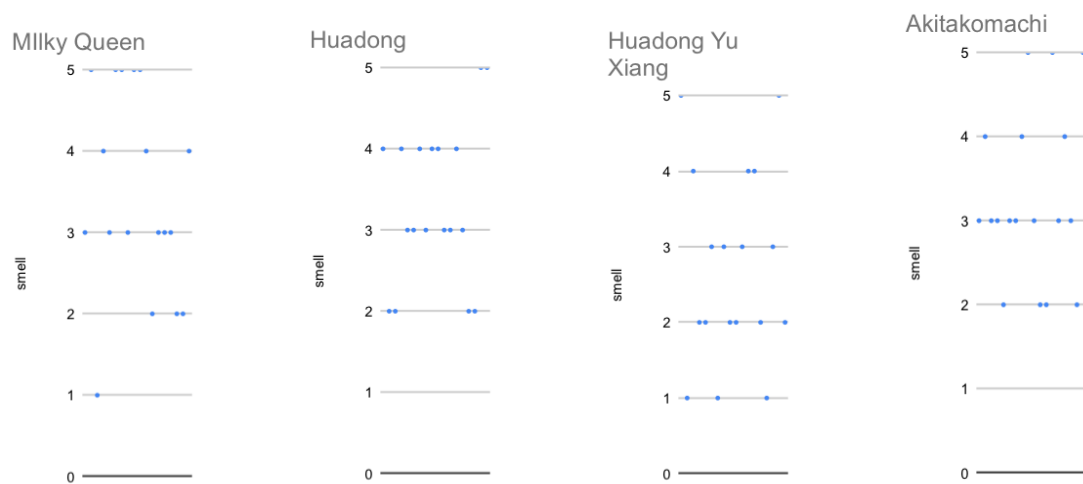


Fig.6 Result chart of smell

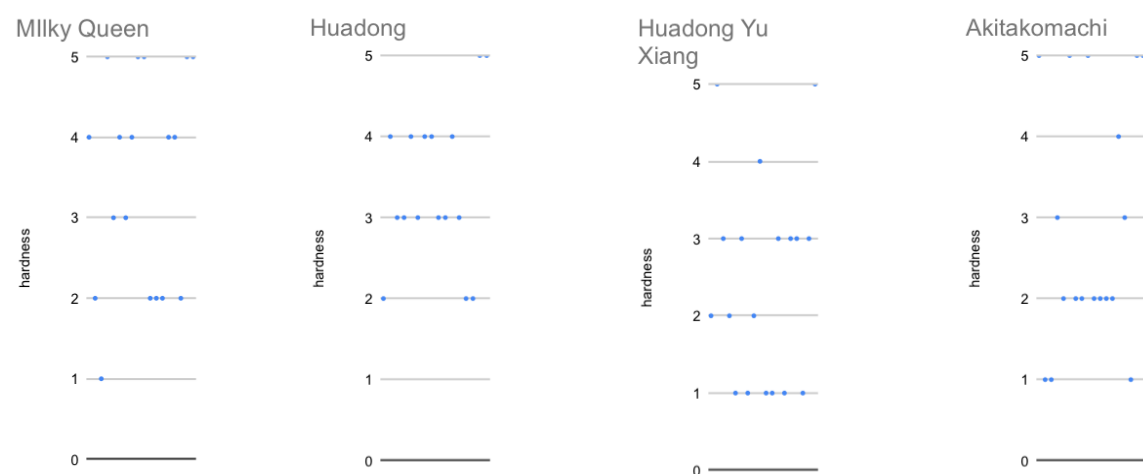


Fig.7 Result chart of hardness

Water absorption:

The water absorption experiment was repeated three times, but the first experiment did not work. The results were different by about 1 g compared to the other two experiments. Therefore, the values from the first experiment were treated as outliers.

Table 4 Result of water absorption experiment

various of Rice	Huadong Yu Xiang	Huadong	Huadong Niunai Qingxiang	Hitomebore	Milky Queen	Akitakoma chi
before (g)	0.980	0.985	0.983	1.004	0.916	0.981
after (g)	1.253	1.252	1.246	1.280	1.192	1.271
difference (g)	0.274	0.267	0.263	0.277	0.276	0.290

Soluble starch:

Experiments were conducted with six different types of rice, each of which produced different colors. Milled rice grains, homogenised (Fig.8).

In the iodine-starch reaction, amylose produces a bluish color and amylopectin a reddish color.

This makes it possible to determine whether there is more amylose or amylopectin. Milky queen produced a reddish color, indicating high amylopectin content. Rice with high amylopectin content is more sticky. When participants actually tasted it, many of them said that Milky queen was sticky. Contrary to popular belief that Huadong rice was dry. Experimental results indicated that the iodine-starch reaction produced a bluish color. This suggests that Huadong rice has a high amylose content, which is closely associated with its texture and amylose concentration (Fig.9).

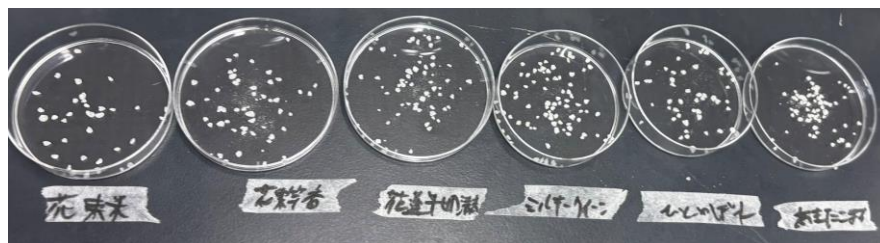


Fig.8: Rice crushed into 1/3

From left to right Huadong, Huadong yu xiang,

Hualing niunai qingxiang, Milky queen, Hitomebore, Akitakomachi.

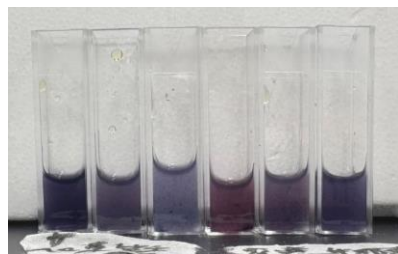


Fig.9: Results of iodine reaction of extracted soluble starch

From left to right Huadong, Huadong yu xiang, Hualing niunai qingxiang, Milky queen, Hitomebore, Akitakomachi.

4. Discussion

Size Measurements:

After analyzing the data, it was found that the sizes of those kinds of rice are almost the same. After researching Japanese and Taiwanese history it was discovered that the Japanese brought rice to Taiwan during the 1900s. It is hypothesized that the size of the rice could not change much in 100 years. As a

result, the size of rice from these two places is almost the same.

Hardness Experiment:

Hitomebore and Milky Queen cracked with about 80 joules. Akitakomachi cracked with about 120 joules. Weights can also be dropped from a height of 8 cm to measure how much energy is required to crack each kind of rice.

The amylose in the rice

This experiment cannot be done just by using iodine solution because this solution can only be used to test if there is amylose in the rice. Therefore, Benedict's reagent was used with amylase to test the glucose to determine the amount of amylose in the rice. However, the same result for the colors of Benedict's reagent was acquired, so it was not possible to analyze them. But we learned that we can not just use these simple solutions to test the amount of the rice.

Tasting Test

If there was not a clear trend for participants to either love or hate the taste (opinions in both directions, or a mixture of positive and negative), then there was also no clear relationship between the smell and hardness (Huadong Yu Xiang). However, if there was a clear trend for participants to either love or hate the taste (a majority had a positive or negative opinion) a relationship between the smell and taste could be found.

There was also a clear relationship between taste and ranking. The decentralization was similar, so we can say the taste of general opinion is directly connected to its ranking. Through these results, we can say it is important to determine a relationship between taste and other factors.

For this research, the participants were Japanese students. So their preference may lean toward Japanese rice.

Water absorption

From the results, it was found that Japanese rice, especially Akitakomachi, absorbs more water than Taiwanese rice. The result is connected with the Hardness Experiment. The two other Japanese rice were cracked with 80 joules, but Akitakomachi was cracked with 120 joules. Thus, it is concluded that greater water absorption leads to a more hard construction of rice.

Soluble starch

Rice that exhibited a bluish colour was generally perceived as dry, whereas rice displaying a reddish colour was rated as glutinous. These findings suggest a strong correlation between the relative amounts of amylose and amylopectin and the textural properties of rice.

5. Conclusion

In this research, we found that rice has a relationship with amylose and amylopectin. We assumed that Japanese rice is more sticky than Taiwanese rice.

Even though we did not make a question of elasticity in the questionnaire, many took note that Japanese rice (Milky Queen and Akitakomachi) were more glutinous. Additionally, in the water absorption experiment, it was found that Japanese rice absorbs more water compared to Taiwanese rice. Thus, the elasticity could be related to water absorption.

In soluble starch experiments, Japanese rice (Akitakomachi, Hitomebore, Milky queen) tended to be higher in amylopectin and Taiwanese rice (Huadong, Huadong yu xiang, Hualing niunai gingxiang) tended to be higher in amylose.

We found that many kinds of rice have some similar properties, such as size and water absorption. Different properties of rice, such as hardness, depend on the place.

6. References

Lu, Shaoli. (2023, March 1). Starting with Changes in Daily Habits: NTU's Lu Shaoli Explains How the Japanese Government Used "Rice" and "Time" to Colonially Control Taiwan. Humanities·Island. https://humanityisland.nccu.edu.tw/Lushaoli_a/

flourfwps. (2011, February 28). 272 Properties of Starch - Amylose and Amylopectin Kinoshita Flour Milling Company. <https://www.flour.co.jp/news/article/272/>

Pumping Straw

Yu-Shan Huang¹, You-I Yang¹, Miku Kamagata², Shin Miyano²

¹*Kaohsiung Municipal Kaohsiung Girls' Senior High School (Taiwan)*

²*Seishingakuen High School (Japan)*

Abstract:

The research used some physical evidence to explain the phenomenon of water spreads while the straw rotates and try to find out how to make the water spread farthest and using the experiment result to prove that the theory we use is correct.

We changed the diameters of the straw, the side length of the straw and the material of the straw. And turns out that if the side length of the straw and the diameters of the straw get longer, the water will spread farther. And we can use this result to make some applications like agricultural sprinklers.

Keywords: 1. Water 2. Straw 3. Centrifugal Force

1 Introduction

1.1 Phenomenon

Fill a bowl with water, take a triangular straw with three holes on the vertexes and partially submerge one of the openings in the water. Rotate the system, and observe as water spreads out of the other two holes in the air.

1.2 Theory

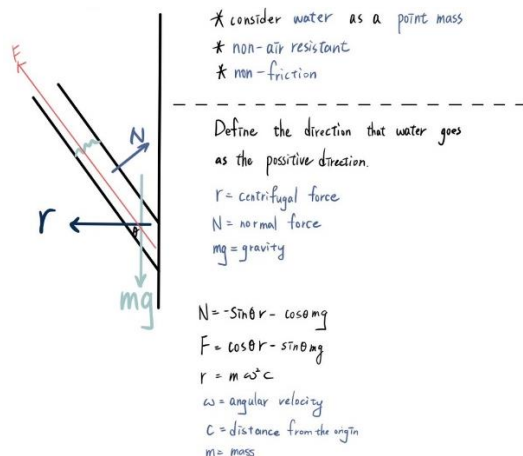


Figure 1: The theory used in the experiments

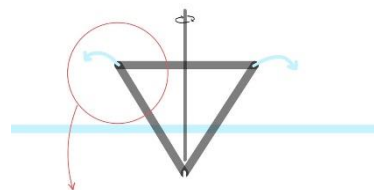


Figure 2: The schematic of the experiments

1.3 Purpose

1.3.1 Discuss the influence of the side length on the range of water spreading

1.3.2 Discuss the influence of the diameter of the straw on the range of water spreading

1.3.3 Discuss the influence of the depth of the straw submerges in the water on the range of water spreading

1.4 Variables

1.4.1 The side length

1.4.2 the diameter of the straw

1.4.3 the depth of the straw

1.5 Equipment



Figure 3: The equipment used in the experiments

1.6 Experiment setup

1.6.1 Make the straws into equilateral triangles

1.6.2 Connect the straw to the drill

1.6.3 Make the straws vertical to the water surface and enter the water

2 Methodology

2.1 Experiment 1

2.1.1 Purpose: Discuss the impact of the side length on the distance water spreads

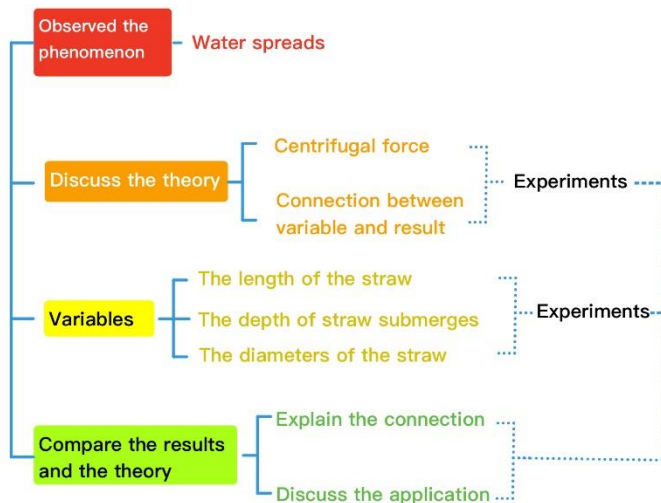


Figure 4: The structure of the whole research

2.1.2 Control Variables

- 2.1.2.1 The angle of the triangular straws: 60°
- 2.1.2.2 The material of the straws: Plastic
- 2.1.2.3 The depth of the straw submerges in the water: 2 cm
- 2.1.2.4 The rotational speed of the drill: 10.3 RPM
- 2.1.2.5 The diameter of the straw: $2r = 0.5\text{cm}$

2.1.3 Independent Variable

- 2.1.3.1 The side length of the triangular straw

2.1.4 Dependent Variable

- 2.1.4.1 The distance that water spreads

2.2 Experiment 2

- 2.2.1 Purpose: Discuss the influence of the diameter of the straw on the range of water spreading

2.2.2 Control Variables

- 2.2.2.1 The angle of the triangular straws: 60°
- 2.2.2.2 The material of the straws: Plastic
- 2.2.2.3 The depth of the straw submerges in the water: 2 cm
- 2.2.2.4 The rotational speed of the drill: 10.3 RPM
- 2.2.2.5 The side length of the triangular straw: 4 cm

2.2.3 Independent Variable

- 2.2.3.1 The diameter of the straw

2.2.4 Dependent Variable

- 2.2.4.1 The distance that water spreads

2.3 Experiment 3

- 2.3.1 Purpose: Discuss the influence of the depth of the straw submerges in the water on the range of water spreading

2.3.2 Control Variables

- 2.3.2.1 The angle of the triangular straws: 60°
- 2.3.2.2 The material of the straws: Plastic
- 2.3.2.3 The rotational speed of the drill: 10.3 RPM
- 2.3.2.4 The side length of the triangular straw: 4 cm
- 2.3.2.5 The diameter of the straw: $2r = 0.5\text{cm}$

2.3.3 Independent Variable

- 2.3.3.1 The depth of the straw submerges in the water

2.3.4 Dependent Variable

- 2.3.4.1 The distance that water spreads

3 Results

3.1 Experiment 1

Table 1: The results of changing the side length

Straw Length	Number of Times	1st	2nd	3rd	4th	5th	6th	7th	Avg.
	Distance of Water Spreading								
3 (cm)		31 (cm)	31 (cm)	32 (cm)	33 (cm)	32 (cm)	34 (cm)	32 (cm)	32 (cm)
4 (cm)		50 (cm)	56 (cm)	53 (cm)	56 (cm)	49 (cm)	52 (cm)	52 (cm)	53 (cm)
5 (cm)		67 (cm)	68 (cm)	67 (cm)	63 (cm)	71 (cm)	69 (cm)	70 (cm)	68 (cm)
6 (cm)		100 (cm)	101 (cm)	98 (cm)	97 (cm)	103 (cm)	101 (cm)	101 (cm)	100 (cm)

3.2 Experiment 2

Table 2: The results of changing the diameter

Straw diameters(2r)	Number of Times	1st	2nd	3rd	4th	5th	6th	7th	Avg.
	Distance of Water Spreading								
0.5 (cm)		50 (cm)	56 (cm)	49 (cm)	52 (cm)	52 (cm)	53 (cm)	56 (cm)	53 (cm)
1 (cm)		60 (cm)	67 (cm)	69 (cm)	58 (cm)	70 (cm)	68 (cm)	66 (cm)	65 (cm)

3.3 Experiment 3

Table 3: The results of changing the The depth submerges in the water

The depth submerges in the water	Number of Times	1st	2nd	3rd	4th	5th	6th	7th	Avg.
	Distance of Water Spreading								
0.5 (cm)		43 (cm)	45 (cm)	40 (cm)	47 (cm)	43 (cm)	46 (cm)	39 (cm)	43 (cm)
1 (cm)		50 (cm)	56 (cm)	53 (cm)	56 (cm)	49 (cm)	52 (cm)	52 (cm)	53 (cm)
2 (cm)		57 (cm)	62 (cm)	66 (cm)	55 (cm)	61 (cm)	58 (cm)	59 (cm)	60 (cm)

4 Discussion

4.1 Experiment 1

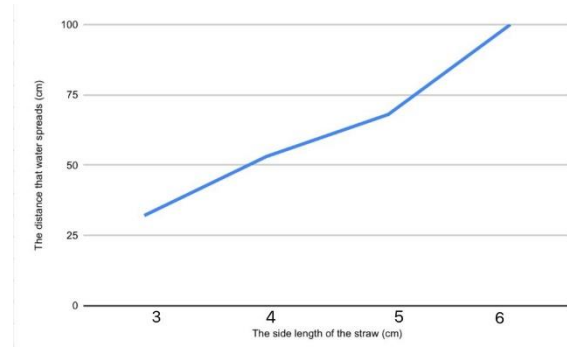


Figure 5: The influence of the side length on the range of water spreading

Through this chart, we can find out that the longer the length of the straw is, the farther water spreads. Thus, the result matches our theory.

4.2 Experiment 2

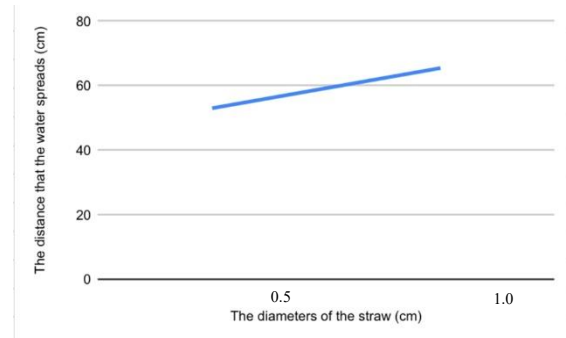


Figure 6: The influence of the diameter on the range of water spreading

In this chart, we can find out that the longer the diameters of the straw are, the farther water spreads. We consider it is caused by the bigger diameter can load more water and that would decrease the friction parameter.

4.3 Experiment 3

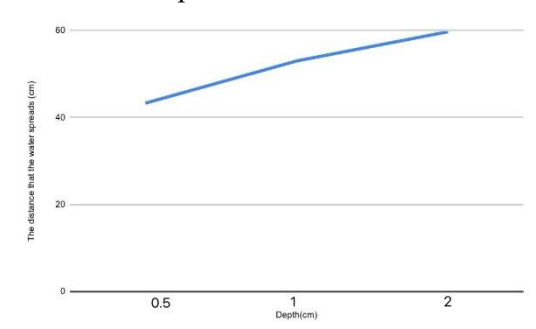


Figure 7: The influence of the depth on the range of water spreading

Through this chart, we can find out that the deeper the straw is submerged, the farther water spreads. We think that it's because if the straw submerges deeper, the water would be closer to the vertex, and it would waste less energy.

5 Conclusion

5.1 Experiment 1

When the side length of the straw **increased**, the distance that the water can spread will also **increase**.

5.2 Experiment 2

When the diameters of the straw **increased**, the distance that the water can spread will also **increase**.

5.3 Experiment 3

When the depth of the straw submerges in the water **increased**, the distance that the water can spread will also **increase**.

6 References

6.1 Pressure (2024, 5 1). Wikipedia . <https://zh.m.wikipedia.org/zh-tw/%E5%8E%8B%E5%BC%BA>

6.2 Centrifugal force (2024, 5 4). Wikipedia . <https://zh.wikipedia.org/zh-tw/%E9%9B%A2%E5%BF%83%E5%8A%9B>

Learning behavior of fruit flies (*Drosophila melanogaster*)

Kazuki Shoho¹, Tomonosuke Oe¹, Yurika Matsumoto¹, Chang Yu Han², Huang You Ruel², Huang Ching En², Kao Chi Hsiang²

¹Hatsushiba Ritsumeikan Junior and Senior High School (Japan)

²Kaohsiung Municipal Kaohsiung Senior High School (Taiwan)

Abstract:

Learning is an essential process for every organism, knowing how much and what organism could learn is also important. In our research, we aim to investigate whether the fruit fly *Drosophila melanogaster* shows learning behavior under specific conditions. First, each one of them was placed in a box with Red, Green, Blue and Yellow papers. The time they spent on each color was recorded to understand their preference. Yellow is the most preferred, while green is the least. Second, they were trained to like green, by which we hope to know their learning ability. They are found to be trainable. In the last experiment, caffeine(50, 100, 250, 500ppm) was added into the food to understand whether caffeine would influence their learning behavior. Caffeine was found to cause fruit flies to show different learning outcome.

Keywords: fruit fly; learning behavior; color preference; caffeine

1. Introduction

Learning behavior is a very interesting topic for us as high school students. *Drosophila melanogaster* is a common model organism for many animal researches. They are easy to rear, highly reproductive, provide abundant samples for experiments, and are simple to observe.(fig.1) We hope to make observations of this species and make inference from our research for vertebrates. Besides, caffeine effect on learning of *Drosophila* also interests us because there is always a debate that young people should not consume coffee, which a very aromatic and delicious drink for adults. This research aims to test 3 hypotheses: (1)Fruit flies show color preferences. (2)Fruit flies are capable of learning. (3)Caffeine makes fruit flies learn better.

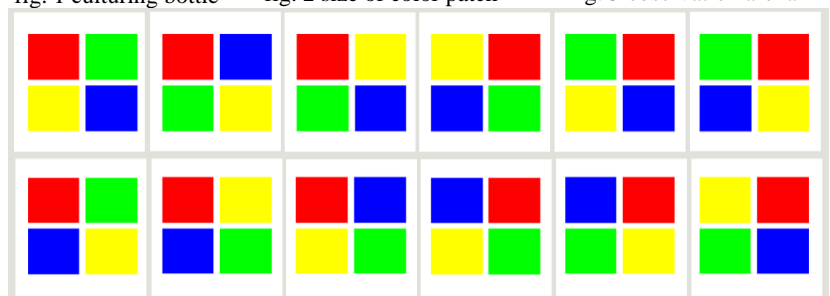
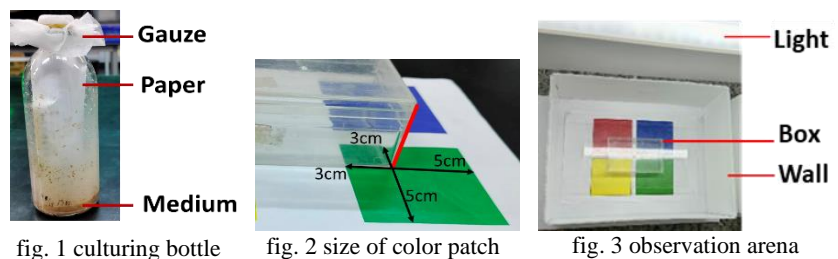


fig. 4 orientation of color patches for each trial

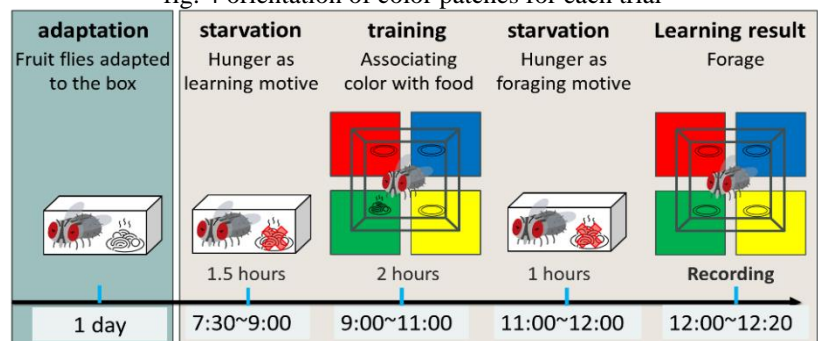


fig. 5 experiment procedure of learning behavior experiment

2. Methodology

2-1 *Drosophila* rearing

Drosophila melanogaster were cultured under a 9-hour light/15-hour dark cycle at 25–27°C. The cultivating medium consisted of 8g of sugar, 15g of water, 15g of yeast extract, 3g of barley, and 15g of vinegar. Ten pairs of 3~5-day-old adults were used as parents for reproduction. The flightless variant of *Drosophila* was chosen for this research because they cannot fly away. It is easier for manipulation and continual trainings.(fig.1)

2-2 Experiment setup

2-2.1 Color preference

In the observation arena, we set up walls to avoid interference from surrounding area. Also, LED lights were placed beneath the boxes to control the light source.(fig.3) Colored patches were set up to understand its preference on 4 colors - red, green, blue, and yellow. Yellow is the color commonly adopted for fly traps, while red, green, and blue are components colors. There are 12 combinations of orientation of these 4 colors. 24 flies were used for each set of experiments. (fig.4) Each fly was isolated and provided with food, the same recipe as the cultivating medium, in a single observation box for adaptation for 1 day. For recording, color patches were placed underneath the box and flies' choices were filmed for 20 minutes. The time flies spent on each color was recorded to understand which color was preferred.

2-2.2 Learning behavior observation

The learning behavior experiment consists of two parts. The first part is adaptation, where fruit flies are allowed to adapt to the experimental box(observation arena), and food is provided. In the second part, flies were trained to associate food with specific colors. The training phase consisted of 3 stages: 1.Fruit flies are starved to motivate learning(1.5 hr.). 2. A plate of food was provided in the green patch and empty food plates were placed in the other color patches(2 hr.). 3.Then, flies were fasted for 1 hour, followed by restoring color patches and only empty plates on all color patches. Finally, within 20 minutes, we recorded the amount of time the flies spent in areas of different colors to evaluate if their color preference had changed.(fig.5) 24 flies were used and all of them were trained for consecutive 3 days. Their choice of color were recorded every day, by which we can understand whether association between training times and color preference was significant.

2-2.3 Caffeine effect experiment

The experiment procedure is identical as the former experiment(fig.5), except for the recipe of food provided during the adaptation stage and the training stage. The caffeinated food was prepared by replacing the water with 4 different concentrations of caffeine solution(50ppm, 100ppm, 250ppm, 500ppm).(Aleksandra H. Nall *et.al*,2016; Asbah A,2021; Sonia Tremblay,2022)(The sample size(24 flies) and recording method was also identical as the previous experiment.

2-3 Statistical Analysis

Randomized Block Design ANOVA (RBD ANOVA) was used to know if there is significant preference among four colors. If significant difference was observed, then Tukey HSD was adopted to make pair-wise comparisons to determine which color is significantly preferred.

3. Results

3-1 Color preference

Table. 1 color preference experiment

	sample	1	2	3	4	5	6	7	8	9	10	11	12	13	14	15	16	17	18	19	20	21	22	23	24	means	
Male fruit flies	R	123	635	0	0	227	506	0	12	545	0	351	536	0	224	267	118	0	197	70	677	267	467	221	458	245.9	RBD ANOVA P= 0.008
	B	153	48	0	1200	320	167	0	0	651	0	403	134	0	116	234	266	0	160	0	72	347	203	241	105	200.8	
	G	519	74	0	0	400	227	0	15	0	0	116	126	0	294	189	82	0	280	0	67	345	110	210	333	141.1	
	Y	84	11	1200	0	198	55	1200	1098	0	1200	314	124	1200	320	222	183	1200	261	1128	190	108	283	299	242	463.3	
Female fruit flies	R	42	131	76	353	35	340	0	32	128	300	14	567	89	1200	133	34	220	87	1200	0	0	283	389	1165	284.1	RBD ANOVA P=0.25
	B	162	9	130	0	38	60	0	37	61	74	968	123	0	0	130	351	155	105	0	1200	0	180	194	12	166.2	
	G	2	480	449	0	1051	282	1126	1050	570	20	212	228	375	0	542	358	608	630	0	0	960	198	309	23	394.7	
	Y	901	560	333	845	76	495	74	36	427	799	6	178	730	0	168	357	149	252	0	0	0	262	154	9	283.8	

Male fruit flies exhibit a distinct preference for colors, with yellow being the most preferred and green the least favored. In contrast, female fruit flies do not display significant color preferences; while green scores relatively higher, no specific color stands out as particularly preferred.(fig.6)

3-2 Learning Behavior Observation

For the experiment, male fruit flies will be selected for behavioral training. The objective is to condition them to develop a preference for green. After undergoing the training process, they were observed to spend more time on green; however, this increase in time did not translate into a significant preference for the color. It is assumed that *Drosophila* initially approached the green area in search of food. However, upon arriving

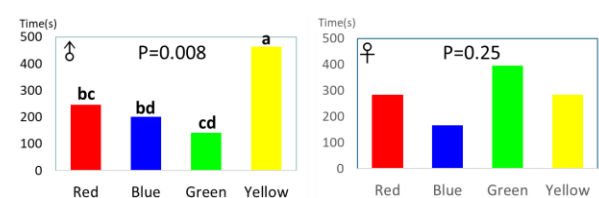


fig. 6 Color preference of fruit flies

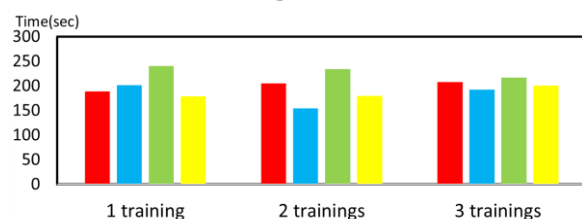


fig. 7 learning behavior experiment

there, no food could be found, which might have affected the flies' cognition. Since there was no reward associated with the designated color(green), the *Drosophila* may return to the color(yellow it preferred before the training.)(fig.7) Therefore, the observation interval should be shortened to 3 minutes to better track its behavior.

Table. 2 learning behavior observation experiment

1 training	Sample	1	2	3	4	5	6	7	8	9	10	11	12	13	14	15	16	17	18	19	20	21	22	23	24	means	RBD ANOVA P = 0.73
	R	361	208	195	112	204	316	162	100	174	145	0	160	10	164	144	320	224	4	197	71	654	180	251	171	188.625	
	B	174	203	153	123	67	87	173	235	203	196	26	12	864	278	177	30	201	850	195	67	47	174	137	171	201.792	
	G	106	283	404	256	264	168	302	196	331	265	0	665	17	98	107	514	146	20	206	637	35	299	265	186	240.417	
	Y	159	149	120	190	132	155	125	161	153	218	868	7	10	247	330	33	232	15	147	92	85	164	205	289	178.583	
2 trainings	Sample	1	2	3	4	5	6	7	8	9	10	11	12	13	14	15	16	17	18	19	20	21	22	23	24	means	RBD ANOVA P = 0.52
	R	350	22	0	259	297	306	44	74	192	214	183	558	0	140	537	505	27	471	157	55	0	191	176	169	205.292	
	B	128	5	0	368	93	110	80	139	166	249	258	20	0	308	0	242	337	102	264	98	85	226	218	211	154.458	
	G	199	4	175	80	175	158	681	349	258	204	184	96	900	223	282	54	132	126	253	221	234	285	206	133	233.833	
	Y	118	867	205	58	258	148	76	135	199	118	157	17	0	122	0	59	325	139	130	493	164	142	161	216	179.458	
3 trainings	Sample	1	2	3	4	5	6	7	8	9	10	11	12	13	14	15	16	17	18	19	20	21	22	23	24	means	RBD ANOVA P = 0.97
	R	102	214	454	80	133	187	85	174	278	58	75	26	174	153	167	230	443	135	492	218	35	47	900	127	207.792	
	B	195	186	154	156	84	200	290	173	114	147	565	300	203	176	0	174	79	150	59	406	101	405	0	295	192.167	
	G	237	224	84	389	380	238	225	234	198	418	123	203	331	151	697	151	102	198	216	139	194	0	0	81	217.208	
	Y	329	172	81	175	136	162	254	200	261	164	104	300	153	272	0	157	202	178	110	72	556	428	0	347	200.542	

After partitioning the observation time into 3-minute interval, some trends were observed. In all groups with different training levels, fruit flies spent more time in green during the first 9 minutes but shifted to red in the last 6 minutes. Flies with more training times associated food with color more quickly. Those with 2 trainings did so between 3 to 9 minutes, while those with three trainings did so between 0 to 6 minutes. After 9 minutes, the flies moved to the red area. We assumed that because they couldn't see red, which could imply a darker place; therefore, learning that no food was in green makes them move to red for resting.(fig.8)

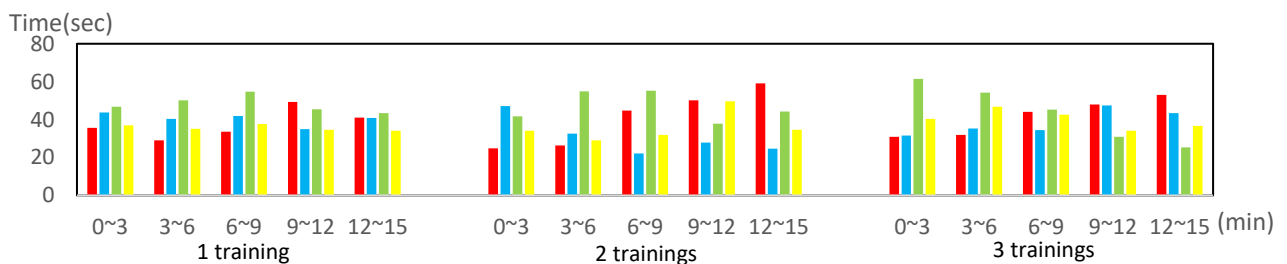


fig. 8 learning behavior observation experiment with male(interval)

3-3 Caffeine effect on learning Behavior

After 1 training, caffeine did not appear to influence the learning behavior of fruit flies, though it generally seems to have a negative effect. After 2 trainings, caffeine began to alter their behavior depending on the concentration. At 50 ppm, the flies show a delayed preference for green, while at 100 ppm, there is a significant improvement in their learning behavior. At 250 ppm, the flies spend more time in both the green and red, and at 500 ppm, the delayed preference for the green. After 3 trainings, caffeine continued to affect learning, with the flies spending less time in the

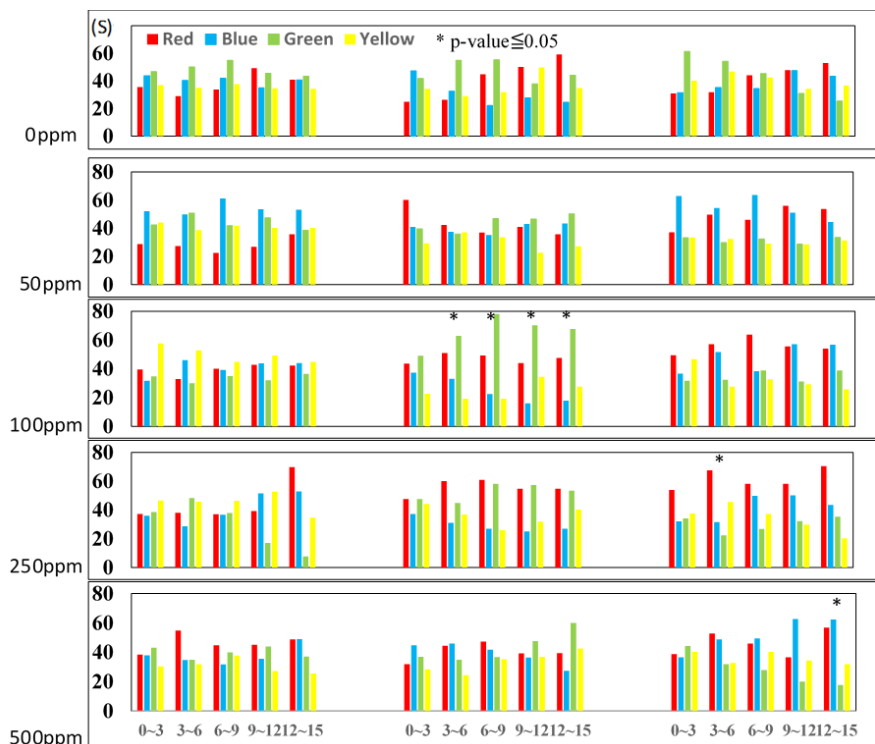


fig. 9 Caffeine effect on learning Behavior experiment

green and more time in the blue and red. At higher concentrations, such as 250 ppm and 500 ppm, the flies significantly preferred the blue and red. Once they realize there is no food in the green area, they tend to move to the red to rest. Because fruit flies cannot see the red, the red may imply dark to them. Overall, a suitable concentration of caffeine, such as 100 ppm, appears to enhance the learning behavior of fruit flies.(fig.9)

4. Conclusion

Male fruit flies exhibit a distinct preference for yellow, and least favor for green. This finding provides a foundation for further research on how color influences their natural behaviors and decision-making processes. Fruit flies are capable of learning, and their behavior adapts significantly with repeated training. The more training sessions they undergo, the faster their behavior changes, suggesting a strong capacity for associative learning. This adaptability highlights the potential of fruit flies as a model organism for studying memory and learning mechanisms. Caffeine has a notable impact on the learning behavior of male fruit flies. When exposed to suitable amounts of caffeine, their learning ability improves, resulting in better retention and performance. Remarkably, after three training sessions, caffeinated fruit flies consistently move toward red or blue, instead of green.

5. Discussion

Male fruit flies show the preference of yellow; we think that it is because rotten fruit usually shows yellowish coloration, which naturally attracts fruit flies. Learning behavior changes are correlated with levels of training. In other words, the more times they are trained, the faster they will learn. Caffeine changes fruit flies learning behavior; however, only the moderate concentration(eg. 100ppm) improved their awareness of the association between food and color patches. High concentrations changed their behavior and the effect of training times. We suggest that they might have stayed awake for too long due to the caffeine intake. As a result, after 3 trainings, they were tired and preferred to rest in the red and blue areas.

6. Reference

- Aleksandra H. Nall, Iryna Shakhmantsir, Karol Cichewicz, Serge Birman, Jay Hirsh & Amit Sehgal. Caffeine promotes wakefulness via dopamine signaling in *Drosophila*. Scientific Reports. Sci Rep 6, 20938 (2016). <https://www.nature.com/articles/srep20938>
- Asbah A, Ummussaadah U, Parenthen N, Putri A S W, Rosa R A, Rumata N R, Emran T B, Dhama K, Nainu F. Pharmacological Effect of Caffeine on *Drosophila \ melanogaster*: A Proof-of-Concept *in vivo* Study for Nootropic Investigation. National Library of Medicine. Archives of Razi Institute. 2021 Dec 30;76(6):1645–1654. <https://pmc.ncbi.nlm.nih.gov/articles/PMC9083854/>
- Sonia Tremblay, Yanqiqi Zeng, Aixin Yue, Kiana Chabot, Abigail Mynahan, Stephanie Desrochers, Sarra Bridges, S Tariq Ahmad. Caffeine Delays Ethanol-Induced Sedation in *Drosophila*. National Library of Medicine. Biology (Basel). 2022 Dec 30;12(1):63. <https://pmc.ncbi.nlm.nih.gov/articles/PMC9855986/>

The Relationship Between Surface Shape and Airflow

Masaaki Sano¹, Canon Takahashi¹, Yulin Chen², Sean Liao², Kevin Lu²

¹ *Institute of Science Tokyo High School (Japan)*

² *Kaohsiung Municipal Kaohsiung Senior High School (Taiwan)*

Abstract:

As a development in reducing the wind load on electric wires, we made the cross-sectional shapes of electric wires circles and polygons. We measured the peeling points and wind force. And we investigated the difference in air resistance due to the cross-sectional shapes of electric wires. For our experiment, we carried out an airflow experiment (STHS) and a wind tunnel experiment (KSHS). In the airflow experiment, we measured the relationship between voltage and wind speed, observed airflow that flows around the samples and measured the peeling point. In the tunnel experiment, we put the sample on a cart and measured the force that the wind gave to the samples. As a result, in the airflow experiment, the peeling point of the triangle appears at more back than other samples and the peeling point did not change when the voltage was changed. In the tunnel experiment, the force giving wind load to the triangle was the least among other samples even when the voltage was changed. From these things, we can know the air resistance of the triangle is less than the other shapes.

Keywords: Surface shapes; Airflow; Air resistance; Electric Wire; Peeling point

1. Background and purpose

Typhoon Kemi, which made landfall in Taiwan in July 2024, caused severe damage to about 700,000 homes with power outages, in addition to landslides, flooding, and inundation damage.^[1] The breakage of power lines has a major impact on infrastructure. The causes of wire breaks include flying objects, but it is also known that strong winds can cause wires to sway, leading to collisions and subsequent breakage, or that they can break due to fatigue fracture caused by the up-and-down movement induced by wind.^{[2][3]} Broken power lines pose serious hazards, such as electric shocks and fires, leading to secondary damage.^[4] Therefore, as another policy, research is being conducted on electric wires that are less susceptible to strong winds. If electric wires with wind-resistant shapes are developed, they can reduce swaying and collisions during strong winds. This is expected to reduce damage from power outages and maintain lifelines in the event of a disaster.

2. Method

2-1 Research principle and division of roles

This study aims to research the relationship between voltage and wind velocity and determine how circular and polygonal shapes affect wind resistance as surface shapes of electric wires. Circular, triangular, square, and pentagonal polygons will be used to evaluate the correlation between the position of each peeling point (which an air flow leaves an object) and aerodynamic drag.

Hypothesis

- When the vertex of regular polygons gets wind, the air resistance is less than when the side gets wind.
- When regular polygons have fewer vertices, the air resistance is less.

The following two experimental methods will be used in this study

1. “Experiment of airflow on an object” (STHS)

We examine the relationship between voltage and wind speed and observe the airflow on the surface of an object. Incense smoke will be used to visualize the flow, and a video of the airflow will be taken. By analyzing this video, the location of the peeling point can be determined and the effect of the shape can be evaluated.

2. “Wind Tunnel Experiment” (KSHS)

Circular and polygonal samples will be placed in a controlled environment and changes in air resistance will be measured. The samples are placed on a cart and video is taken with and without wind. By

analyzing this video, we will confirm the change in acceleration with and without wind and evaluate the effect of wind speed on the movement of the sample.

2-1 Experiment of airflow on an object

2-1-1 Experiment steps

1. Construct the device shown in Figure 1
2. Research the relationship between voltage and wind speed
We do it every experimental day
3. Set up in the experimental device
4. When incense smoke builds up, turn on the propeller
5. Take a video of the airflow and temperature with a smartphone
6. Find the position of the peeling point from the video
7. Consider the difference of peeling point by each condition device

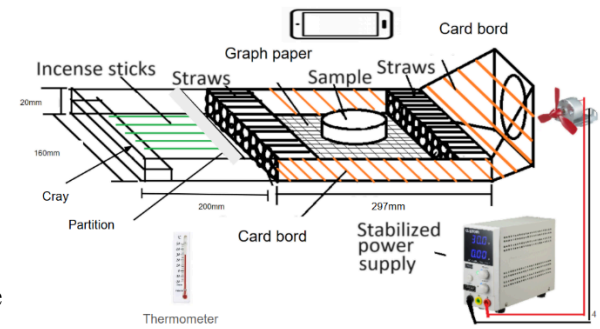


Figure 1 STHS experimental

2-1-2 Comparison and evaluation method

Samples were circular, triangular, square, and pentagonal polygons. The more downstream the peeling point was, the lower the resistance was, so we looked for the peeling point from the video and evaluated the angle to see how far downstream the peeling point was.

2-2 Wind Tunnel Experiment

2-2-1 Experiment methods

(1) Pressure

We use a fan to blow air at the object, measure the pressure on both sides of the object, and then calculate the difference between the two readings. Using the formula $F=P \times A$, we can determine the force caused by air resistance.

(2) String

We use a fan to blow air at the object and thread a string through a keychain ring attached to the top of the object. By measuring the angle of depression and conducting basic analysis, we can calculate the air resistance.

(3) Small Car

We attach the small car to the object we want to measure, place it on the device we created, turn on the fan, record a video of it, and then use Tracker to analyze the video and Desmos for data analysis.

2-2-2 Comparison and Evaluation Methods

In method (1), the pressure readings fluctuated continuously, and the difference between the two values was too small to yield reliable results. Therefore, we explored alternative methods. In method (2), the wind is unstable, causing the angle to change continuously, leading to considerable measurement uncertainty. In method (3), the wind is not strong enough to overcome the maximum static friction, preventing the car from moving. To address this problem, we improved the device repeatedly, including building a small wind tunnel to make the wind stronger and more concentrated. We also used a slope to help it overcome the maximum static friction. By deducting the force when the car is empty, we can neutralize the effects of both the slope and friction.

3. Results and discussion

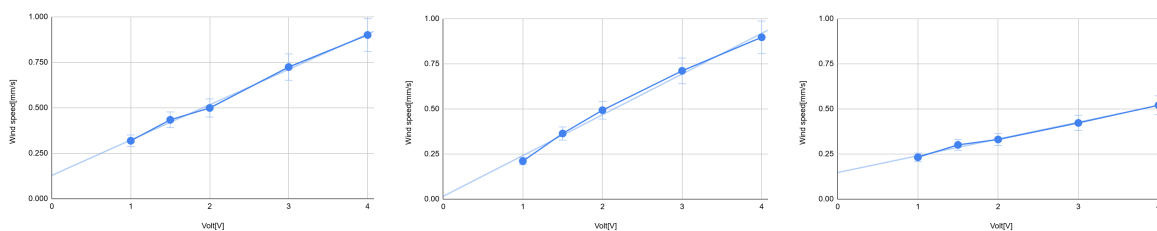


Figure 2~4 Relationship between voltage and wind speed (Left: 11/11, Center: 11/12, Right: 11/13)

Date	11/11	11/12	11/13
Temperature	18°C	18°C	18°C
Humidity	82%	68%	44%
Slope	0.149	0.226	0.0931
Intercept	0.129	0.0158	0.147

Table 1 Relationship between voltage and wind speed

Shape(front)	1V	1.5V	2V	3V	4V
Triangle(vertex)	61.34	61.04	61.9	61.26	60.96
Triangle(side)	118.32	118.72	118.14	118.52	119.34
Square(vertex)	92.36	90.96	91.74	90.32	92.18
Square(side)	135.66	134.82	135.06	135.08	134.72
Pentagon(vertex)	108.52	108.18	108.62	109.24	109.18
Pentagon(side)	144.22	143.96	144.14	143.92	143.8
Circle	98.94	97.88	96.3	94.34	91.28

Table 2 Relationship between sample shape and peeling point

3-1 Experiments of airflow through an object (STHS)

3-1-1 Relationship between voltage and wind speed

The temperature value was constant at 18°C for each date in Table 1. This suggests that humidity likely affected the relationship between voltage and wind speed. The slope for 11/11 in Table 1 was 0.149, and the slope became steeper with higher humidity. This is because the air is lighter when humidity is high, so its viscosity decreases. This is thought to be because the propeller is more likely to pull in air, which is affected at high voltages. The slope of 11/13 in Table 1 was 0.0931, and the slope became more gradual with lower humidity. This is because air is heavier when humidity is low, which increases the viscosity of the air. This makes it harder for the propeller to draw in air, which is thought to have a greater effect at low voltages.

3-1-2 Relationship between shapes of samples and peeling point

For the polygonal peeling points in Table 2, the peeling point appeared farther downstream when the wind was directed at the vertices compared to when it was directed at the sides. This result suggests that wind at the apex has less aerodynamic drag. For the polygonal peeling points in Table 2, the more angles there were, the more the peeling point appeared forward. The results indicate that triangular samples exhibited the least aerodynamic drag. The peeling points of the polygons in Table 2 did not change when the voltage was changed. This suggests that the same peeling point would be reached even in strong winds.

3-2 The relationship between shape and air resistance(KSHS)

Shape(Front)	a(no wind)(m/s ²)	a(wind)(m/s ²)	Δa (m/s ²)	F(dyne)	Shape(Front)	a (no wind)(m/s ²)	a(wind)(m/s ²)	Δa (m/s ²)	F(dyne)
Triangle(Vertex)	0.204	0.249	0.045	45.225	Triangle(Vertex)	0.204	0.455	0.251	252.225
Triangle(Side)	0.164	0.240	0.076	76.380	Triangle(Side)	0.164	0.597	0.433	435.165
Square(Vertex)	0.173	0.225	0.052	110.320	Square(Vertex)	0.173	0.881	0.708	1644.684
Square(Side)	0.183	0.068	0.115	243.340	Square(Side)	0.183	0.554	0.371	861.833
Pentagon(Vertex)	0.191	0.376	0.185	429.755	Pentagon(Vertex)	0.191	1.037	0.846	1965.258
Pentagon(Side)	0.222	0.330	0.108	250.884	Pentagon(Side)	0.222	0.587	0.365	847.895
Circle	0.152	0.207	0.055	152.295	Circle	0.152	0.505	0.353	977.457

Table 3. The difference in accelerations (wind speed:1.3m/s) and their drags

Table 4. The difference in accelerations (wind speed:4.0m/s) and their drags

In the beginning, we thought that the farther the peeling point is, the lower the air resistance would be. However, based on our experimental results, there is no direct correlation between the peeling point and air resistance; we also need to consider the geometric properties of the shape. Theoretically, when analyzing the drag of objects, both the effective area (the equivalent area after considering geometric properties) and the peeling point must be taken into account. After researching relevant information online, we found that the theory mentioned in the first paragraph better explains the behavior of spherical objects, such as golf balls. The more sides a polygon has, the more its front side resembles that of a cylinder. Therefore, squares at a wind speed of 4.0 m/s and pentagons conform to the previously mentioned theory. However, for prisms with fewer sides, the effective area significantly influences drag, which is why triangles and squares at a wind speed of 1.3

m/s do not align with the theory. In the case of the triangle, its shape is less similar to a circle, reducing the influence of the peeling point. Instead, the primary factor affecting air resistance is the wind pushing the object. Since both the vertex and the sides have the same contact area, the area itself does not need to be considered separately. However, the vertex experiences some neutralization of the force caused by the wind due to the angle between the object's surface and the wind direction, whereas the side is directly impacted by the wind. This explains why the side experiences higher air resistance. In contrast, in the case of the square and pentagon, their shapes are more similar to circles composed of numerous sides, so the peeling point has a more substantial effect. This is why they align with the theory we mentioned earlier.

4. Conclusion

4-1 Discussion of our research

Initially, it was believed that a farther peeling point would reduce air resistance, but experiments showed no direct correlation and highlighted the importance of geometric properties. Drag analysis requires considering both effective area and peeling point. Squares and pentagons align with the theory as peeling points have a more substantial effect on shapes resembling circles. However, triangles do not, as their effective area significantly influences drag on triangles. The results of airflow experiments and wind tunnel experiments showed that when the cross-sectional shape is a triangle and the vertex of the triangle receives the wind, air resistance remains low even if the voltage is changed. In other words, we think that it is possible to prevent the electric wire from swaying due to strong winds by making the electric wire triangle. Therefore, we think it reduces the chance of touching each electric wire and causing fatigue damage by swaying.

4-2 Issue

However, in fact, wind comes from various directions, and the wind in the experiment came from one direction. So it is necessary to develop a way to point the apex to the wind direction. In addition, Replacing existing electric wires with triangular ones would be costly and time-consuming, so it is necessary to consider something that can be attached later. In addition, a triangular shape has a surface. Therefore, future research should explore strategies to prevent snow buildup on triangular electric wires.

5. References

- [1]THE PARTNERS CO.LTD. (2024, July 25).《Typhoon No.3 of 2024》Typhoon No.3 crossed Taiwan, 2 people died•279 people injured (top news) / Taiwan. Y's consulting group.
<https://www.ys-consulting.com.tw/news/116622.html>
- [2]Nariyuki Kurisu. (2023, February 17). What is a galloping phenomenon ! ? The phenomenon in which each electric wire sways because of strong wind and touch. Disaster newspaper.
<https://bousai.nishinippon.co.jp/15594/>
- [3]Jun Fukuda. (2020, December 6). Why are electric wires safe even when it rains? You think you know but do not know the secrets of electric wires. News Switch. <https://newswitch.jp/p/24812>
- [4]Nariyuki Kurisu. (2023, May 15). When the high-voltage or electric wires break...?The key point for preventing accidents is. Disaster newspaper. https://bousai.nishinippon.co.jp/5559/#index_id3
- [5]Toshiaki Yoshiura, Hiroshi Nakamoto, Takeshi Nakamura, Kouji Terasaki, Kiyonori Watanabe. (2000). Development of Low Wind-Pressure Electric Wire.
https://www.jstage.jst.go.jp/article/ieejpes1990/120/12/120_12_1723/_pdf
- [6]ZHUANG, ZI-DE, CHEN, YI-ZHEN, WU, JIA-RU, WANG,XIAO-QI. Observe the path of wind through the surface of an object. <https://twsf.ntsec.gov.tw/activity/race-1/49/pdf/030111.pdf>
- [7]flying609. (2020, November 3). Introduction to aerodynamics #6 Turbulence, resistance, and boundary layer (Boundary Layer). Aviation Notes of Flying Potato Boy.
<https://flying609.wordpress.com/2020/11/03/%E7%A9%BA%E5%8B%95%E8%B6%85%E5%85%>

A5%E9%96%806-%E7%B4%8A%E6%B5%81%EF%BC%8C%E9%98%BB%E5%8A%9B%EF%
BC%8C%E9%82%8A%E7%95%8C%E5%B1%A4boundary-layer/

Drop and Rebound

Alex Chen¹, Franky Chan¹, Joe Juang¹, Maya Morito², Aoi Nozaki²

¹Kaohsiung Municipal Kaohsiung Senior High School (Taiwan)

²Waseda University Honjo Senior High School (Japan)

Abstract:

Liquid splashes are common and sometimes annoying in our daily lives. Therefore, the purpose of this study is to investigate the form in which factors could potentially impact the liquid rebound (Worthington jet). Marbles were used as a dropping object in our experiments. We set up a slow-motion camera to capture images of rebound and use “Tracker” to collect data. In our experiments, dropping height and liquid depth are determined to be significant factors in Worthington jet.

The height of liquid rebound has a positive correlation with dropping height and the increase is highly linear, while liquid rebound becomes more inconsistent as dropping height increases. The height of liquid rebound also has a positive correlation with water depth. In terms of salt solution, as density increases, liquid rebound shows not only a declining trend at first but also a rising trend at the end. Viscosity causes the rebound to be increasingly lower when salt solution is less denser than 1.12 g/cm^3 , while surface tension causes increasingly higher liquid rebound when it is denser than 1.12 g/cm^3 . This study definitively answers the question regarding correlation between Worthington jet, and certain factors involving dropping height, liquid depth, and dissolved salt. Nevertheless, viscosity and surface tension still require further research work in order to determine the mechanism of how they cause impacts on Worthington jet.

Keywords: Worthington jet; liquid rebound; salt solution; dropping height; liquid depth

1. Introduction

Water is an essential part of our daily lives, yet we often find ourselves splashed by it. Whether it's during a thrilling diving competition or cooking soup, splashes are a common occurrence. These splashes include the phenomenon of Worthington jet.

The mechanism of Worthington jet is as follows. As marble impacts on the surface of liquids, an air column is formed, temporarily increasing the surface area of liquid. Due to surface tension, as a result, liquid seeks to minimize its surface area, causing water to rebound. In this study, we conducted the experiments to study the impacts caused by dropping height, liquid depth, and liquid density based on the mechanism of Worthington jet.

2. Methodology

- We conducted each experiment 40 times and organized the data using box plots.
- Experiment 1: We attempted to drop marbles into various liquid solutions to observe the relationship between certain solution properties and the splash height. The liquids we used were as follows: alcohol, water, salt solution, sugar solution, and potato starch solution.
- Experiment 2: We changed the height (H) of where marbles were dropped (H=20, 30, 40, 50, 60, 70, 80, 90 cm), while the water depth (d) remained 10 cm.
- Experiment 3: We changed the depth (d) of the water (d=5, 7.5, 10, 12.5, 15 cm), while the dropping height (H) remained 30cm.
- Experiment 4: We add salt into water to change the density of the liquid, while dropping height remained 30 cm and the water depth remained 10 cm.

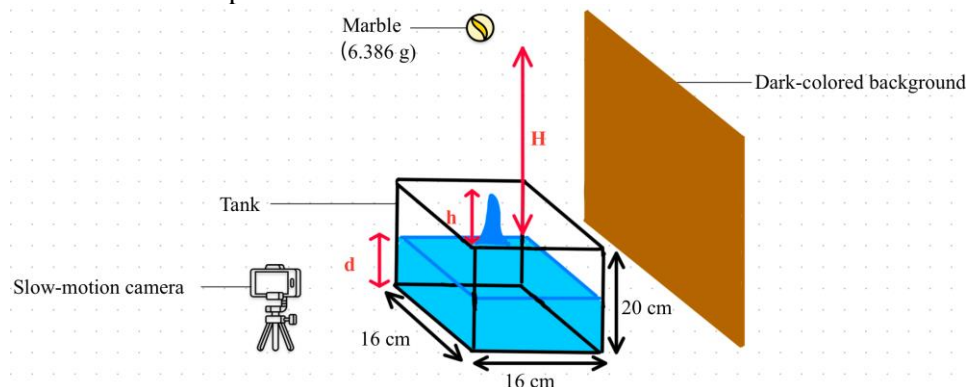


Figure 1. Experimental equipment

3. Results

- Experiment 1:

- Table 1. shows the height of liquid rebound when a marble is dropped from the same height into equal depths. Alcohol had a rebound height of 4 cm, while water and potato starch solution both produced 3 cm. Salt and sugar solutions had the highest rebound at 4.5 cm.

	Water	Salt solution	Sugar solution	Alcohol	Potato starch solution
Density (g/cm ³)	1.00	1.12	1.29	0.80	1.50
Liquid rebound (cm)	3.0	4.5	4.5	4.0	3.0

Table 1. The relationship between liquid rebound and different liquid

- Experiment 2:

- In experiment 2, we changed the dropping height and observed the height of liquid rebound. The result is as it shows in Figure 2, the higher the dropping height, the higher the liquid rebound.
 - In the box plot, the interquartile range (IQR) reflects the discreteness. Consequently, according to Figure 2, we noticed that at lower dropping height, the discreteness is smaller, suggesting the liquid rebound is more consistent. Relatively, at higher dropping height, the discreteness is larger, suggesting the height of liquid rebound is more inconsistent.

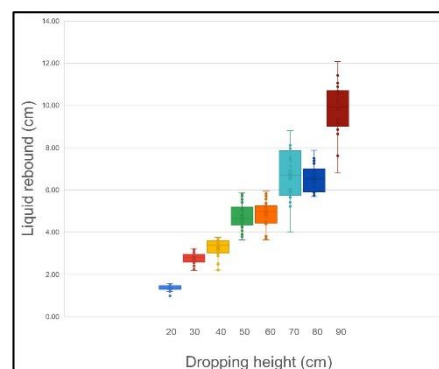


Figure 2. Liquid rebound-Dropping height box plot

- In order to look into the relationship between dropping height and liquid rebound, we calculated the amount of energy using mechanical energy formula and made Table 2.

Dropping height (cm)	20	30	40	50	60	70	80	90
Relative initial mechanical energy of marble (Standard value)	1.0	1.5	2.0	2.5	3.0	3.5	4.0	4.5
Relative terminal mechanical energy of liquid rebound (Standard value)	1.000	2.038	2.414	3.504	3.594	4.865	4.835	7.233

Table 2. Relative mechanical energy of liquid rebound table. Relative initial mechanical energy of marble and relative terminal mechanical energy of liquid rebound are calculated using potential energy formula. We assume that the mass of the liquid droplet remains constant and use means to represent for liquid rebound at different height. We set the data collected from 20 cm dropping height as standard value to show the ratio.

- According to Table 2 and Figure 3, we can observe that there is a positive correlation between liquid rebound and dropping height. In the linear regression model, the equation is $y=1.549x-0.5744$ and R^2 is 0.9372, which suggests that the increase in liquid rebound is highly linear.
- Experiment 3:
 - According to Figure 4, it shows that greater water depths result in higher liquid rebounds. However, the increase is not strictly linear. At shallower depths (e.g., 5 cm), the liquid rebound remains relatively low and consistent, whereas at deeper depths (e.g., 15 cm), the rebound height increases significantly, accompanied by greater variability.
 - To investigate the relationship between liquid depth and the height of liquid rebound, we calculated the standard deviation of the data and expressed the results as relative percentages of the maximum value. Additionally, although the marble's height remains constant—implying the same potential and kinetic energy upon entering the water—greater water depths allow the liquid to rebound higher. Specifically, in the group with a water depth of 5 cm, the rebound height was reduced to only 86% of that observed in the group with a water depth of 15 cm.

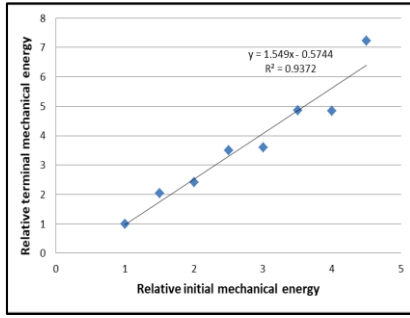


Figure 3. Relative liquid rebound-Relative dropping height scatter diagram

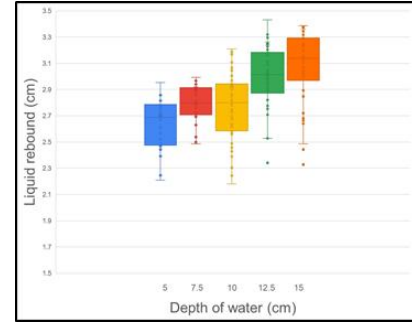


Figure 4. Liquid rebound-Depth of water box plot

Depth (cm)	5	7.5	10	12.5	15
Average Rebound Height (cm)	2.632	2.786	2.765	3.001	3.065
Standard Deviation	0.184	0.14	0.252	0.241	0.281
Percentage Relative to Maximum (%)	86%	91%	90%	98%	100%

Table 3. The percentage of rebound heights relative to maximum (Depth 15cm)

- Experiment 4:
As demonstrated in Experiments 2 and 3, both the dropping height and water depth influence the liquid rebound. Therefore, in the current investigation, both factors were controlled. As salt is gradually dissolved in water, the rebound height of water droplets initially decreases. However, when the density of the salt solution reaches approximately 1.12 g/cm^3 , this trend reverses (as shown in **Figure 5**).

We infer that the rebound height is primarily determined by surface tension and viscosity. Viscosity tends to reduce rebound height, while surface tension increases it. By combining these findings with the trend observed in **Figure 5**, it can be inferred that viscosity predominantly influences the rebound height below a density of 1.12 g/cm^3 , whereas surface tension becomes the dominant factor above this threshold.

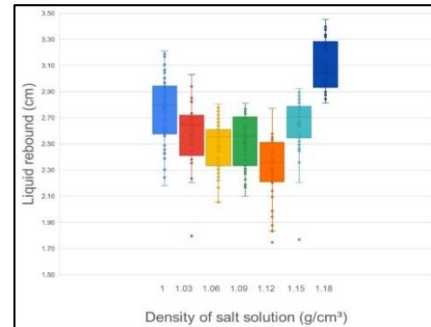


Figure 5. Density of salt solution-Liquid rebound box plot.

4. Discussion

- Experiment 1:
 - After conducting preliminary experiments, we discovered that factors such as density, viscosity, and surface tension, in addition to height and depth, could potentially influence the height of the liquid rebound. Therefore, we decided to select density, which is relatively easier to measure, as one of the variables.
- Experiment 2:
 - At higher dropping position, marbles possess more initial mechanical energy, which is determined by its height. It leads to formation of larger and longer air column, thus contributing to higher liquid rebound.
 - As dropping height increases from 20 cm to 90 cm, the standard deviation becomes larger. It reflects that the possibility of unstable liquid rebound increases. Some factors such as the structural imperfection in air column, which happens at greater dropping height, may contribute to instability of liquid rebounds. Liquid rebounds thus become more unstable and inconsistent as dropping height increases.
- Experiment 3:
 - Greater water depth provides more space for the marble to generate a complete air column during its descent. A more complete air column releases more energy upon rebound, resulting in a higher splash.
 - The depth of water significantly impacts the height of liquid rebound. At shallower depths (e.g., 5 cm), the rebound height is relatively low and consistent. As the depth increases to

- 15 cm, the rebound height rises noticeably while showing only slight variability.
- At greater water depths, more energy propagates through the liquid, resulting in more complex splash dynamics. This includes dispersed droplets, which occur more frequently at deeper depths.
- Experiment 4:
 - The observed trend in the height of liquid rebound on salt solutions may be influenced by two primary factors:

Surface Tension: As the density of the salt solution increases, its surface tension also rises (as shown in **Figure 6**). Surface tension is the cohesive force acting at the liquid's surface, which tends to minimize surface area. After the marble impact creates an air cavity, surface tension drives the liquid to restore its original shape. Stronger surface tension generates a greater restorative force, leading to a higher liquid rebound. This relationship can be summarized as:

Density \uparrow \rightarrow Surface Tension \uparrow \rightarrow Height of liquid rebound \uparrow

Viscosity: Increasing the density of the salt solution also leads to higher viscosity (as shown in **Figure 7**). Greater viscosity increases internal friction within the fluid, dissipating kinetic energy more effectively during impact. This energy dissipation reduces the rebound height of the droplet. The relationship can be summarized as:

Density \uparrow \rightarrow Viscosity \uparrow \rightarrow Height of liquid rebound \downarrow

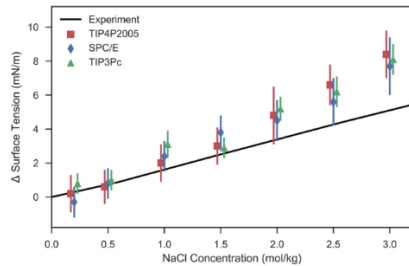


Figure 6. Salt concentration-Surface tension line chart (Thomas R et al, 2018)

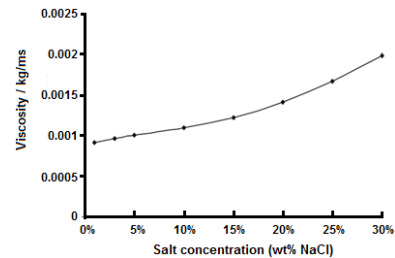


Figure 7. Salt concentration-Viscosity line chart (Andi et al, 2012)

Density is positively correlated with concentration : Concentration = Density * 1/Molecular weight

5. Conclusion

- The height of liquid rebound has a positive correlation with dropping height and the increase is highly linear. At higher dropping position, marbles possess more initial mechanical energy, which is determined by its height. It leads to formation of larger and longer air column, thus contributing to higher liquid rebound.
- Liquid rebound becomes more inconsistent as dropping height increases. It could result from imperfection in air column when marbles drop into liquids.
- The height of liquid rebound has a positive correlation with water depth. We speculate that this is because when the marble enters the water, a larger air column is able to form, which can generate a greater liquid rebound. However, the depth of the liquid significantly restricts the travel distance of the air column, thereby reducing the final rebound height.
- The depth of water significantly impacts the height of liquid rebound, but the overall variability remains relatively, in comparison with that in Experiment 2, low across all depths.
- Viscosity affects the rebound to be progressively lower when salt solution is less than 1.12g/cm³, while surface tension leads the water rebounds increasingly higher when it is denser than 1.12 g/ cm³. We consider that viscosity primarily reduces the rebound height of a droplet when the fluid density is below 1.12, while surface tension dominates and leads to a higher rebound height above this density threshold.
- When the density comes to 1.185 g/ cm³, the salt solution has approached saturated. On the moment, the height of water rebound is higher than it does in pure water.

6. References

1. Thomas R. Underwood & H. Chris Greenwell (2018). The Water-Alkane Interface at Various NaCl Salt Concentrations: A Molecular Dynamics Study of the Readily Available Force Fields. *Nature*, 8, 5, <https://doi.org/10.1038/s41598-017-18633-y>
2. Rustandi, Andi; Adyutatama, Muhammad; Fadly, Enriko; and Subekti, Norman (2012). Corrosion Rate of Carbon Steel For Flowline and Pipeline as Transmission Pipe in Natural Gas Production with Co2 Content, *Makara Journal of Technology*, 16(1), 60, <https://scholarhub.ui.ac.id/mjt/vol16/iss1/9>

The study of microplastics in marine animals in the seas of Thailand and Japan

Nalinrat Homwisetwongsa¹, Praewa Piyasoontrawong¹, Kanoko Shigihara², Tsukina Shigihara²

¹*Chitralada School (Thailand)*

²*Fukushima Prefectural Fukushima High School (Japan)*

Abstract:

Microplastics (less than 5 mm) contamination has recently posed a serious environmental threat to marine ecosystems and human health, as they can accumulate in the body through seafood consumption. This research aims to better understand which sea has a higher quantity and examine characteristics (shape, color, and size) of microplastics in seafood. The Thai team analyzed mackerel and mussels from the Gulf of Thailand and the Andaman Sea, while the Japanese team studied mackerel and clams from Japan's Pacific coast. Organic matter was digested with 30% hydrogen peroxide and 1% potassium hydroxide. Filtered microplastics were dried, inspected under a microscope, and categorized by shape and color. In the Andaman Sea microplastics were found most abundantly in fish flesh (31.4%), followed by mussels (28.3%), stomachs (20.4%), and the least in gills (19.9%). In the Gulf of Thailand microplastics were found most abundantly in mussels (32.9%), followed by fish flesh (24.1%), stomachs (23.8%), and the least in gills (19.2%). In the Pacific side of Japan were found most abundantly in fish flesh (27.3%), followed by stomach and clam (25.0%) and the least in gills (22.7%).

This study found slight variations in microplastic contamination between the Andaman Sea and the Gulf of Thailand, while levels in Japanese fish were more consistent. Overall, contamination levels across all regions were comparable, highlighting the widespread distribution of microplastics in the environment and their impact on ecosystems. Moreover, analyzing the shape, color, and characteristics of microplastics helps identify their sources, while ongoing research is crucial for assessing future risks to ecosystems and human health.

Keywords: microplastics; marine animals; contamination

1. Introduction

Microplastics are tiny pieces of plastic, smaller than 5 mm, that cannot be seen with the naked eye. They come from the breakdown of larger plastic items like bottles and plastic bags, which take a long time to decompose. These microplastics end up in seas and oceans, becoming pollutants that harm the environment and ecosystems. Because of their small size, microplastics are eaten by plankton and move up the food chain through different marine animals. Eventually, they reach humans when seafood is consumed. When people eat seafood, they may also consume microplastics, which can build up in the body and cause health problems. These problems include hormonal changes, issues with blood vessels, cancer risks, and a weakened immune system. Although the exact health effects of microplastics are not yet fully understood, they are considered a hidden danger. Studying microplastic contamination in food provides important information that can help develop measures to protect human health.

2. Methodology :

Step 1: Sample Preparation

1.1 Select 5 mackerels and 5 mussels (clams) of similar weight and size. Clean them with fresh water to minimize external contamination.

1.2 For the mackerels : dissect the 5 fish to separate 5 stomachs, 5 gills, and the flesh from all 5 fish. Each sample is finely ground using an electric grinder. Each portion of the sample is placed into five beakers, with 1 gram per beaker. This results in 15 beakers.

1.3 For the mussels (clams) : blend all 5 mussels together into a fine consistency. Each portion of the sample is placed into five beakers, with 1 gram per beaker. This results in 5 beakers.

Step 2 : Digestion of Organic Matter

2.1 Add equal amounts of the following chemicals into all 20 beakers:

- 80 mL of 30% hydrogen peroxide (H₂O₂).
- 16 mL of 1% potassium hydroxide (KOH).

2.2 Place beakers on a magnetic stirrer. Set the stirring speed to 900 rpm for 2 hours until fully digested into a clear solution.

Step 3 : Separation of Microplastics

Filter the digested solution using the prepared filter papers to separate any undissolved materials. Use the same Whatman™ filter papers to filter microplastics from the solution. Dry the filtered microplastics in an Oven at 50°C for 1 hour to ensure complete dryness.

Step 4 : Identification of Microplastic Shape and Color

5.1 Examine the dried microplastics under a microscope (ZEISS Stemi 305).

5.2 Count the number of microplastic particles and measure their size.

5.3 Classify the shape and color of the microplastics.

5.4 Record all observations.

3. Results and discussion :

Thailand

From the experiment conducted between August and October 2024, the following results were obtained: Andaman sea

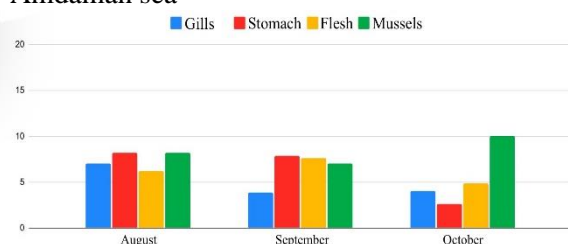


Figure 1. A graph illustrating the amount of microplastics in mackerels and mussels per 1 gram from the Andaman Sea between August and October 2024

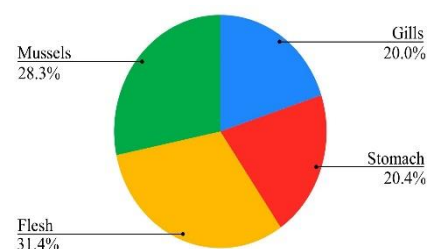


Figure 2. A graph illustrating the number of microplastic pieces in mackerels and mussels from the Andaman Sea between August and October 2024

Microplastics were found most abundantly in fish flesh (31.4%), followed by mussels (28.3%), stomachs (20.4%), and the least in gills (19.9%)

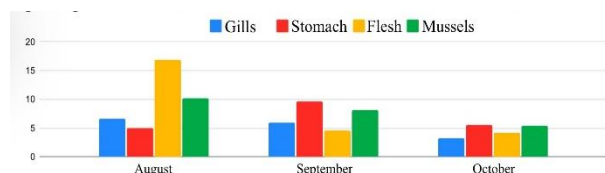


Figure 3. A graph illustrating the amount of microplastics in mackerels and mussels per 1 gram from the Gulf of Thailand between August and October 2024

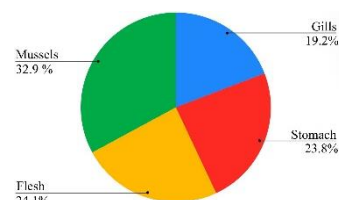


Figure 4. A graph illustrating the number of microplastics pieces in mackerels and mussels from the Gulf of Thailand between August and October 2024

Microplastics were found most abundantly in mussels (32.9%), followed by fish flesh (24.1%), stomachs (23.8%), and the least in gills (19.2%)

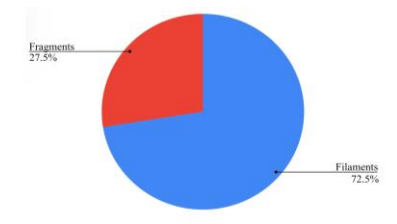


Figure 5. A graph illustrating the shape of microplastic pieces from the Andaman Sea and the Gulf of Thailand

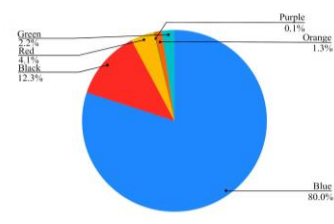


Figure 6. A graph illustrating the colors of microplastic pieces from the Andaman Sea and the Gulf of Thailand

Overall, blue colored microplastics were the most common color(80.0%) followed by black(12.3%), red(4.1%), green(2.2%), orange(1.3%) and the least was purple(0.1%). Additionally, filament shaped microplastics were predominant (72.5%), followed by fragments (27.5%).

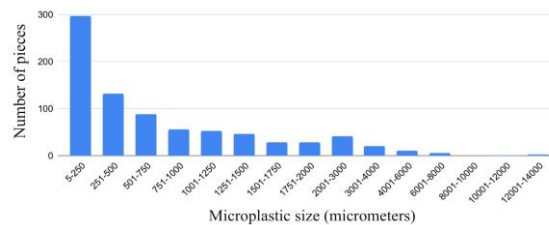


Figure 7. A graph illustrating the size of microplastics found in the Andaman Sea and the Gulf of Thailand

The sizes of microplastics found in marine animal samples from the Andaman Sea and the Gulf of Thailand ranged from the smallest, 5-250 micrometers (μm) with 297 pieces, to the largest, 12001-14000 micrometers (μm) with 2 pieces (as shown in Table).

This study did not analyze the type of microplastics to confirm their plastic composition using an FT-IR spectrometer (Perkin Elmer: Spectrum Two) due to limitations in available equipment.

Japan

- We were able to conduct three months' experiments on fish (September, November, December), but were only able to conduct two months' experiments on clams (November, December).
- Microplastics were found in marine animal's bodies at all months.
- Overall, the amount of microplastics did not change.

From the experiment conducted in November and December 2024, the following results were obtained:

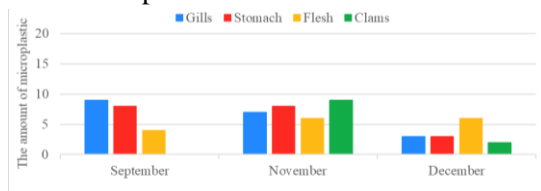


Figure 8. A graph illustrating the amount of microplastics in mackerels and clams per 1 gram from the Pacific side of Japan in September, November, and December 2024

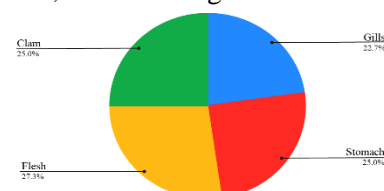


Figure 9. A graph illustrating the number of microplastic pieces in mackerels and clams from the Pacific side of Japan in November, and December 2024

- Microplastics were found most abundantly in fish flesh (27.3%), followed by stomach and clam (25.0%) and the least in gills (22.7%).

From the experiment conducted in September, November, and December 2024, the following results were obtained:

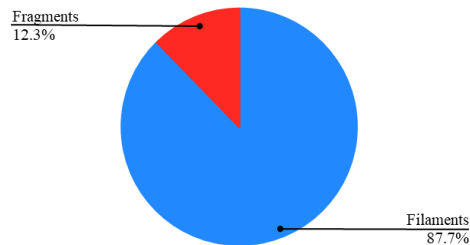


Figure 10. A graph illustrating the shape of microplastic pieces from the Pacific side of Japan

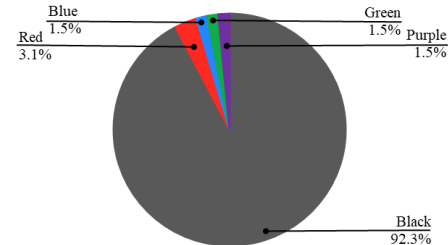


Figure 11. A graph illustrating the colors of microplastic pieces from the Pacific side of Japan

- Filament shaped microplastics were predominant (87.7%), followed by fragments(12.3%).
- Black colored microplastics was the most common color(92.3%) followed by red(3.1%), and the least is blue(1.5%), green(1.5%), purple(1.5%).

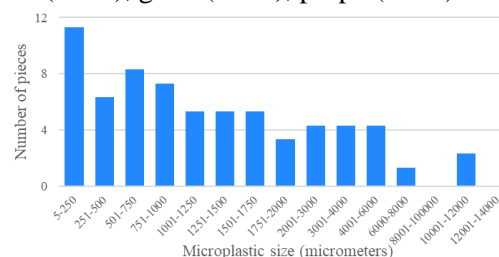


Figure 12. A graph illustrating the size of microplastics found in the Pacific side of Japan

- The sizes of microplastics found in marine animal samples from the Pacific Ocean side of Japan ranged from the smallest, 5-250 micrometers (μm) with 11 pieces, to the largest, 10001- 12000 micrometers (μm) with 2 pieces.

4. Conclusion :

Thailand

Results show similar microplastic contamination in marine animals from the Andaman Sea and Gulf of Thailand, highlighting their widespread distribution and ecological impact. Examining the shape, characteristics, and color of microplastics proves to be valuable for identifying their sources. For instance:

- The shape of microplastics can reveal their source and the extent of their breakdown.
- The color of microplastics can help researchers determine the type of products they originate from. Clear microplastics often come from plastic bottles or bags, while black microplastics may originate from industrial plastics, potentially containing heavy metals. Blue, red, green, and other colored microplastics may come from toys, which could contain lead contamination.

Research tracking microplastics in the environment enables scientists to analyze the risks posed by microplastics to ecosystems and human health in the future. Furthermore, the study found that microplastics sized 5–250 micrometers were most common, posing risks to Thailand’s marine ecosystem. They can harm marine life by causing digestive blockages, toxin accumulation, and may

contaminate seafood consumed by humans. This highlights the urgent need for better plastic waste management to protect marine environments.

Japan

This study concludes that there was not much difference between the number of microplastics found in various parts of mackerel and the number of microplastics found in clams, indicating the distribution of microplastics in the pacific ocean side of Japan in the environment and their impact on ecosystems.

Among the microplastics found, some were fragment-shaped, but filaments were the most common. Since there were many filaments, it is possible that those microplastics originated from plastic cloths and plastic fishing nets.

The color of microplastics was the highest proportion of black, and others were blue, red, green, and purple. From this, many of the microplastics found are thought to be derived from industrial plastics that may contain heavy metals and toys that may contain lead contamination.

Comparison

- Distribution: Thailand saw slightly varied contamination levels between fish flesh and mussels across regions, while Japan showed more uniform contamination across fish tissues.
- Shapes: Both countries observed a high proportion of filament-shaped microplastics.
- Colors: Thailand had a mix of colors with blue being predominant. While, Japan observed a significant dominance of black-colored microplastics
- Implications: Both countries highlight the need for identifying microplastic sources to mitigate their impact on marine ecosystems and human health. Thailand emphasizes the variety of potential sources (e.g., toys, bags), while Japan's black microplastics suggest heavy industrial influence.

5. References :

Eswar M., Saranya V., Lalitha G., Matias S., Wei-Hsin C., et al. (2024). Microplastics in marine ecosystems: A comprehensive review of biological and ecological implications and its mitigation approach using nanotechnology for the sustainable environment, *Environment Research*, 1-18. <https://www.elsevier.com/locate/envres>

Kumar R., Verma A., Shome A., Sinha R., Sinha S., et al. (2021). Impacts of plastic pollution on ecosystem services, sustainable development goals, and need to focus on circular economy and policy interventions. *Sustainability* 13 (issue 17). <https://doi.org/10.3390/su13179963>.

Puntip W., Apinya C. and Wachirah J. (2019). Microplastic Contamination in Marine Animals Used as Seafood : *The 58th KU Annual Conference*, 397-407.

S.E. Nellms., J. Barnett., A. Brownlow., N.J. Davidson., R. Deaville., et al. (2019). Microplastics in marine mammals stranded around the British coast: ubiquitous but transitory. *Scientific Reports*. 9:1075. <https://doi.org/10.1038/s41598-018-37428-3>.

Sonali P., Somava N., Shreya B., Susmita M. (2024). Unveiling the effects of microplastic pollution on marine fauna. *Blue Biotechnology*. 1:6. <https://doi.org/10.1186/s44315-024-00006-6>.

Comparative Analysis of Extract Alone Versus Extract with Blood

Jidapa Kawngam¹, Lucklaor Chulajata¹, Kaoru Iida², Taiki Yoshimura²

¹*Chitralada School (Thailand)*

²*Ritsumeikan High School (Japan)*

Abstract:

In this study, the interaction between *Eclipta prostrata* Linn. extract, *Artemisia vulgaris* extract, and blood was investigated, focusing on structural changes observed through UV-Vis spectrophotometry. Extracts were prepared by soaking dried and powdered *Eclipta prostrata* Linn. in ethanol, followed by filtration and dilution with distilled water. Pig blood was gradually added to the extract, and interactions were analyzed by observing changes in absorption spectra at wavelengths of 400–500 nm (Thailand) and 400–800 nm (Japan), corresponding to hemoglobin absorption.

The results showed that, in the Thai experiment, the absorbance peak decreased as the extract interacted with hemoglobin, indicating aggregation and structural changes in the blood. This aggregation resulted in a clearer solution, allowing more light to pass through. In contrast, the Japanese experiment revealed a trend toward significance in the OD600 values via a T-test, though no distinct agglutination effect was observed.

These findings highlight the potential of *Eclipta prostrata* Linn. extract to induce structural changes in blood, suggesting possible applications in hemostasis.

Keywords: *Eclipta prostrata* Linn., hemoglobin interaction, UV-Vis spectrophotometer, blood aggregation, *Artemisia vulgaris*

1. Introduction

Human bodies respond to wounds by constricting blood vessels to reduce blood flow to the affected area. This triggers primary hemostasis, during which platelet adhesion and aggregation occur to form a platelet plug on the damaged blood vessel surface. Following this, secondary hemostasis is activated, with a sequential stimulation of coagulation factors, leading to the formation of fibrin strands that integrate and encase the platelet plug. This process results in fibrin stabilization, strengthening the blood clot.

The project developers have drawn inspiration from local wisdom regarding the use of *Eclipta prostrata* Linn. and *Artemisia vulgaris* (known for their properties and active compounds that promote platelet production) to stop bleeding from wounds.

2. Methodology

Thailand

Preparation of the extract

1. Grind 40 g of dried *Eclipta prostrata* Linn into powder
2. Soak the powder in 400 mL of 95% Ethanol for 24 hours
3. Filter the extract.
4. Dilute 1 mL of the extract with distilled water in 100 mL of Volumetric flask.
5. Dilute 1 mL of pig blood with distilled water in 100 mL of Volumetric flask.

Evaluation

1. Put distilled water in a cuvette and start running the UV-Vis spectrophotometer for the baseline
2. Put the diluted extract in a cuvette and run the machine.
3. Put the diluted blood in a cuvette and run the machine.
4. Drop 10 drops of the whole pig blood into the same cuvette and run the machine.
5. Leave it for 10, 20, and 30 minutes, then run the machine again
6. Analyze each graph

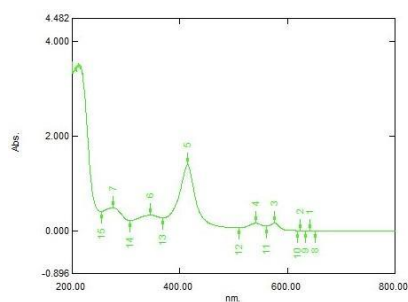


Figure 1. The spectrum of a whole pig blood dilute with distilled water

Table 1. Absorbance in Figure 1.

Solution	Absorbance	Wavelength (nm.)
Diluted pig blood	1.414	414.50

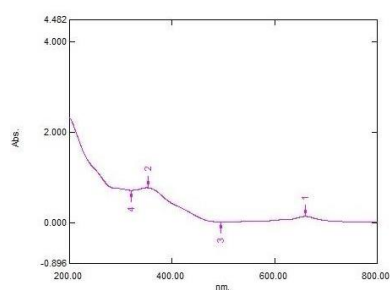


Figure 2. The spectrum of the extract diluted with distilled water

Table 2. Absorbance in Figure 2.

Solution	Absorbance	Wavelength (nm.)
Diluted Extract	0.776	352.50

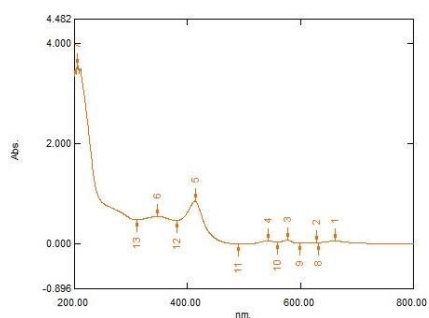


Figure 3. The spectrum of the solution showing the change of the extract mixed with blood

Table 3. Absorbance in Figure 3.

Solution	Absorbance	Wavelength (nm.)
Mixing between the extract and blood	0.851	413.50

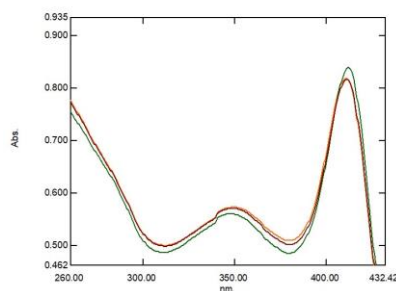


Figure 4. The spectrum of the solution after having been left for 10 20 and 30 minutes
— 10 minutes — 20 minutes — 30 minutes

Table 4. Comparison of the absorbance in Figure 4. focusing in the wavelength range 400-500 nm

Solution	Absorbance	Wavelength (nm.)
left for 10 minutes	0.840	412.50
left for 20 minutes	0.817	411.50
left for 30 minutes	0.818	411.00

Japan

2-1. Materials

Reagents: Sodium citrate-treated pig blood (4% sodium citrate solution mixed with blood ratio of 1:9)

Dried *Artemisia vulgaris* leaf powder

2-2. Chemicals

0.9 (w/v) % NaCl solution

99.5 (v/v) % ethanol

0.025 mol/L calcium chloride solution

2-3. Preparation of *Artemisia vulgaris* extract

Dried *Artemisia vulgaris* leaf powder was mixed at a ratio of 1 g of the powder with 75 mL of 99.5% (v/v) ethanol. The mixture was then put into an evaporator to obtain the *Artemisia vulgaris* extract.

2-4. Confirmation of Blood Coagulation Effects

Pig blood was treated with sodium citrate, which binds calcium in the blood and inhibits coagulation. Therefore, calcium chloride solution was added to restore coagulation function.

1. Preparation: In a test tube, mix 40 mL of 0.9% (w/v) NaCl solution with 25 drops (approximately 1.25 mL) of the porcine blood, and stir the mixture.
2. Step: Divide the stirred mixture equally into two test tubes, adding 2 mL of 0.9% (w/v) NaCl solution. 2 mL of 0.9% (w/v) NaCl to one and 2 mL of calcium chloride solution to the other.
3. Incubation: Place the test tubes in a water bath at 35°C to 40°C for 5 minutes. Filter the solution through Kimwipes and transfer it to cuvettes. Measure the absorbance using a spectrophotometer, using water with an absorbance of 0 as the baseline.
- 4.

2-5. Experiment on Coagulation Promotion by *Artemisia vulgaris*

To the sodium citrate-treated porcine blood, calcium chloride solution and *Artemisia vulgaris*

extract were added to restore coagulation function. Since the *Artemisia vulgaris* extract contains ethanol, a control group was created by mixing calcium chloride solution with ethanol.

1. Preparation: In a test tube, mix 40 mL of 0.9% (w/v) NaCl solution with 25 drops (approximately 1.25 mL) of the porcine blood, and stir the mixture.
2. Step: Divide the stirred mixture equally into two test tubes. To one tube, add 2 mL of the extract diluted with 100 mL of calcium chloride solution; to the other, add 2 mL of ethanol diluted with 100 mL of calcium chloride solution.
3. Incubation: Place the test tubes in a water bath at 35°C to 40°C for 5 minutes. Filter the solution through Kimwipes and transfer it to cuvettes. Measure the absorbance using a spectrophotometer, using water with an absorbance of 0 as the baseline.

2-6. Statistical Analysis

The data were analyzed using a t-test, with significance set at $p < 0.05$.

3. Results

Thailand

An absorption spectrophotometry was used to compare the peak of the substance. After dropping 10 drops of blood in the extract. When the light in a spectrophotometer passes through the solution, the detector will transfer the result into an absorbance graph.

From Figure 3, when the extract was mixed with blood, the peak value decreased from 1.414 to 0.851, indicating a change. However, factors such as the color of the substance or the dilution of the solution make it unclear to draw a definitive conclusion about the cause of this change.

From Figure 4, when the mixture was left for 10, 20, and 30 minutes, the spectrum lines showed a slight decrease in the peak value as well

Japan

Result 1: From Method 2-5, the absorbance of the group with saline (n=3) was 2.1926 ± 0.069 , while the absorbance of the group with calcium chloride (n=3) was 1.4000 ± 0.062 ($p=0.00028$). A lower absorbance indicates greater transparency, which is attributed to the generation of fibrin due to coagulation and its subsequent removal through filtration. This result indicates that sodium citrate-treated blood coagulates upon the addition of the calcium chloride solution.

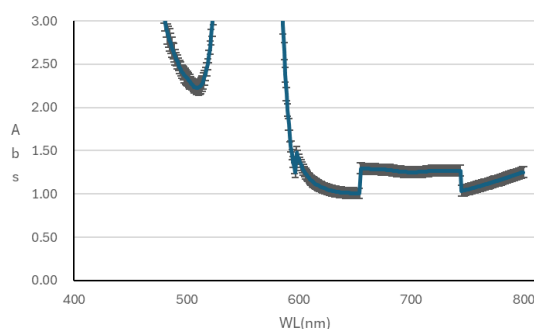


Figure 4

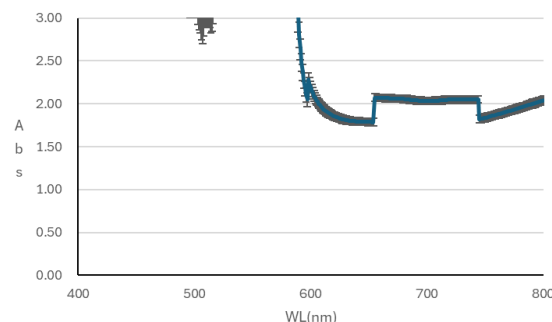


Figure 5

Figure 4. Wavelength and absorption of light for a saline and pig blood solution.

Figure 5. Wavelength and absorption of light for a saline, pig blood, and CaCl₂ solution

Result 2: From Method 2-6, the absorbance of the group with *Artemisia vulgaris* extract (n=3) was 1.3021 ± 0.056 , while the absorbance of the group with ethanol (n=3) was 1.4129 ± 0.044 ($p=0.0938$). Similar to Result 1, the lower absorbance suggests that fibrin was generated through coagulation and removed via filtration, indicating a trend towards enhanced coagulation with the addition of *Artemisia vulgaris* extract.

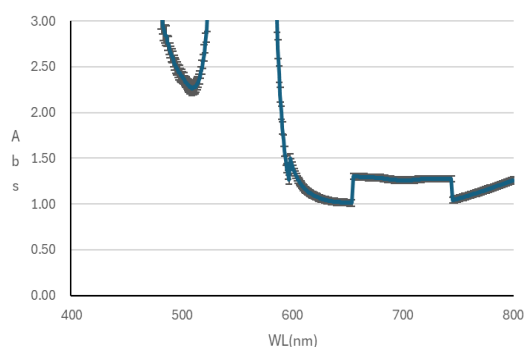


Figure 6

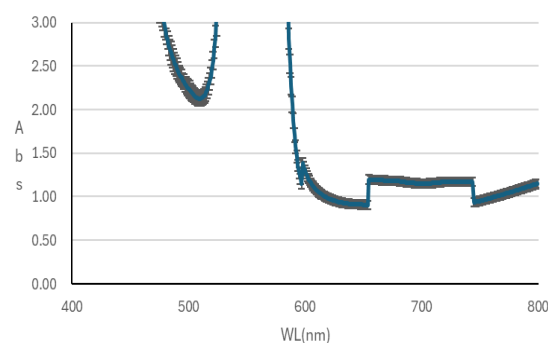


Figure 7

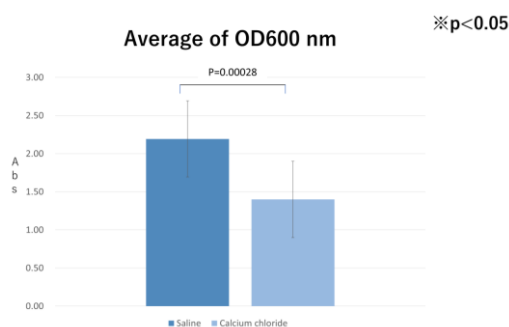


Figure 8

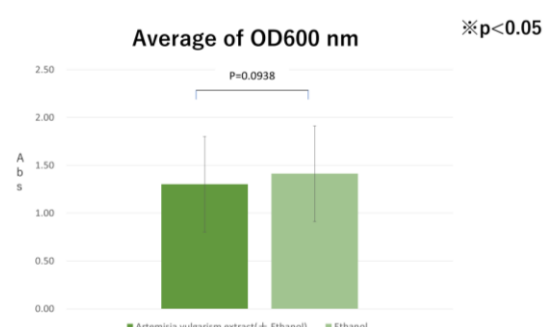


Figure 9

Figure 6. Wavelength and absorption of light for a saline , porcine blood, CaCl_2 , and *Artemisia vulgarism* extract solution.

Figure 7. Wavelength and absorption of light for a saline water, porcine blood, CaCl_2 , and ethanol solution.

Figure 8. Result of *T-test* between saline water and CaCl_2 aq.

Figure 9. Results of *T-test* between CaCl_2 aq and CaCl_2 aq + ethanol and CaCl_2 aq + *Artemisia vulgarism* extract.

Discussion: The results of the experiments investigating whether *Artemisia vulgaris* promotes secondary hemostasis by facilitating fibrin formation showed no significant promoting effect. This suggests that a different mechanism may be involved in the hemostatic effect of *Artemisia vulgaris*. For example, there is a possibility that the tannins abundant in *Artemisia vulgaris* may help the hemostatic effect by causing astringent action. Additionally, the sample size in this experiment was small, and the t-test results may not accurately reflect significant differences. Since platelet aggregation was not directly compared or evaluated, it's still possible that *Artemisia vulgaris* effects primary hemostasis by promoting platelet activation or aggregation. Furthermore, considering the thinking that *Artemisia vulgaris* acts when applied directly to the bleeding site, it may be due to its astringent action or other effects. Thus, further studies and experimental approaches from different perspectives are needed to better understand the hemostatic effects of *Artemisia vulgaris*.

4. Conclusion

The extract from *Eclipta prostrata* Linn. exhibited changes in absorbance when mixed with blood. However, these results cannot conclusively identify the substances responsible for the peaks or the causes of the changes, as factors such as solution dilution and color may influence the results. In contrast, the extract from *Artemisia vulgaris* showed no changes in absorbance. Therefore, the evaluation methods used in this study are deemed unsuitable. To obtain more reliable and conclusive results, the LTA (Light Transmission Aggregometry) method, a standard technique for measuring platelet function by assessing how light passes through a platelet suspension, is recommended.

5. References

1. Pawadee Chinudomwong, Karan Paisooksantivatana & Narin Khongjaroensakun. (2020). *A Study of Reference Interval for Platelet Aggregation Test Using Light Transmission Aggregometry in Thai Population*. Mahidol University.
2. Suwanna Semsri, et al. (2017). Effects of extracts from *Eclipta prostrata*, *Chromolaena odorata*, *Centella asiatica*, and *Terminalia chebula* on the blood coagulation system. *HCU Journal of Science and Technology*, 2017(3), 42-53. Retrieved from <https://medplant.mahidol.ac.th/user/reply.asp?id=7459>.
3. Cleveland Clinic. (2021). Hemostasis. Retrieved December 17, 2023, from <https://my.clevelandclinic.org/health/symptoms/21999-hemostasis>.
4. Kornkanok Akeyothinwong, et al. (2019). Antioxidant activity and bioactive compounds of Kameng (*Eclipta prostrata* Linn.) extracts. *Thai Journal of Science and Technology*.
5. (n.d.). UV-visible absorption spectra of blood and EB diluted in water. Retrieved from https://www.researchgate.net/figure/UV-Visible-absorption-spectra-of-blood-and-EB-diluted-in-water-A-Five-microliters-of-a_fig1_267273300.
6. Ocean Optics. (n.d.). Whole blood analysis. Retrieved from <https://www.oceanoptics.com/blog/whole-blood-analysis/>
7. Akeyothinwong, K., Sakkayawong, N., & Damrianant, S. (2020). Antioxidant activity and bioactive compounds of Kameng (*Eclipta prostrata* Linn.) extracts. *Thai Journal of Science and Technology*, 9(1), 46-47.
8. Ohkura, N. Plant-Derived Substances with Hemostatic Effects. *The Chemical Times*, 243(1), 22-27. Kanto Chemical.
9. Okuda, T. (1983). The Utility of Tannins. *Journal of the Brewing Society of Japan*, 78(10), 728-732.
10. Tomiyama, Y., Sato, K., Ozaki, Y., Shimizu, M., Tamura, N., Nishikawa, M., ... & Hato, T. (2016). Introduction and Commentary on "Standardization of Light Transmission Platelet Aggregation Testing: Recommendations from the Platelet Function Standardization Subcommittee of the International Society on Thrombosis and Haemostasis." *Journal of the Japanese Society on Thrombosis and Hemostasis*, 27(3), 365-369.
11. Toda, S. (2012). A Study on the Antioxidant Effects of *Artemisia* (Yomogi). *Bulletin of Kansai University of Health Sciences*, 6, 20-32.
12. Tsukada, M. (1991). 2. Platelet Function Tests and Their Issues. *Journal of the Japanese Society of Internal Medicine*, 80(6), 822-827.

Developing Hemostatic Agents Using Different Plants

Noa Sato¹, Tomoho Yasuda¹, Natsuki Yoshimatsu¹,

Mathis Dubas², Teepob Tajchakavit², Suphachat Sriharan²

¹ Nara Prefectural Seisho High School (Japan)

² Chulalongkorn University Demonstration Secondary School (Thailand)

Abstract:

Portulaca oleracea and *Chamaesyce maculata* are known to have hemostatic effects, but the mechanism has not been elucidated. The purpose of this study was to reveal that these plants transform fibrinogen into fibrin. These plants were added to a fibrinogen solution and the absorbance value for each plant was measured. The absorbance values of the experimental plots were defined by samples containing distilled water and either *Portulaca oleracea* or *Chamaesyce maculata* with fibrinogen subtracted from blank samples without fibrinogen. The results showed that the absorbance values of the experimental plots were significantly greater than those of the control (t-test $p < 0.05$) when *Portulaca oleracea* was added (t-test $p > 0.05$), while there was no significant difference for *Chamaesyce maculata* (t-test $p > 0.05$). This data suggests that *Portulaca oleracea* converted fibrinogen into fibrin. It is known that thrombin cleaves fibrinogen, exposing polymerization sites and resulting in fibrin monomers. These monomers then polymerize to form fibrin polymers, which are stabilized by transglutaminase (factor XIIIa), leading to hemostasis. (Takeo et al. 2013). Transglutaminase is also known to be present in plants. Previous research and these results suggest that the transglutaminase in *Portulaca oleracea* converted fibrinogen into fibrin.

Keywords: *Portulaca oleracea*; *Chamaesyce maculata*; fibrinogen; fibrin; hemostatic effects

1. Introduction

Plants are often used in Chinese medicine and some species are known to have hemostatic effects. However, the mechanism and components of hemostasis in these plants have not been revealed. This study aims to clarify them. Hemostatic agents are generally derived from animal sources, such as bones and skins of cattle, pigs, and human plasma proteins. Therefore, if plant-derived hemostatic agents could be developed, they would be a viable alternative to animal-derived hemostatic agents and could be used as a quick response to disasters and other emergencies, contributing to SDG3, “Good Health and Wellbeing.”

2. Methodology

[Experiment 1 - Japan]

The purpose of this experiment was to clarify that four different plants: *Portulaca oleracea*, *Portulaca grandiflora*, *Chamaesyce maculata*, and *Prunus yedoensis* transform fibrinogen into fibrin. A fibrinogen solution was prepared by mixing 1 mg of fibrinogen with 1 mL of distilled water. Next, a sample plant filtrate was prepared by mixing ground plants and distilled water at a ratio of 1:3. Then, 2950 µg of fibrinogen solution and 50 µL of plant filtrate were placed in a 3 mL cell, and absorbance value for each experimental plot was measured. The fibrinogen solution was kept at 37°C using a hot water bath. For the boiled *Portulaca oleracea*, it was ground and boiled at 100°C for 15 minutes. For the control, the samples were distilled water with fibrinogen; sample blanks were distilled water. For the experimental plot, the samples were distilled water with plant filtrate and fibrinogen, and sample blanks were distilled water with plant filtrate. The absorbance value of each plot was measured. The absorbance of fibrinogen alone is calculated by subtracting the absorbance of the sample blank from the sample. This was done three times for each plot.

[Experiment 2 - Thailand]

The purpose of this experiment was to investigate the effects of *Portulaca oleracea*, commonly known as purslane, on the speed of blood coagulation to determine whether it accelerates or slows down the process. Purslane is a plant known for its medicinal properties, and its potential influence on coagulation could have implications for its use in treating blood-related conditions. The experiment began with the preparation of extracts, where the plant material was thoroughly crushed and mixed with water in two different concentrations: a high concentration of 80 g/L and a low concentration of 16 g/L. For each

concentration, 12.5 ml of the solution was prepared to ensure consistent testing. The mixtures were then centrifuged to remove solid residues, leaving a clear liquid extract for analysis. To investigate the impact of storage conditions on the extracts' effectiveness, they were stored in two controlled environments: a deep-freeze condition at -20°C and a refrigeration condition at -4°C. These varying temperatures were chosen to evaluate how storage stability might influence the plant's properties. Finally, the prepared extracts were tested for their effects on blood coagulation using turbidity as a measurement method. Turbidity levels served as an indicator of coagulation speed, with changes in clarity correlating to the plant's influence on the process. This experiment provides insights into the potential medical applications of *Portulaca oleracea* in blood-related treatments.

3. Results

The following photos show the results of each experiment. *Portulaca oleracea* and *Portulaca grandiflora* were cloudier and whiter than the control (Figure 1, 2). There were almost no differences between *Chamaesyce maculata*, *Prunus yedoensis*, and the control (Figure 3, 4).



Figure 1

Portulaca oleracea (raw)

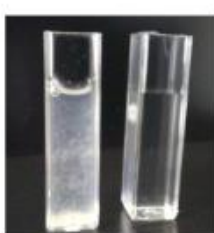


Figure 2

Portulaca grandiflora



Figure 3

Chamaesyce maculata

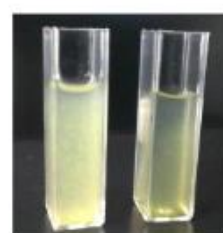


Figure 4

Prunus x yedoensis

Left: sample (plant filtrate of each plant, distilled water, fibrinogen solution)

Right: control (distilled water, fibrinogen solution)

The absorbance value for each experimental plot is shown in Figure 5. The absorbance values of the raw and boiled *Portulaca oleracea* and *Portulaca grandiflora* were significantly higher than those of the control. The increase in absorbance can be attributed to an increase in solid fibrin. Therefore, it is suggested that *Portulaca oleracea* (raw and boiled) and *Portulaca grandiflora* had the ability to transform fibrinogen into fibrin. On the other hand, *Chamaesyce maculata* and *Prunus yedoensis* were not significantly different from the control. Since *Prunus yedoensis* is not known to have hemostatic effects, we used it as a negative control to confirm that not all plants can transform fibrinogen to fibrin. There was no significant difference between raw and boiled *Portulaca oleracea*, where the proteins were deactivated, but the absorbance value was smaller in the boiled one.

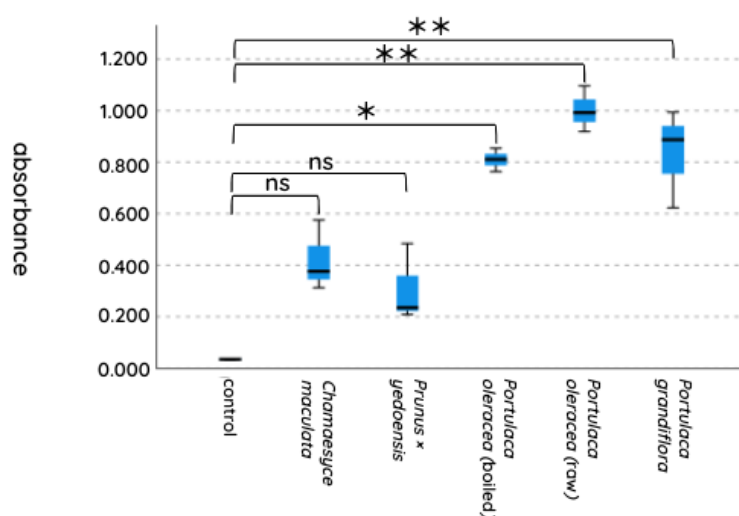


Figure 5. The absorbance values of the sample blank from the sample. Type of plant. (Experiment 1)

4. Discussion

From previous studies, thrombin cleaves the polymerization site of fibrinogen so that it comes to the surface. Fibrinogen becomes a fibrin monomer with the polymerization site visible and is polymerized by transglutaminase into fibrin polymer, which is known to stop bleeding. *Portulaca oleracea* and *Chamaesyce maculata* have transformed fibrinogen into fibrin. Plants are also known to have transglutaminase, as explained earlier.

5. Conclusion

The results from previous studies and this study suggest that transglutaminase transformed fibrinogen into fibrin rather than thrombin. These results indicate that the hemostatic effect is achieved by transforming fibrinogen into fibrin in *Portulaca grandiflora* and *Portulaca oleracea*. The enzyme called transglutaminase was considered to be involved in this process because transglutaminase is known to be generally included in plants. The fact that the absorbance value of boiled *Portulaca oleracea* was lower than that of raw one was considered to be due to the deactivation of the enzyme. However, despite the enzyme becoming deactivated, *Portulaca oleracea* did not have the same hemostatic effect as *Prunus yedoensis*, and its absorbance value remained high. This is considered to be due to the presence of a substance that does not lose its function even when *Portulaca oleracea* is boiled. It is suggested that *Portulaca oleracea* uses both the enzyme, which is a protein, and an unknown substance that does not lose its function when boiled, to transform fibrinogen into fibrin.

6. References

- AXEL. Standard Quartz Cell for Spectrophotometer. AXEL. <https://axel.as-1.co.jp/asone/d/2-7644-02/>
- Chugh, V., Mishra, V., Dwivedi, S., & Sharma, K. (2019). Purslane (*Portulaca oleracea* L.): An underutilized wonder plant with potential pharmacological value. ~ 236 ~ *the Pharma Innovation Journal*, 8(6), 236–246. <https://www.thepharmajournal.com/archives/2019/vol8issue6/PartE/8-5-92-356.pdf>
- FUJIFILM Wako Pure Chemical Corporation. Fibrinogen, from Human Plasma. FUJIFILM. <https://labchem-wako.fujifilm.com/us/product/detail/W01W0106-0369.html>
- Ibrahim, N., Ibrahim, S., Elbahaie, E., Kh, A., & Asalah. (2017). POSSIBLE MITIGATING EFFECTS OF CALORIC RESTRICTION OR PORTULACA OLERACEA L. (PURSLANE) EXTRACT ON COAGULATION AND FIBRINOLYTIC PROCESSES OF OBESE RAT. *Open Access Journal International Journal of Medical Research and Pharmaceutical Sciences*, 4(1), 2394–9414. <https://www.ijmrpsjournal.com/Issues%20PDF/Vol.4/January-2017/2.pdf>
- Kobra Shirani, Bamdad Riahi-Zanjani, Seyed Navid Omidkhoda, Barangi, S., & Karimi, G. (2023). The hematopoietic potential of methanolic and aqueous extracts of *Portulaca oleracea* in a phenylhydrazine model of anemia. DOAJ (DOAJ: Directory of Open Access Journals), 13(1), 85–96. <https://doi.org/10.22038/ajp.2022.20965>
- Kojima Pharmacy. *Portulaca oleracea*. *Kojima Pharmacy Kanpodou*. <https://kanpoudou.com/news/五行草スベリヒユ/>
- Nguyen T. Van Anh, and Le H. Luyen. “Potential Inhibitory Effects on Human Platelet Aggregation and Blood Coagulation of the Aerial Part of *Portulaca Oleracea* L.” *Trop J Nat Prod Res*, vol. 8(1), no. Tropical Journal of Natural Product Research, 1 Feb. 2024, pp. 6001–6005, <https://www.tjnpr.org/index.php/home/article/view/3417>
- TAKEO, Kazuhiro, et al. (2013). Diversity of Fibrinogen: Its Structure, Function, and Molecular Evolution. *Journal of Hemostasis and Thrombosis*, 24(3), 300-317.
- Takuma KAWASAKI, et al. (2017). Simple Method for Density Measurement of Cultured Algae Applying an Absorption Spectrometer. *Journal of Fisheries Technology*, vol. 9 (1), 27–31. https://www.fra.go.jp/home/kenkyushokai/book/fish_tech/files/090104.pdf
- United Nations. THE 17 GOALS. *United Nations*. <https://sdgs.un.org/goals>
- WDB Co., Ltd.. Spectrophotometer. *Kenkyu.net*. <https://www.wdb.com/kenq/dictionary/absorption-photometer>.

- Wide Area Administration Association of Amami Islands. *Chamaesyce maculata*. *Amami Islands bioresource Web Database*.
https://www.amami.or.jp/Seibutsusigen/Detail_plant/Plant_detail_600.html
- Mu, K., Liu, Y., Liu, G., Ran, F., Zhou, L., Wu, Y., Peng, L., Shao, M., Li, C., & Zhang, Y. (2023). A review of hemostatic chemical components and their mechanisms in traditional Chinese medicine and ethnic medicine. *Journal of Ethnopharmacology*, 307, 116200–116200. <https://doi.org/10.1016/j.jep.2023.116200>
- Zeng, Z., Nallan Chakravarthula, T., & Alves, N. J. (2020). Leveraging Turbidity and Thromboelastography for Complementary Clot Characterization. *Journal of Visualized Experiments*, 160. <https://doi.org/10.3791/61519>

The Study of Cellulose Fiber Water Filter from Bamboo and Teas

Chihiro Ishihara¹, Megumi Yokoyama¹, Nitchawee Piromchotesiri², Polawat Poowarattanakul²

¹ Ichikawa High School (Japan)

² Kamnoetvidya Science Academy (Thailand)

Abstract:

Since both Japan's and Thailand's rice farming are sensitive to water contamination, reliable water management is strongly required, especially in Thailand where water quality management is below standard. Bamboo and tea, both abundant agricultural products in Thailand and Japan, were selected for their high fiber content, biodegradability, and durability, making them suitable for water filtration applications. Bamboo fibers are known for their high cellulose content and durability, and tea fibers are similarly rich in fiber, making both materials ideal for filtration applications. To explore their filtration potential, this study synthesized cellulose fibers from both materials using H₂O₂ and HNO₃. The experiment involved fiber visualization and analysis using Scanning Electron Microscopy (SEM) and water purification efficiency testing through UV-Vis Spectrophotometry to observe absorbance changes linked to particle reduction in water. Results indicated that bamboo fibers, with finer diameters and softer textures, showed higher filtration efficiency compared to tea fibers. Increasing the concentration of H₂O₂ further enhanced water purification performance. This study highlights the potential of bamboo and tea agricultural waste for sustainable water filtration solutions, contributing to eco-friendly waste management and improved water quality in both Japan and Thailand.

Keywords: cellulose fiber; water filtration; bamboo; tea leaves; agricultural waste

1. Introduction

Both Thailand and Japan are particularly vulnerable to water contamination due to their reliance on rice farming, which poses serious risks to food security and public health. In Thailand, water quality challenges are largely driven by eutrophication, caused by nutrient runoff from agricultural fertilizers and untreated wastewater. A study in the Nakhon Nayok River basin found that aquaculture significantly contributes to nitrogen pollution, requiring a 12% reduction in nitrogenous waste to mitigate its impact [5]. These issues highlight inadequacies in Thailand's water management systems, including weak regulations, insufficient wastewater treatment, and poor enforcement of environmental standards [6].

Similarly, parts of Japan face tap water contamination from nitrate nitrogen derived from agricultural fertilizers, which poses cancer risks when consumed in excess. To address these issues, cellulose fibers are being developed for water purification. Synthesized by agricultural by-products like bamboo and tea, these fibers offer sustainable and effective solutions.

- **Bamboo**, widely available in both Thailand and Japan, produces approximately 800 kg to 1 metric ton of agricultural waste daily in Thailand alone [2]. Its high cellulose content, strength, and durability make bamboo fibers ideal for filtration materials [3].
- **Tea leaves**, a significant agricultural product in Japan, consist of about 60% insoluble fiber and generate by-products like stems and lower-quality leaves. These by-products hold potential for filtration applications due to their high fiber content [1][7].

This study focuses on comparing cellulose fibers derived from agricultural waste, produced using straightforward methods and commonly available chemical substances. The objective is to identify the optimal conditions for creating efficient water filters and to compare the outcomes between Thailand and Japan.

2. Methodology

2.1. Cellulose Fiber Synthesize

2.1.1. Bamboo Fiber Preparation

1. Collect several bamboo branches.
2. Separate the stems and leaves.
3. Heat the bamboo stems at **60°C for 24 hours** in a Memmert universal oven.
4. Blend the bamboo stems using a regular blender until they are finely ground.
5. Prepare **three sets of 5 g** of blended bamboo.

2.1.2. Chemical Treatment Setup

6. Prepare the following solutions in labeled beakers:
 - **Beaker 1:** 34 ml of 30% H₂O₂ and 200 ml of 3.2M HNO₃.
 - **Beaker 2:** 34 ml of 30% H₂O₂ and 200 ml of 3.2M HNO₃.
 - **Beaker 3:** 68 ml of 30% H₂O₂ and 200 ml of 3.2M HNO₃.
7. Add **5 g of blended bamboo** to each beaker.

2.1.3. Reaction Process

8. Subject each beaker to the following conditions:
 - **Beaker 1:** Stir and heat using a magnetic stirrer and hot plate at **60°C for 24 hours**.
 - **Beakers 2 and 3:** Stir at room temperature using a magnetic stirrer for **24 hours**.

2.1.4. Post-Reaction Processing

9. Dilute the solution in each beaker with DI water, adding an amount equal to the solution volume in the beaker.
10. Prepare the vacuum filtration setup, including:
 - Vacuum flask
 - Rubber bung
 - Funnel
 - Filter paper
 - Rubber tubing
 - Vacuum pump
11. Filter the solution until only cellulose fibers remains.
12. Wash the cellulose fibers thoroughly with DI water.
13. Remove the cellulose fibers from the filter and allow them to dry completely.

2.1.5. Tea Leaf Fiber Synthesis

14. Repeat steps 2.1.1 to 2.1.4, substituting dried tea leaves for bamboo stems in all processes.

2.2. Physical Properties of the Filter

2.2.1. Color and Texture

1. Take a picture of each filter after it dried.
2. Touch and noted down the texture.

2.2.2. Scanning Electron Microscope Analysis

1. Cut the fiber into a small piece.
2. Paste the specimen fiber onto the Scanning Electron Microscope stage. Cover all specimen with the carbon tape to guarantee the conductive.
3. Measure the diameter and size of the fiber.

2.3. Water Purification Efficiency Analysis

2.3.1. Filtration System Setup

1. Set up a vacuum filtration system as described in section 2.1.10, replacing the filter paper with the cellulose fibers obtained from section 2.1.

2.3.2. Water Sample Collection

2. Collect a sample of unpurified water from a natural water source (e.g., pond, lake, or river).

2.3.3. Filtration Process

3. Filter the unpurified water using the setup from section 2.2.10.
4. Label the purified water samples according to the cellulose fiber used during filtration.

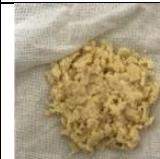

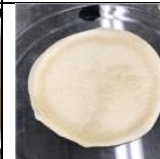
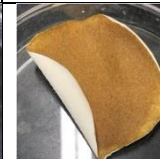




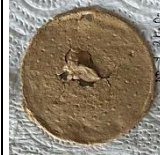



2.3.4. UV-Vis Spectrophotometry Analysis

5. Transfer each purified water sample into quartz cuvettes.
6. Measure the absorbance of each sample using a UV-Vis spectrophotometer.
 - Scan wavelengths from 300 nm to 800 nm.
 - Use the unpurified water sample as the baseline for comparison.
 - Use the DI water sample as the control for clear water sample.

3. Results and Discussion

3.1. Physical Properties of the Filter

Table 1. Effect of Temperature and H₂O₂ Volume on Bamboo and Tea Cellulose Fiber

Sample		Bamboo1	Bamboo2	Bamboo3	Tea1	Tea2	Tea3
Japan	Picture						
	Picture						

From our experiment, the color of cellulose fibers from bamboo was quite similar, ranging from light brown to deep brown. This consistent brown coloration may be caused by residual lignin and other natural compounds inherent in bamboo. In bamboo Beaker 3 (Japan), the palest color was observed, likely due to the highest level of bleaching. In contrast, tea cellulose fibers showed more variation in color, ranging from near black to off-white. The whiteness in some tea samples indicates effective removal of natural pigments and impurities during chemical treatment and post-reaction processing, while darker shades suggest that residues remained, potentially due to less efficient decomposition. Tea Beaker 2 (Thailand) showed the darkest color, which might reflect a less intensive decomposition process and greater retention of organic matter.

In terms of texture, bamboo-derived cellulose fibers were softer and more flexible compared to tea-derived fibers. Additionally, the yield percentage of bamboo fibers was lower than that of tea fibers, possibly due to bamboo having less undecomposable material than tea.

These differences in color, texture, and yield would affect how the filters perform in practical applications. Bamboo filters, with their consistent coloring, provide a more uniform baseline for material analysis. Darker tea-derived filters, with higher fiber density and residual content, could retain more organic matter but might reduce water flow.



Figure 1. Picture of Bamboo Cellulose Fiber under SEM, Kamnoetvidya Science Academy

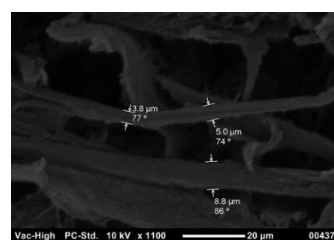


Figure 2. Picture of Tea Cellulose Fiber under SEM, Ichikawa High School

The two images above show fiber that was synthesized under typical conditions using a scanning electron microscope. The fibers are from Thailand and Japan. It demonstrates that the fiber's diameter is approximately micrometers.

Table 2. Average Cellulose Diameter Sorted by H₂O₂ Mass and Reaction Temperature

		Temperature		
		30°C	40°C	60°C
H ₂ O ₂ Mass	37.4g	5.3	2.8	2.9
	74.8g	2.4	0.9	3.9

Table 2 shows that an increase in reaction temperature led to a decrease in fiber diameter. This is caused by the temperature increase causing the molecules to move in active thermal motion, enabling the chemical substances to collide with each other more frequently and encouraging the reaction.

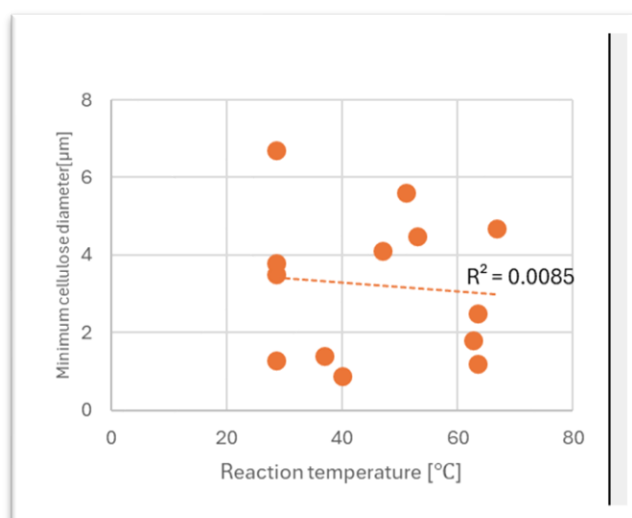


Figure 3. Reaction temperature and the minimum diameter of acquired cellulose

Plotting the data in graph, the trend line is the approximate straight line of the data shown in dots. Moreover, as shown in figure 2, increasing the mass of H₂O₂ also decreased the diameter of the fiber in most of the samples. This behavior can be attributed to the role of H₂O₂ as a regenerating agent for HNO₃, which acts as an oxidizer. The HNO₃ facilitates the breaking of hydrogen bonds in cellulose, leading to finer fibers. [8]

As it could be seen in figure 3, we were unable to see a correlation between the reaction temperature and cellulose diameter.

3.2. UV-Vis Spectrophotometry Analysis

UV-visible spectrophotometry measures water quality by detecting specific substances, color, and suspended solids. Lower absorbance values indicate cleaner water, reflecting the effectiveness of the purification process.

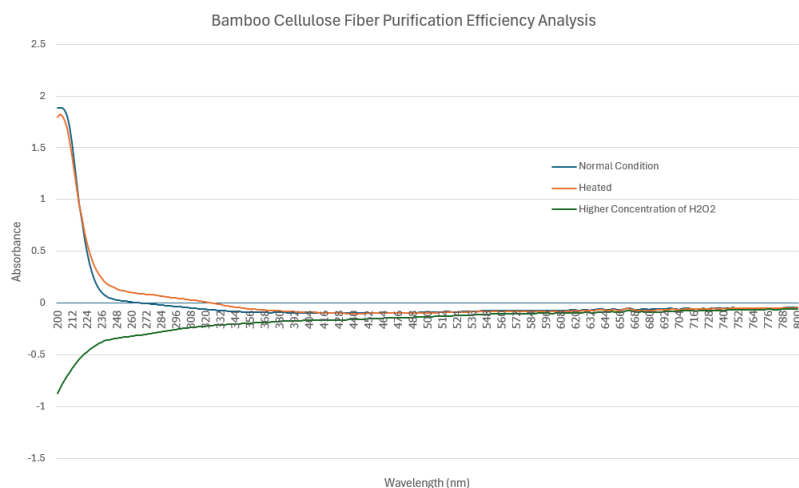


Figure 4. Purification analysis of cellulose fibers synthesized from bamboo with three different conditions including normal condition, heated, and high amount of H_2O_2 .

Using natural water as the baseline, the absorbance difference reflects the effectiveness of bamboo cellulose fibers. Based on literature review [9], variations between filters are observed in the 200 to 800 nm wavelength range. Figure 4 above shows the comparison of UV-Vis Spectrophotometry result of water after filtered by three different bamboo filters. The filter synthesized with a high H_2O_2 volume shows the best performance, achieving the lowest absorbance at small wavelength. The other two filters, synthesized under standard conditions or with heat, yield similar results.

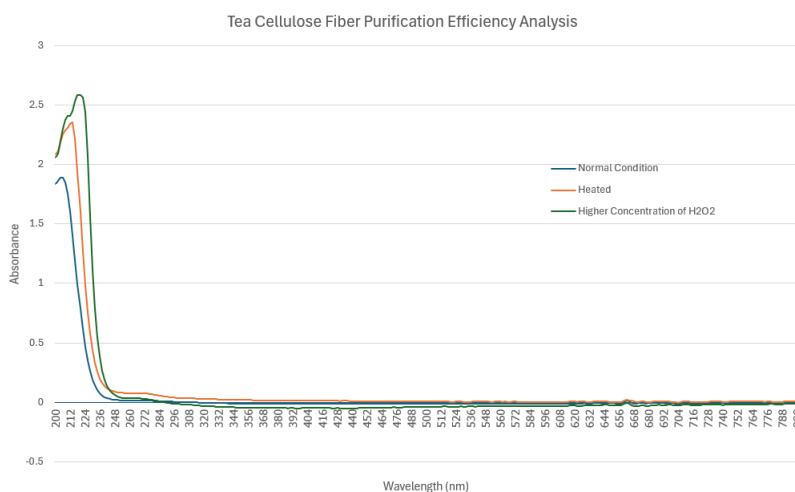


Figure 5. Purification analysis of cellulose fibers synthesized from tea with three different conditions including normal condition, heated, and high amount of H_2O_2 .

Figure 5 above shows the comparison of UV-Vis Spectrophotometry result of water after filtered by three different tea filters. The filter synthesized with a high H_2O_2 volume performs best, showing the lowest absorbance peak around 200 nm, though all three filters exhibit similar trends.

Both tea and bamboo filters achieve optimal performance under high H_2O_2 conditions, followed by normal and high-temperature conditions. Increasing the amount of H_2O_2 could potentially enhance filtering efficiency further.

4. Conclusion

This study demonstrates the simple process to synthesize cellulose fiber from bamboo and tea agricultural waste. Using common chemical compounds such as H_2O_2 and HNO_3 in chemical treatment and using temperature and number of substances as the independent variables.

Compared to tea-derived cellulose fibers, which are more waterproof and more difficult for water to penetrate, bamboo-derived cellulose fibers have softer textures and more uniform colors. SEM is used to analyze fiber diameter in greater detail. The findings showed weak relationships between temperature, H_2O_2 volume, and fiber diameter, the finer the fiber, the higher the concentration. Higher H_2O_2 volume filters perform best, obtaining the lowest absorbance values and demonstrating superior water purification efficiency, according to UV-Vis spectrophotometry analysis. This demonstrates how the performance of tea and bamboo filters could be improved by further optimizing the H_2O_2 concentration.

Overall, the goal of this study was to offer viable and sustainable water purification solutions. It could contribute to both Thailand and Japan in agricultural waste problem and water pollution which lead for an environmentally friendly approach.

5. Acknowledgements

We want to gratefully acknowledge our advisors, Dr. Prasongporn Ruengpirasiri, Mr. Jin Ihara, and Mr. Yuki Miyazawa, for their essential assistance, support, and direction during this research. Thanks to Teacher Siriporn Suntiworapong and Natthaputtiya Klayposri, KVIS Laboratory teacher who always guide us to success the experiment. Their expertise and perceptive feedback have been beneficial to our research's progress. We are incredibly grateful for the time and effort they committed in guiding us while motivating me to engage with different concepts and methods in our work.

6. References

- Bai, X., He, Y., Quan, B., Xia, T., Zhang, X., Wang, Y., ... & Wang, M. (2022). Physicochemical properties, structure, and ameliorative effects of insoluble dietary fiber from tea on slow transit constipation. *Food Chemistry: X*, 14, 100340.
- Hornaday, F. (2024, April 29). WongPhai and Planboo bring Biochar to Thailand - Planboo. *Planboo*. <https://planboo.eco/wongphai-and-planboo-bring-biochar-to-thailand/#:~:text=Bamboo%20waste%20management&text=The%20province%20of%20Prachinburi%2C%20as,into%20a%20zero%2Dwaste%20industry>.
- Liu, D., Song, J., Anderson, D. P., Chang, P. R., & Hua, Y. (2012). Bamboo fiber and its reinforced composites: structure and properties. *Cellulose*, 19(5), 1449–1480. <https://doi.org/10.1007/s10570-012-9741-1>
- Suzuki, S., & Nakagoshi, N. (2011). *Sustainable management of satoyama bamboo landscapes in Japan*. https://doi.org/10.1007/978-4-431-87799-8_15
- Thitanuwat, B., & Wongsoonthornchai, M. (2021). Estimation of Nitrogen Loading to Surface Water from Agriculture Based Area and Its Application for Water Pollution Mitigation. *Environment & Natural Resources Journal*, 19(3).
- Thinphanga, R. F. & P. (2023, August 5). Tackling Thailand's water problems. <https://www.bangkokpost.com>. <https://www.bangkokpost.com/opinion/opinion/2623807/tackling-thailands-water-problems>
- Wikipedia contributors. (2024, November 22). *Tea culture in Japan*. Wikipedia. https://en.wikipedia.org/wiki/Tea_culture_in_Japan
- Wang, J., Li, X., Song, J., Wu, K., Xue, Y., Wu, Y., & Wang, S. (2020). Direct Preparation of Cellulose Nanofibers from Bamboo by Nitric Acid and Hydrogen Peroxide Enables Fibrillation via a Cooperative Mechanism. *Nanomaterials*, 10(5), 943. <https://doi.org/10.3390/nano10050943>
- Uchiyama, T. (2022, August 15). Water Analysis using a UV-Visible Spectrophotometer | JASCO. JASCO Inc. <https://jascoinc.com/applications/water-analysis-uv-visible-spectrophotometer/>

Measuring Sugar In The Fruits To Serve As A Resource

Bongkodkan PLANANTAKUNTORN¹, Panisara PHADUNGWONG¹, Thitaree LANJANASTIENCHAI¹

Kouki FUKAGAWA², Ami YARA²

¹*Patumwan Demonstration School, Srinakharinwirot University (Thailand)*

²*Tokai University Takanawadai Senior High School (Japan)*

Abstract:

Recently, the number of diabetes patients in the world has been increasing. Therefore, we focused on the diet of diabetic patients. Among the diets, we focused on fruits. In our experiment, we measured four fruits in each of Thailand and Japan, three of which used the same fruits, and one of which used seasonal or famous fruits in Thailand and Japan. We then measured the sugar content of each fruit three times. In Thailand, we used watermelon, melon, orange, and longan. In Japan, we used watermelon, melon, orange, and pear. The purpose of the experiment was to measure the sugar content of fruits and increase the options of fruits that diabetic patients can eat. The results of the experiment showed that melon had the lowest sugar content in both Thailand and Japan, and orange had the highest sugar content. And because the sugar content of watermelon was low, we thought that the sugar content of fruits in the Cucurbitaceae family might be low.

Keywords: sugar content, diabetes, fruit

1. Introduction

As diabetes rates rise, people become more aware of the health risks associated with it, preferring to eat healthier and choosing fruits over snacks or desserts because they believe it is better for their health and to avoid excessive sugar consumption, but each fruit contains varying amounts of sugar, which may lead to sugar overconsumption. As we became aware of this issue, we decided to evaluate the sugar content of popular fruits in Thailand and Japan in order to learn more and provide consumers in both countries with more options when it comes to fruit selection.

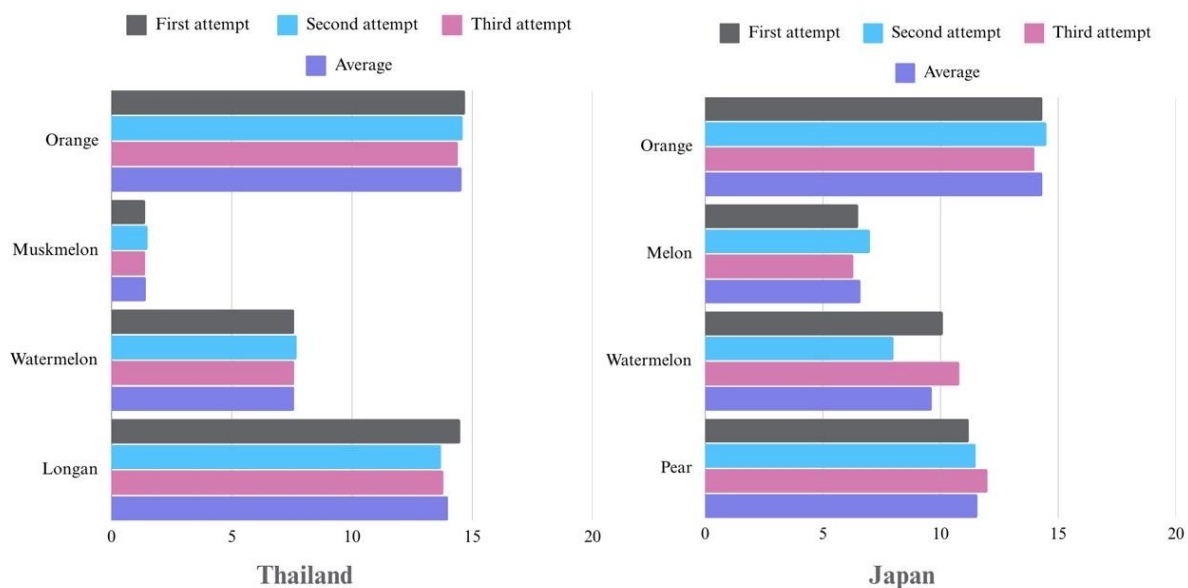
2. Methodology

1. Start by cutting the fruit into small pieces and crushing it thoroughly to extract the juice effectively. And transfer the crushed fruit pulp into a beaker.
2. Draw up the extracted juice using a dropper.
3. Pour the juice into the inverted sugar refractometer and let it measure the amount of sugar.
4. Repeat steps 2 and 3 at least three times, then analyze the recorded data to identify a trend or pattern in the sugar content.
5. Summarize the findings, drawing conclusions based on the consistent measurements obtained.

3. Result

Thailand		Japan	
Fruits	Sugar (%w/w)	Fruits	Sugar (%w/w)
Watermelon	7.6	Watermelon	9.63
Muskmelon	1.43	Melon	6.6
Orange	14.56	Orange	14.33
Longan	14	Pear	11.57

4. Discussion



5. Conclusion

The results of the study show that the fruit with the lowest sugar content is the melon in Japan and Thailand, respectively. Next to melons, watermelons were also found to have low sugar content. This led us to believe that fruits in the Cucurbitaceae family do not have high sugar content. Based on this, it was expected that zucchini and squash would also have low sugar content. Next, it was found that the fruit with the highest sugar content was the orange in Japan and Thailand, respectively. Using the same approach as for the low-sugar fruit, we can expect oranges to be high in sugar content for the tangerine family, to which they belong. Based on these facts, we thought that fruits of the Cucurbitaceae family should be recommended for diabetics. As a future perspective, we thought that investigating more fruits in more families would broaden the food choices for diabetics.

6. Acknowledgements

We would like to express our sincere gratitude to our Thai and Japanese teammates, our supervisors, for their guidance and support throughout this research. Special thanks to JTB advisors for their valuable feedback. We also appreciate the financial support from Patumwan Demonstration School, Srinakharinwirot University & Tokai University Takanawadai Senior High School teachers. Lastly, we are grateful to our family and friends for their encouragement and understanding.

7. References

- [1] A. Trifiro, G. Saccani, S. Gherardi, E. Vicini, E. Spotti, M. P. Previdi, M. Ndagijimana, S. Cavalli, C. Reschiotto; *J. Chromatogr. A.*, 770, 243 (1997).
- [2] L. E. Rodriguez-Saona, S. F. Fry, M.A. McLaughlin, E.M. Calvey; *CarbohydrRes*, 336, 63 (2001).
- [3] G. P. Meade, J. C. P. Chem, 'Sugar cane Handbook', Wiley Group, (1985).
- [4] F. Cadet, F. W. Pin, C. Rouch, C. Robert, P. Baret; *Biochim. Biophys. Acta*, 1246, 142 (1995).
- [5] J. Prodoliet, C. Hischenhuber, *Z. Lebensm. Unters Forsch. A*, 207,1 (1998).
- [6] S. K. Henderson, A. F. Carol, J. D. Domijan; *J.Chem. Educ.*, 75, 1122 (1998).

Assessment of Doxorubicin and Ethanol Production Using Japanese and Thai Fruit Waste

Nakanishi Hana², Ananya Maneenut¹, Bhumiphat Srivaranon¹, Patwee Wasunantharat¹, Naka Yuzuki²

¹Patumwan Demonstration School (Thailand)

²Institute of Science Tokyo High School (Japan)

Abstract

Experiments exploring the effective use of inedible parts of fruits using microorganisms were evaluated in producing doxorubicin and ethanol. The fruits used were the same oranges, and the Thai team added papaya and mangoes in total 3 kinds of fruits, and the Japanese team added Japanese pears in total 2 kinds of fruits. In the production of ethanol, the more the fruit contained nutritive components for the microorganisms, the greater the amount produced.

Doxorubicin, an anticancer drug essential for chemotherapy, faces production challenges due to high costs and low yields. This study explores the use of orange, papaya, and mango peel extracts—common agricultural waste in Thailand—as biostimulants to enhance doxorubicin production in *Streptomyces peucetius* fermentation. Peel extracts at concentrations of 50%, 25%, 12.5%, and 6.25% were tested, with yields analyzed using UV-Vis spectrophotometry. The results show that while peel extracts enhance doxorubicin production up to an optimal concentration, excessive levels inhibit fermentation. These findings highlight a novel, sustainable approach to reduce chemotherapy drug costs by optimizing doxorubicin production through agricultural waste valorization.

In the ethanol production experiment, fruits whose peels contain a source of energy for the yeast were easy to grow in this condition to proliferation, leading to more active alcohol fermentation and higher ethanol production. Also, ethanol has the property of evaporating. Thus, fruit peels with a smaller density than water were suitable for this alcohol experiment.

Keywords: microorganism; *Streptomyces peucetius*; natural yeast; doxorubicin; ethanol

1. Introduction

Background and Purpose

Thailand and Japan have common things; waste food, and Thailand waste 272 g/day, Japan waste 140 g/day. As a result, inedible parts of fruit (peels, seed, core) have many volumes. Actual data is this as Table 1.

Table 1. The Rejection rate of each fruit

Fruit consumption	Rejection rate(%)
Banana	40
Orange	35
Papaya	35
Mangoes	35
Grape	15
Japanese pear	15
Apple	8
Strawberry	2

We want to find the method of using the inedible part effectively, through using microorganisms in common. The Thai team focuses on *Streptomyces peucetius*, while the Japanese team focuses on natural yeast on fruit peels. *Streptomyces peucetius* produces doxorubicin which is an anticancer antibiotic used to treat various cancers.

Yeast fermentate in anaerobic and generate ethanol and carbon dioxide to get sugar. Yeast reaction formula: $C_6H_{12}O_6 \rightarrow 2C_2H_5OH + 2CO_2$

For this research's purpose, the Thai team generated doxorubicin, while the Japanese team did alcohol fermentation using fruit peels.

2. Methodology

The common fruit is oranges (*Citrus reticulata*). The Thai team added papaya (*Carica papaya*) and mangoes (*Mangifera indica*) in total 3 kinds of fruits, the Japanese team added Japanese pears (*Pyrus pylofonia*) in total 2 kinds of fruits.

2-1-1. Producing doxorubicin to use *Streptomyces peucetius* (PDS)

① Culturing of *S. peucetius*

Streptomyces peucetius ATCC 29050 was obtained from Thailand Bioresource Research Center. It was inoculated into 125-mL shake flasks containing 20 mL of starter medium (g/L): corn starch, 5; glucose, 5; soybean flour, 30; dry yeast powder, 1; NaCl, 1; KH_2PO_4 , 1; and $MgSO_4 \cdot 7H_2O$, 1. Flasks were autoclaved (121°C, 30 min) and shaken at 150 rpm, 28°C for 3 days

② Extraction of Fluids from Fruit Peels

The fruit peels were rinsed with tap water, dried at room temperature for 30 minutes, and torn into small pieces. Twenty grams of peels were finely ground with a mortar and pestle, then mixed with 20 mL of filtered water. The mixture was squeezed through a cloth strainer, filtered with a 0.45-micron syringe filter, and centrifuged at 6000 rpm for 10 minutes. The supernatant was diluted into four concentrations (50%, 25%, 12.5%, and 6.25% w/v) for each fruit, with the process performed once per fruit (Figure 1).

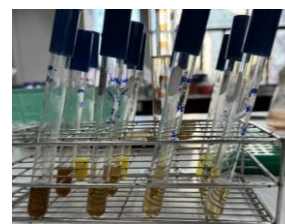


Figure 1. Dilutions of fruit peel extracts

③ Fermentation of *S. peucetius*

Four mL of each concentration of fruit peel extracts were added to its respective 125-mL flask containing 25 mL of fermentation medium. The fermentation medium, in g/L, consisted of: soybean oil, 80; soybean meal, 30; NaCl, 2; and CaCO₃, 3; and all of the fruit extract (Wang et al., 2018). All the media were autoclaved at 121°C for 30 minutes before use. After the growth period in the starter medium, 3 mL of *S. peucetius* starter culture was inoculated into each of the 125-mL shake flasks of fermentation medium (Figure 2). The shake flasks were put on a shaker at 180 rpm and 28°C for 7 days.



Figure 2. Fermentation media inoculated with *S. peucetius*

④ Measurement of Doxorubicin

Fermented solution from each shake flask was put into test tubes, which were centrifuged at 6000 rpm for 10 minutes. The supernatant of each trial was poured into cuvettes and then analyzed using a UV-Vis spectrophotometer at 496 nm. Optical densities of doxorubicin were recorded.

2-2. Producing ethanol to use yeast (STHS)

① **Taking fruit peels:** Took fruit peels and cut it out of 2 cm per side.

② **Preparing sugar solution:** Measuring glucose 30.0 g. Adding ultrapure water 150.0 g. After preparing the sugar solution, we boiled to heat sterilize. After we cooled it to room temperature and prepared sugar solution. Sugar solution is put into fermentation erlenmeyer flasks. At them, we prevented outside air from entering. 10 fruit peels with tweezers were put into one erlenmeyer flask and fermentate in incubator 30 °C (Figure 3)



Figure 3. Fermentation equipment

3. Results & Discussion

Thailand

3-1.

Table 2 summarizes the optical densities obtained for each fruit type across the different concentrations. Optical density (OD) is a measure of how much a substance absorbs light at a specific wavelength. In this experiment, OD reflects the concentration of doxorubicin produced in the fermentation medium. Figure 4 illustrates the OD trends at varying concentrations (50%, 25%, 12.5%, and 6.25%) for *Carica papaya*, *Citrus reticulata*, and *Mangifera indica* respectively.

Table 2. Optical Densities of Doxorubicin in Fermented Solutions with Different Concentrations of Fruit Peel Extracts

Fruit / Concentration	6.25%	12.5%	25%	50%
<i>Carica papaya</i>	0.433	0.858	0.661	0.180
<i>Citrus reticulata</i>	1.194	0.218	0.238	0.126
<i>Mangifera indica</i>	0.0081	0.235	0.781	0.163

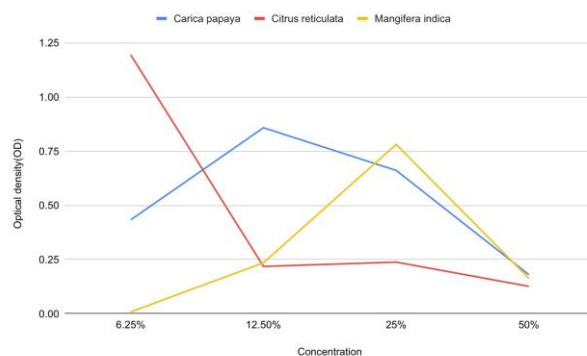


Figure 4. Optical Densities of Doxorubicin in Fermented Solutions with Different Concentrations of *Carica papaya*, *Citrus reticulata*, and *Mangifera indica* Peel Extracts

A Friedman test yielded a p-value of 0.3679, indicating no statistically significant difference in optical density (OD) values across tested concentrations (50%, 25%, 12.5%, and 6.25%) when blocking by fruit type (*Carica papaya*, *Citrus reticulata*, *Mangifera indica*). A Wilcoxon Signed-Rank test comparing peak production values with 50% concentration data ($W=0$, critical value=0 at $\alpha=0.05$) revealed a statistically significant decrease in doxorubicin production at 50%. Inhibitory effects were observed across all fruit types, with OD reductions of 79.0% (*C. papaya*), 89.4% (*C. reticulata*), and 79.1% (*M. indica*).

The experimental data revealed a biphasic response in doxorubicin biosynthesis. At lower concentrations (6.25–25%), the extracts enhanced production, with *C. reticulata* showing the highest stimulation (OD: 1.194) at 6.25%, followed by *C. papaya* (OD: 0.858) at 12.5% and *M. indica* (OD: 0.781) at 25%. This enhancement suggests the presence of beneficial secondary metabolites that may act as precursors or regulatory molecules in the doxorubicin biosynthetic pathway. However, at 50%, production sharply decreased (OD: 0.180, 0.126, and 0.163 for *C. papaya*, *C. reticulata*, and *M. indica*, respectively), indicating that excessive concentrations may create inhibitory conditions through antimicrobial effects, osmotic stress, or feedback inhibition mechanisms.

These inhibitory effects align with previous studies. Muhamad et al. (2017) reported antibacterial activity in *C. papaya* peels, Boudries et al. (2017) demonstrated antimicrobial properties of essential oils from *C. reticulata*, and Koirala et al. (2024) found antioxidant and antimicrobial activity in *M. indica* peels.

Japan

3-2-1.Fermentation(orange)

While fermenting, small bubbles were from the center of the sugar solution. After 1 fermentation day, peels were floated. Smells of alcohol couldn't be felt. From this, peels were gathered in the center of the flask. So the more fermentation went on, carbon dioxide concentration was easy to higher so lead bubbles were centered. Also, the momentum became stronger as day passed. The color of the solution was changed colorless and transparent into yellow. There weren't different from ①, ②, ③, so it wasn't cause concentration.

3-2.2.Fermentation(pear)

Table 4. Ethanol concentration(0~13 day)

Pear	Area value	EtOH(%)
①	5.51	19
②	5.23	18
③	5.02	17
Average	5.26	18

Table 5. Ethanol concentration and number of fruit peels

Pear	EtOH(%)	Number of pieces of peels floating
①	19	8
②	18	6
③	17	2
Average	18	5

While fermenting, big bubbles were from fruit peels. The more fermentation went on, the smells of alcohol became stronger and peels were floated. As from table 4, table 5, there were some relationships between number of floated peels and concentration of ethanol. As to table 5, it is higher concentration, and more the number of floated peels. The color of the solution was changed colorless and transparent into a light yellow color. Also, 1 fermentation day, peels were floated.

3-2-3.The differences of oranges and Japanese pears

Microbe could grow well like this condition; containing protein and oranges and Japanese pears mineral. Oranges and Japanese pears

Table 6. Ingredients of oranges and Japanese pears

	Orange	Pear
Protein(g)	0.9	0.3
Mineral(g)	0.4	0.3

had these values as shown in table 6. From table 6, microorganisms could grow in orange condition, oranges' ethanol concentration is higher than Japanese pear. Also, from 3-2-1,3-2-2, it was different to float and sink peels. Produced ethanol has the property of evaporating, and its density is 0.789~0.7919 g/cm³. Therefore, the condition of Japanese pears was that they evaporate.

4. Conclusion

In summary, this study demonstrates that incorporating *Carica papaya*, *Citrus reticulata*, and *Mangifera indica* peel extracts into fermentation media at lower concentrations (6.25–25%) enhances doxorubicin production in *Streptomyces peucetius*. However, higher concentrations (>50%) inhibit bacterial growth. These findings highlight the potential of fruit peel extracts as sustainable, cost-effective bioenhancers for doxorubicin production while emphasizing the need for precise optimization of extract concentrations. Further research should identify the optimal concentrations and the compounds responsible for inhibitory effects. The Japanese team uses oranges and Japanese pears peels. Eventually, the results of oranges are higher concentration than Japanese pears. Possible factors are proliferation of microorganisms and ethanol properties. The former, they are easy to grow when there are energy sources like protein and minerals. Orange peels include more of them than Japanese pears, so microorganisms could grow in this condition and alcohol fermented, it led to high concentration. The latter, ethanol has the property of evaporating, so peels which are smaller in density than water were suited for alcohol fermentation in this research.

5. Acknowledgements

We would like to express our sincere gratitude to Assistant Professor Somkiat Phornphisutthimas for his exceptional mentorship and for allowing us to use his laboratory at the Department of Biology, Faculty of Science, Srinakharinwirot University.

6. References

- Boudries, H., Loupassaki, S., Ladjal Ettoumi, Y., Souagui, S., Bachir Bey, M., Nabet, N., Chikhouné, A., Madani, K., & Chibane, M. (2017). Chemical profile, antimicrobial and antioxidant activities of *Citrus reticulata* and *Citrus clementina* (L.) essential oils. *International Food Research Journal*, 24 (4), 1782–1792.
<https://www.cabidigitallibrary.org/doi/pdf/10.5555/20173358227>
- FUJIFILM. (n.d.). エタノール (99.5) [Ethanol (99.5)] - FUJIFILM Wako. FUJIFILM Wako Chemical U.S.A. Corporation. Retrieved from <https://labchem-wako.fujifilm.com/jp/product/detail/W01W0105-0045.html>
- Koirala, P., Chunhavacharatorn, P., Suttisansanee, U., Benjakul, S., Katewongsa, K., Al-Asmari, F., & Nirmal, N. (2024). Antioxidant and antimicrobial activities of mango peel and radish peel—a comparative investigation. *Frontiers in Sustainable Food Systems*, 8, Article 1354393. <https://doi.org/10.3389/fsufs.2024.135439>
- MilliporeSigma. (n.d.). 微生物培地の基礎 [Fundamentals of microbial culture]. Retrieved from <https://www.sigmaaldrich.com/JP/ja/technical-documents/technical-article/cell-culture-and-cell-culture-analysis/microbial-cell-culture/microbial-media?msockid=0bbfdcc65642609a3053cf5a57d361fd>
- Ministry of Education, Culture, Sports, Science and Technology-Japan. (1994, October 1). *Food composition database*. Retrieved from <https://fooddb.mext.go.jp/whats.html>
- Muhamad, S. A. S., Jamilah, B., Russly, A. R., & Faridah, A. (2017). *In vitro* antibacterial activities and composition of *Carica papaya* cv. *Sekaki/Hong Kong* peel extracts. *International Food Research Journal*, 24(3), 976–984.
<https://www.cabidigitallibrary.org/doi/pdf/10.5555/20193000050>
- Suzuki, Akinori. (n.d.). Yeast growth. *J-Stage*. Retrieved from https://www.jstage.jst.go.jp/article/jbrewsocjapan1915/69/1/69_1_21/_pdf/-char/ja
- Wang, X., Tian, X., Wu, Y., Shen, X., Yang, S., & Chen, S. (2018). Enhanced doxorubicin production by *Streptomyces peucetius* using a combination of classical strain mutation and medium optimization. *Preparative Biochemistry & Biotechnology*, 48(6), 514–521.
<https://doi.org/10.1080/10826068.2018.146615>

The Study of Moon's Orbit by Kepler's Second Law

Takano Shinpei¹, Rui Sato¹, Phurit Jitpanya², Nanthiporn Sitthilerdchotpakdee², Tanawat Srisamran²

¹*Fukushima Prefectural High School (Japan)*

²*Princess Chulabhorn Science High School Mukdahan (Thailand)*

Abstract:

This report examines the Moon's areal velocity using Kepler's Second Law of Planetary Motion. Observations from Mukdahan (Thailand) and Fukushima (Japan) were conducted using a digital camera to calculate the Moon's distance from Earth and its areal velocity. The Moon's distance was determined daily based on its angular displacement, and the areal velocity was calculated by measuring the swept area over equal time intervals.

The results confirmed the elliptical nature of the Moon's orbit, with a wave-like variation in its distance from Earth. The areal velocity remained nearly constant, with a standard deviation of 10.49% for data from Thailand and 11.93% from Japan. Minor deviations were attributed to environmental and observational errors, including atmospheric interference and image processing limitations. Validation against data from the Stellarium application and traditional methods, such as Light Detection and Ranging (LIDAR) and parallax, supported the findings.

This study provides an accessible and practical method for amateur astronomers to validate Kepler's Second Law using basic tools and computational techniques, offering an alternative to more advanced methodologies while successfully demonstrating the law's applicability.

Keywords: Kepler's Second Law; Moon's orbit; areal velocity

1. Introduction

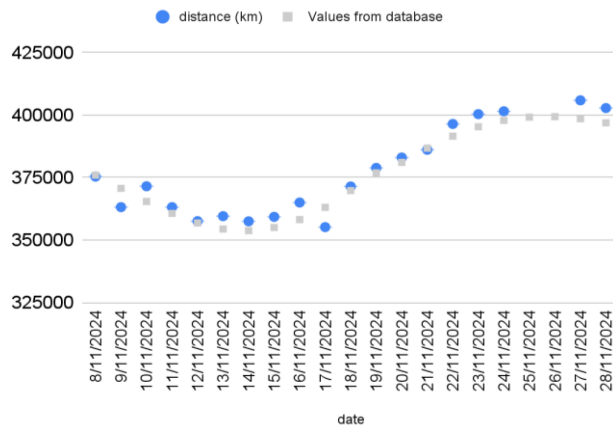
This report aims to study the relationship between the Moon's orbit and Kepler's Second Law, as well as the relationship between the Moon's angular velocity and Kepler's Second Law. While Kepler's Second Law of Planetary Motion, which states that a line joining a planet and the Sun sweeps out equal areas in equal time intervals, has been established for centuries, its practical application is rarely demonstrated.

Observations were conducted in Mukdahan, Thailand, and Fukushima, Japan. Data from Mukdahan are illustrated in Figure 1 (distance from Earth) and Figure 2 (areal velocity trends), with corresponding numerical data in Table 1 and Table 2. Data from Fukushima are represented in Figure 3 (distance) and Figure 4 (areal velocity trends), with corresponding numerical data in Table 3 and Table 4.

2. Methodology

We took some pictures of the Moon, and pictures of two stars to measure the Moon's angular distance. And we calculated the distance between the Earth and the Moon. The moon is photographed at the time of the south center every day during a certain period of clear days, and the distance D [km] from the earth to the moon is measured. The angular distance α [°] that the moon moves in its orbit in about one day appears as the delay time Δt [min] of the moon's south-central time on the next day, and is obtained using the fact that the earth makes one rotation (revolution) in 24×60 min.

The area velocity S_n [km²/day] of any day n is obtained by dividing the area ΔS_n [km²] of the triangle formed by connecting the line segment between the earth and the moon on this day (distance D_n) and the line segment of the moon on the next day $n+1$ (distance D_{n+1}) by the elapsed time.



3. Results

Figure 1: Distance between the Moon and Earth, using Mukdahan Province, Thailand as the observation point. (Circles represent calculated values, while squares represent values from the database.)

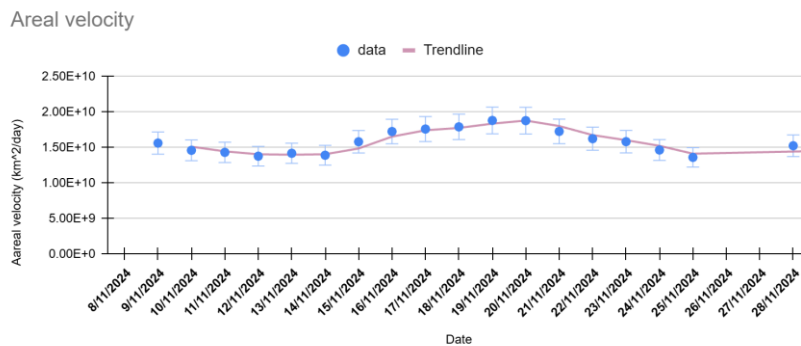


Figure 2: Areal velocity of the Moon over different periods, calculated based on the distance and angular displacement observed daily from Thailand. (the red line shows the trendline.)

Table 1 Calculated distance and database distance between Earth and the moon. (Mukdahan, Thailand)

Date	Calculated distance (km)	Database distance (km)	%Error
8/11/2024	375370.98	375946	0.1529528177
9/11/2024	363164.84	370678	2.026869682
10/11/2024	371517.01	365435	1.664320604
11/11/2024	363164.84	360670	0.6917237364
12/11/2024	357566.56	356844	0.2024862405
13/11/2024	359556.23	354424	1.448048101
14/11/2024	357495.91	353768	1.053772529
15/11/2024	359284.91	355045	1.194189469
16/11/2024	365011.17	358172	1.909465285
17/11/2024	355179.94	363073	2.173959507
18/11/2024	371425.49	369800	0.4395592212
19/11/2024	378860.95	376887	0.5237511509
20/11/2024	382999.29	381053	0.5107662189
21/11/2024	386105.17	386746	0.1656978999
22/11/2024	396426.26	391556	1.243822084
23/11/2024	400356.19	395301	1.278820443
24/11/2024	401493.38	397835	0.9195721844
std			0.6566133095

Table 2 Calculated areal velocity

Date	Areal velocity (km²/48 hours)
8/11/2024	375370.98
9/11/2024	363164.84
10/11/2024	371517.01
11/11/2024	363164.84
12/11/2024	357566.56
13/11/2024	359556.23
14/11/2024	357495.91
15/11/2024	359284.91
16/11/2024	365011.17
17/11/2024	355179.94
18/11/2024	371425.49
19/11/2024	378860.95
20/11/2024	382999.29
21/11/2024	386105.17
22/11/2024	396426.26
23/11/2024	400356.19
24/11/2024	401493.38
mean	15985868491
std	1676168820
%std	10.48531596

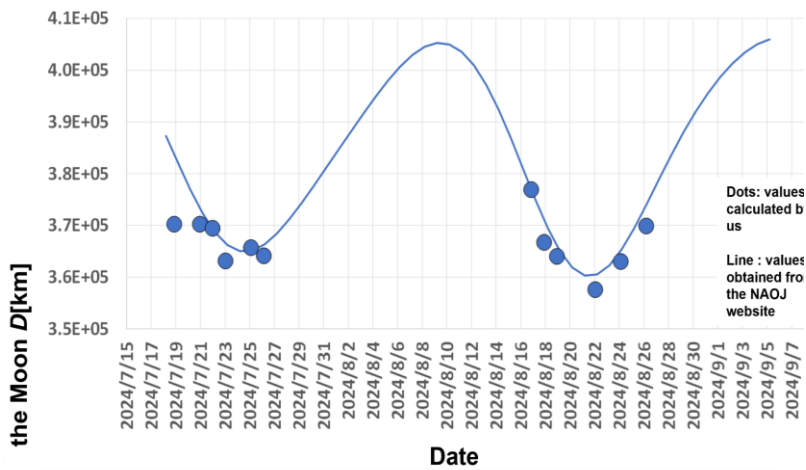


Figure 3: Distance between the Moon and Earth, using Fukushima Prefecture, Japan as the observation point. (NAOJ stands for National Astronomical Observatory of Japan)

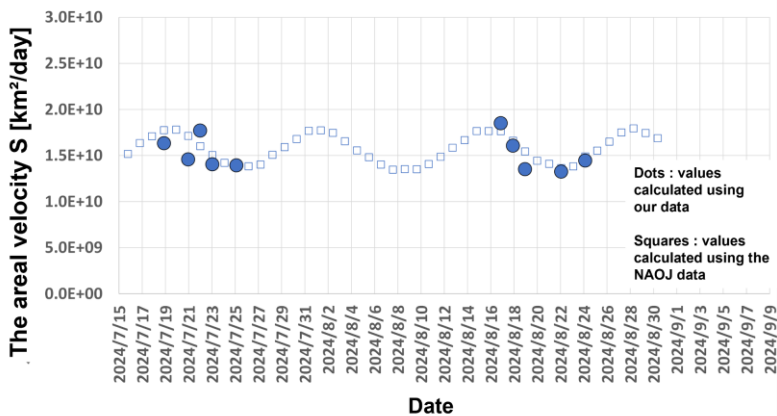


Figure 4: Areal velocity of the Moon over different periods, calculated based on the distance and angular displacement observed daily from Japan.

Table 3 Calculated distance and database distance between Earth and the moon. (Fukushima, Japan)

Date	Calculated distance (km)	Database distance (km)	%Error
18/7/2024	370229.1385	383687	3.51
20/7/2024	370229.1385	373273	0.82
21/7/2024	369425.7776	369277	0.04
23/7/2024	363122.258	366486	0.92
25/7/2024	365684.9886	365066	0.17
26/7/2024	364120.7762	366239	0.58
16/8/2024	376903.1954	376932	0.01
17/8/2024	366697.6699	370999	1.16
18/8/2024	364009.5586	365995	0.54
22/8/2024	357565.8463	360383	0.78
24/8/2024	363011.6495	365110	0.57
26/8/2024	369884.4135	373994	1.10
		std	0.8145

Table 4 Calculated areal velocity (Fukushima, Japan)

Date	Areal velocity (km ² /48 hours)
18/7/2024	16329332335
20/7/2024	14576388380
21/7/2024	17701203776
23/7/2024	14045449491
25/7/2024	13926294384
26/7/2024	
16/8/2024	18502342186
17/8/2024	16063540170
18/8/2024	13512702939
22/8/2024	13253820468
24/8/2024	14446303139
26/8/2024	
mean	15235737727
std	1817099489
% std	11.9265606

4. Discussion

4.1 Distance

The experiment presented a wave-like relationship between the Moon's distance from Earth (Figure 1 and 3) and the daily time interval, identifying points of closest and farthest distances. This observation confirms that the moon does not orbit the earth in a perfect circle.

4.2 Areal velocity

The areal velocity of the moon was calculated to validate Kepler's Second Law, commonly applied to the motion of celestial bodies such as stars and planets. The results revealed that the areal velocity remains nearly constant (Figure 2 and 4) as indicated by the low slope of the trendline and 10.49% deviation percentage. However, minor daily fluctuations were observed. These variations are attributed to changes in the moon's angular motion and its varying distance from the earth, both of which affect gravitational forces and the moon's orbital velocity.

5. Conclusion

Kepler's second law of planetary motion has already been proven a long time ago. However, the application of the law is rarely seen. Utilizing the digital camera and a computer program provided us with an approximate value of the moon's distance from the earth which is then used to calculate orbital swept area. The relative error observed in calculated areal velocity is 0.815 percentages. We believe the errors were caused by the camera's resolution, noises, mist, moonlight flare, and our error in the image processing. These factors ultimately made our data discrepant compared to the data we retrieved from an application called "Stellarium" using the coordinates of Mukdahan, Thailand. Usually, the distance between the Earth and the moon is routinely measured using Light Detection And Ranging (LIDAR) stations which bounce laser pulses off of the retroreflecting mirrors placed on

the Moon by the Apollo astronauts (Mangum, 2016). Another approach is to use the parallax to find the moon's distance. Therefore the method we proposed provides another option for amateur astronomers with telescopes to try and experiment with the moon using Kepler's second law themselves.

6. Acknowledgements

We would like to express our deepest gratitude to the late Yoshiyuki Shimizu, who donated the telescope to Fukushima High School.

7. References

LESA. (n.d.). The motion of planets: Kepler's laws. *LESA*. Retrieved June 5, 2024, from <https://www.lesa.biz/ดาราศาสตร์/การเคลื่อนที่ของดาวเคราะห์/กฎของเคปเลอร์>.

LESA. (2024, October 10). แพลนแลกซ์: สมบัติของดาวฤกษ์. *LESA*. Retrieved from <https://www.lesa.biz/ดาราศาสตร์/สมบัติของดาวฤกษ์/แพลนแลกซ์>.

Stellarium. Stellarium web: Online planetarium. Retrieved June 5, 2024, from <https://stellarium-web.org>.

Astronomical Society of Japan. (2017). *T02: Celestial motion studies*. Retrieved from <https://www.asj.or.jp/jsession/old/2017haru/yokou2017/T02.pdf>.

Celestial Wonders. *Star angle calculator*. Retrieved from <http://celestialwonders.com/tools/starAngleCalc.html>.

National Astronomical Observatory of Japan. *Moon phase calculator*. Retrieved from <https://eco.mtk.nao.ac.jp/cgi-bin/koyomi/cande/moon.cgi>.

Producing Bioethanol From Food Waste Utilizing Yeast Fermentation

Hanna Abe¹, Rion Orihara¹, Karin Daimon¹

Phansiri Thongpreecha², Kullaphat Promarak², Jiraphat Chaisoontorn²

¹Kobe high school (Japan)

²PCSHSM (Thailand)

Abstract:

This study comes from the fact that ethanol is currently widely used, whether in experiments or medicine. This study is also a comparison and wants to know about the materials of waste that can be found in everyday life, namely Sticky rice, noodle, banana, watermelon peel, corncob, rice cake, potato, flour, rice and cabbage, which are used in the experiment to compare the amount of alcohol obtained from the fermentation process. These materials will go through the process of changing carbohydrates or cellulose into sugar, which is glycolysis and fermentation of the obtained sugar with yeast through the fermentation process. The steps are as follows: soaking materials with 2.5 molar NaOH for 18 hours at 60 °C and then soaking with 0.5 % w/v H₂SO₄ and fermentation with *Saccharomyces cerevisiae* yeast at 8 % w/w for 48 hours at 30 °C and measuring the alcohol content with a refractometer. The results showed different alcohol contents The ingredients used are diverse and the results vary greatly: Sticky rice 3.6 % v/v, noodle 1.8 % v/v, banana 0.7 % v/v, watermelon peel 0.4 % v/v, corncob 0.1 % v/v, rice 11 % v/v, flour 14.5 % v/v, rice cake 27 % v/v, potato 34 % v/v and cabbage 33 % v/v.

Keywords: Bioethanol; *Saccharomyces cerevisiae* yeast; fermentation; alcohol refractometer

1. Introduction

The development of renewable energy sources is one of the important approaches that can help reduce dependence on fossil fuels, which are limited energy sources that have long-term environmental impacts. Therefore, there is support and research to find new alternatives for sustainable energy production with minimal environmental impact. One interesting renewable energy source is ethanol, which can be produced by fermenting carbohydrates in various materials, especially from food waste, which has cellulose, starch and sugar as the main components.

Ethanol production from food waste has received much attention in recent years because food waste has been a major problem in many countries, which is often discarded without any benefit. Although these food wastes can be used to produce renewable energy, like the production of ethanol from various energy crops that are widely used in industry, using these food wastes not only reduces waste but can also be used to produce ethanol, which can be used as an alternative energy source for fossil fuels.

Food waste that can be used to produce ethanol includes materials that are high in starch or carbohydrates left over from daily consumption. The production process for ethanol from these food wastes has an important step: decomposing carbohydrates in these raw materials into sugar, which will be fermented with yeast to produce ethanol and carbon dioxide gas. This process can be used both at the household and commercial levels.

Reducing waste and using resources sustainably. Food waste is often an environmental problem that requires effective management. Using this food waste to produce ethanol reduces the amount of waste and makes the use of resources worthwhile.

The production of ethanol from food waste can help reduce the use of fossil energy sources such as oil and natural gas, which have both limitations in their use and impacts on the environment, including climate change. Including creating added value from food waste.

Food waste that is often discarded can be utilized in many aspects, such as the production of ethanol as an alternative energy, the production of supplementary products from the fermentation process, and reducing the cost of waste management. The development of an ethanol production system from food waste has the potential to be used in industry and education in the future.

The selection of food waste in the experiment came from observing the amount of food wastes in cafeterias in Thailand and Japan 's schools, sticky rice, noodle, banana, watermelon peel, corncob, rice cake, potato, flour, rice and cabbage, which are selected the most. Therefore, it was compared for ethanol production in the experiment.

From the above, writing a project report on the topic of ethanol production from food waste is important in terms of presenting the research process and related experiments to understand the appropriate method of using various food wastes as materials for producing alternative energy. It can also help develop sustainable energy production technology in the future, including reducing the environmental impact from the use of natural resources in the traditional way.

2. Methodology

2.1) The method of Thailand's Experiment

- (1) Crush the sample(food) to speed up the reaction.
- (2) Put it in a glass bottle. Add NaOH 2.5 molar in a ratio of 10:1
solution (ml): material (g) control temperature at 60 Celsius 18 hours in a water bath.
- (3) Neutralize with distilled water and add H₂SO₄ 0.5 %/w in a ratio of 10:1
solution (ml): material (g) to control temperature at 100 Celsius for 3 hours in a water bath.
- (4) Adjusting to pH 5.12 by distilled water.
- (5) Filtering by sheet cloth to separate out the solid part.
- (6) Fermentation by Baker's yeast 8% w/w (0.24 g) with 3 g of material and 10 ml of distilled water control at 30 Celsius for 48 hours.
- (7) Analyze obtaining ethanol by an alcohol refractometer.

Table 1. Amount of alcohol in each material (Thailand)

material	Amount of Alcohol (% v/v)
Sticky rice	3.6
Noodle	1.8
Banana	0.7
Watermelon peel	0.4
Corn cob	0.1

Table 2. The amount of alcohol obtained from each measurement and the average value (Thailand)

Material	Amount of Alcohol (% v/v)			
	Test 1	Test 2	Test 3	Average
Sticky rice	3.7	3.5	3.6	3.6
Noodle	1.8	1.8	1.8	1.8
Banana	0.7	0.9	0.5	0.7
Watermelon peel	0.5	0.6	0.4	0.4
Corn cob	0.1	0.1	0.1	0.1

2.2) The method of Japan's Experiment

- (1) Crush the sample(food) to speed up the reaction.
- (2) Put it in a glass bottle. Add NaOH 2.5molar 10 ml control temperature at 60 Celsius 18 hours in a water bath.
- (3) Neutralize with H₂SO₄ and add H₂SO₄ 0.5 % w/w 10 ml to control temperature at 100 Celsius for 3 hours in a water bath.
- (4) Adjusting to pH 6
- (5) Fermentation by Baker's yeast 0.3 g control with 3 g of material at 30 Celsius for 48 hours.
- (6) Filter the alcohol
- (7) Analyze obtaining ethanol by an alcohol refractometer.

Table 3. Amount of alcohol in each material (Japan)

material	Amount of Alcohol (% v/v)
Rice	11
Flour	14.5
Rice cake	27
Potato	34
Cabbage	33

3. Results

The number was significantly higher in the Japanese experiment, possibly due to differences in the equipment used in Thailand and Japan.

The results of the experiment found that when measuring the amount of alcohol from food waste, measured by a handheld refractometer, it was found that potato had the highest alcohol content at 34% v/v, cabbage at 33% v/v, rice cake at 27% v/v, flour at 14.5%, and rice at 11% v/v.

And the experiment using a digital refractometer found that sticky rice had the highest alcohol content at 3.6% v/v, noodle at 1.8% v/v, banana at 0.7% v/v, watermelon peel at 0.4% v/v, corncob at 0.1% v/v.

4. Discussion

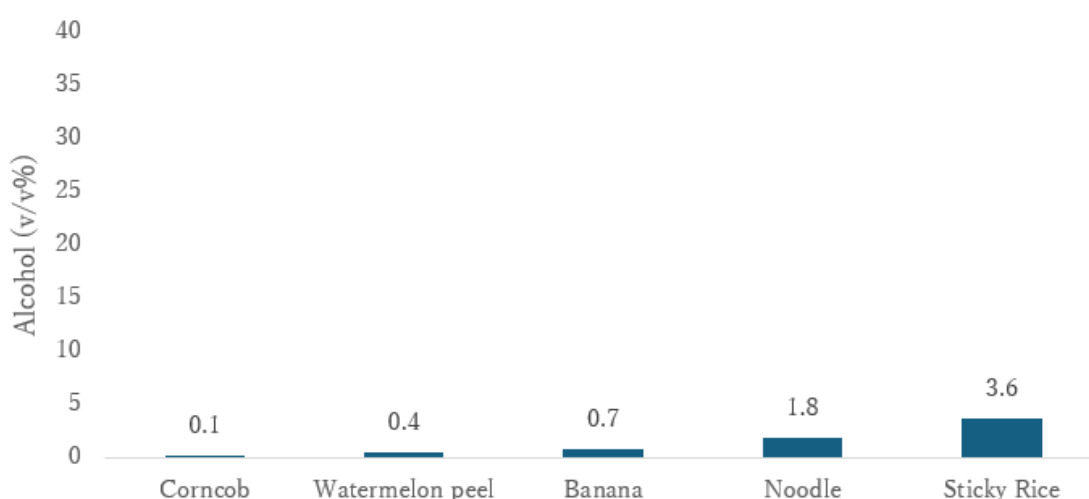


Figure 1. Amount of alcohol in each material
By digital refractometer alcohol (Thailand)

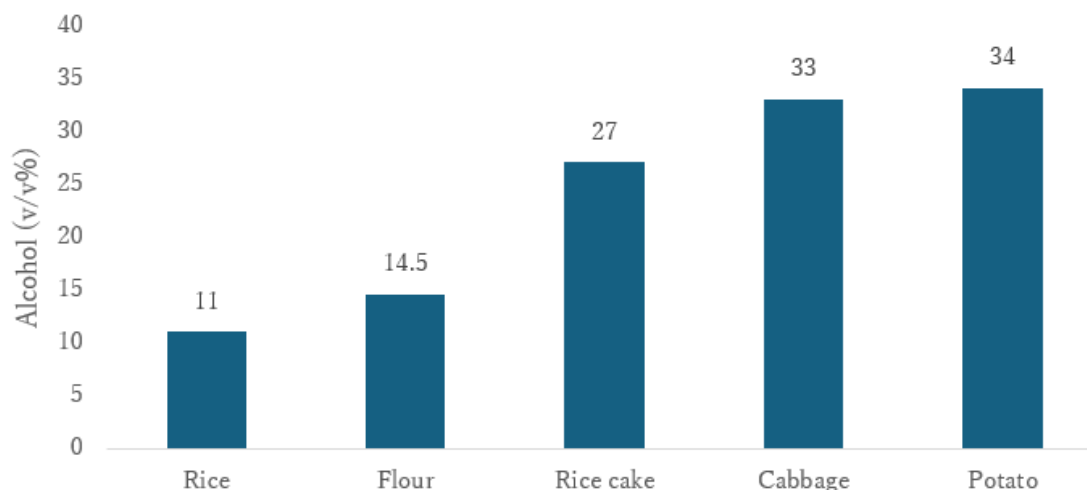


Figure 2. Amount of alcohol in each material
By handheld refractometer (Japan)

5. Conclusion

From the experimental results, the highest amount of alcohol is 34 % v/v of potato and the second highest is 33 % v/v of cabbage. On the other hand, the lowest amount of alcohol was 0.1 % v/v of corncob. This shows that any material with a high carbohydrate content, when converted to sugar for use in the fermentation process, will be able to produce a higher amount of alcohol than a substance with a lot of cellulose as a component. All materials used in the experiment are able to produce alcohol.

6. References

- Ruchala, Justyna, et al. "Construction of advanced producers of first- and second-generation ethanol in *Saccharomyces cerevisiae* and selected species of non-conventional yeasts (*Scheffersomyces stipitis*, *Ogataea polymorpha*)." *Journal of Industrial Microbiology and Biotechnology*, vol. 47, no. 1, 1 Jan. 2020, pp. 109-132, <https://doi.org/10.1007/s10295-019-02242-x>.
- Jahanbakhshi, Ahmad, and Rouhollah Salehi. "Processing watermelon waste using *saccharomyces cerevisiae* yeast and the fermentation method for bioethanol production." *Journal of Food Process Engineering*, vol.42, no.7,22 Oct.2019, <https://doi.org/10.1111/jfpe.13283>.
- Temam Gameda Genemo, et al. "Optimizing bio-ethanol production from cabbage and onion peels waste using yeast (*saccharomyces cerevisiae*) as fermenting agent." *International Journal of Life Science Research Archive*, vol.1, no.1, 30Sept.2021, pp.024-035, <https://doi.org/10.53771/ilsra.2021.1.1.0012>.
- Conventional ethanol production from corn and sugarcane." *Gasoline, Diesel and Ethanol Biofuels from Grasses and Plants*, 19 Apr. 2010, pp. 73-83, <https://doi.org/10.1017/cbo9780511779152.006>.
- Izmirlioglu, Gulten, and Ali Demirci. "Ethanol production from waste potato mash by using *saccharomyces cerevisiae*." *Applied Sciences*, vol.2, no.4,22Oct.2012, pp. 738-753, <https://doi.org/10.3390/app2040738>.

Comparision and consideration of damage by *Lantana camara* in Japan and Thailand

Jin Yoshinouchi¹, Mao Joukou¹, Nozomi Hashimoto¹, Chollada Rakthamanoon², Siriphadsorn

Tunsrisuwan², Pattarapol Boonsom² Supervisor: Mr. Yuta Wakayama¹, Ms. Daranee Chaiyaveij²

¹*Ehime Prefectural Matsuyamaminami High School (Japan)*

²*Princess Chulabhorn Science High School Pathum Thani (Thailand)*

Abstract:

In recent years, invasive species have become a problem. This is because the invasion of non-native species can have a serious impact not only on ecosystems, but also on humans and the agriculture, forestry, and fisheries industries during our exploration of exotic plants in Japan and Thailand, we came across a plant called *Lantana camara*. *Lantana camara* is very fertile, and its unripe fruits contain a toxic substance. We actually grew *Lantana camara* from seedlings and experimented to see if the growth rate, longevity, leaf size, and number of flowers differed between Japan and Thailand in different climates. As a result, the color of *Lantana camara* leaves and flowers was darker and more distinct in Thailand than in Japan. In addition, more flowers were produced in Thailand than in Japan. Therefore, *Lantana camara* was found to live longer at about 30°C. They also found that there were differences in flower-visiting insects, with aphids in Thailand and ants in Japan being found in *Lantana camara*.

Commonalities between the two countries were that multiple peaks in the number of blooms were observed and that the stems of *Lantana camara* were divided into four sections from the base. From these, we were able to discuss the reasons for the phenomenal invasion of *Lantana camara*.

Keywords: *Lantana camara*; growth rate; invasive species

1. Introduction

In recent years, invasive species have become a problem. This is because the invasion of non-native species can have a serious impact not only on ecosystems, but also on humans and the agriculture, forestry, and fisheries industries. *Lantana camara* is a familiar alien plant both in Japan (Ehime Prefecture) and Thailand and has been selected as one of the 100 worst invasive alien species in the world. Therefore, we thought that clarifying the conditions under which *Lantana camara* can easily grow would be useful in stopping further erosion and exterminating the plant.

2. Methodology

(1) Plant lantana seeds in pots. (Table1)

(2) Take pictures of the lantana growing for about two months.

(3) Record the daily growth and compare the speed of growth between Thailand and Japan.

[necessities]

pots, soil, lantana seeds, smartphone (recording media, camera), ruler

Table 1. Growing conditions

Growing Environment	Place in a well-drained location in full sun
watering	Do this every day
fertilizer	Without fertilizer
planting mix	Commercial culture soil mixed with 30% inorganic, fertilizer-free soil
transplantation	No replanting



Figure 1. Lantana camara grown in Japan



Figure 2. Lantana camara grown in Thailand

3. Results

Lantana camara loses its flowers and begins to wither after 56 days in Japan and 64 days in Thailand. The first week was set as 0, and the subsequent changes were plotted on a graph. (Figure5) (Figure6) We obtained the following results from these figures and graphs.

- The weather in Thailand is constant at about 30°C (86°F), but in Japan the temperature is gradually dropping from 30°C (86°F) to 20°C (68°F).
- The Japanese lantana camara grew larger in size than the Thailand ones. (Figure5) (Figure6)
- Multiple peaks in the number of blooms were observed in both countries.
- In both countries, the stem of the lantana camara was split into four pieces from the base. (Figure9) (Figure10)
- Aphids in Thailand and ants in Japan were found in Lantana camara.
- The colors of the leaves and flowers of Lantana camara were darker and more distinct in Thailand than in Japan.
- More flowers bloomed in Thailand than in Japan. (Figure7) (Figure8)

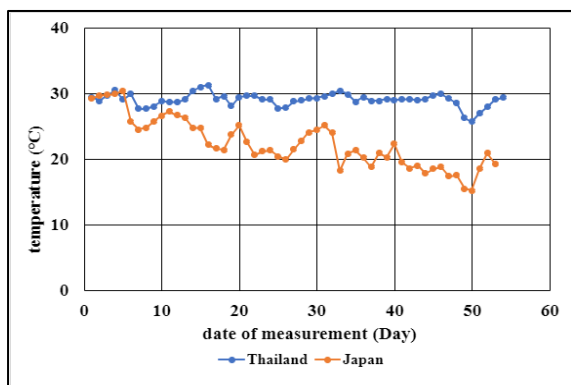


Figure 3. Temperature on the day of the study

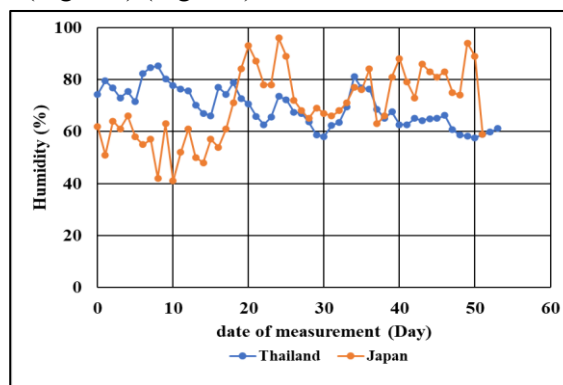


Figure 4. Humidity on the day of the study

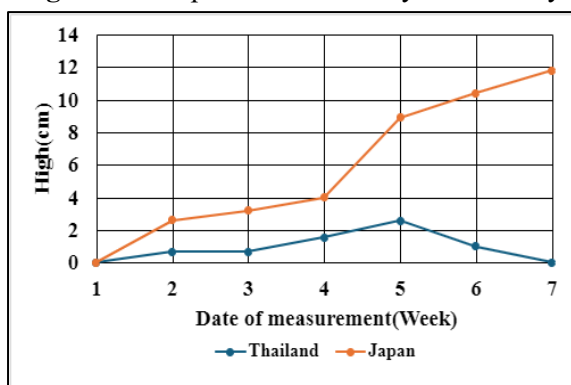


Figure 5. Lantana camara height change

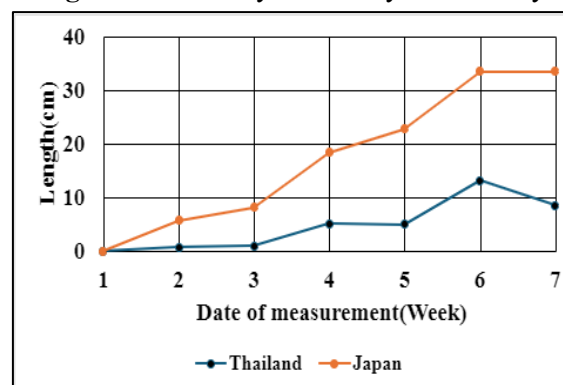


Figure 6. Lantana camara Length change

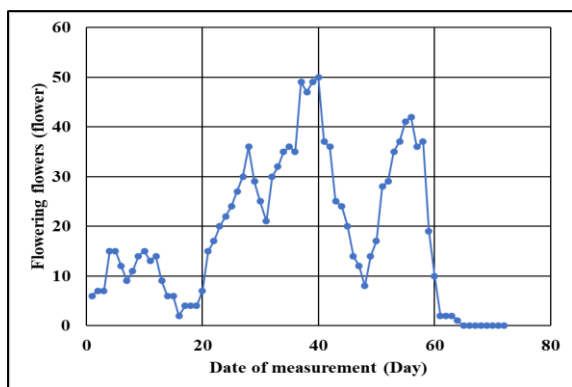


Figure 7. Number of blooms in Thailand

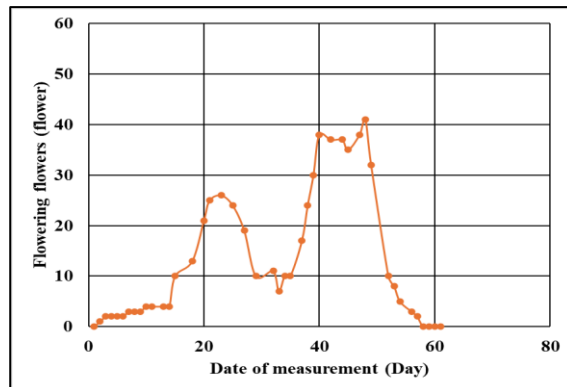


Figure 8. Number of blooms in Japan



Figure 9. Lantana camara stem in Thailand



Figure 10. Lantana camara stem in Japan

4. Discussion

The reason it took longer for Thailand's Lantana camara to wither than Japan's Lantana camara may be because Thailand's temperatures were warmer and more stable than Japan's. Also, according to Figure 7 and 8, high temperatures can have a positive effect on the number of flowers of Lantana camara. However, according to Figure 3, 5 and 6, too high temperatures can negatively affect the development of Lantana camara.

Lantana camara's characteristic of having a stem that divides into four parts from the base may allow it to survive in confined spaces. The amount of soil was ambiguous and made a difference in the length of "a". This may have caused a large difference in the horizontal length and vertical length. (Figure11) (Figure12)



Figure 11



Figure 12

5. Conclusion

Lantana camara lives longer at about 30°C. In addition to it, temperature differences may affect the number of flowers, height and length. We needed to think more about the conditions under which we were making our observations.

6. References

- LOVEGREEN (2024). What is Lantana? How to grow and cultivate | Plant Guide
<https://lovegreen.net/library/flower/p89057/> August 18, 2024
- Ehime University, Faculty of Education (2018) How to use Image J” file6.pdf (ehime-u.ac.jp)
<https://www.ed.ehime-u.ac.jp/~muko-lab/img/file6.pdf> July 2, 2024
- Weather Underground (1994) Weather Underground Bangkok, Thailand Weather History
<https://www.wunderground.com/history/weekly/th/bangkok/VTBD/date> December 24, 2024
- Japan Meteorological Agency (1956) Japan Meteorological Agency | Search past weather data
https://www.data.jma.go.jp/obd/stats/etrn/index.php?prec_no=73&block_no=47887&year=2024&month=09&day=&view=p1

A study comparing water quality between Thailand and Japan

Asaki Kojo¹, Kaho Kunishima¹, Miyamoto Noka¹, Yui Yokoyama¹,

Natchaya Rungrotasanee², Yanita Kaeobuathong²

¹Hyogo Prefectural Akachi-Kita High School (Japan)

²Princess Chulabhorn Science High School (Thailand)

Abstract:

The purpose of this Correspondence is to study the water quality between Thailand and Japan. A total of 5 study points were conducted. Samples were collected using the scooping method during August 2024 - October 2024. Parameters used in water quality analysis were pH, temperature, turbidity, dissolved oxygen (DO) and conductivity.

From the analysis of water quality between Thailand and Japan, it was found that the pH values differ significantly. In the case of Chang Canal, Trang Province, Thailand, the pH ranges from 6.8 to 7.1, while in rivers in Japan, the pH ranges from 7.4 to 9.3. This indicates that the water in Thailand's rivers is neutral, whereas the water in Japan's rivers is more alkaline. Moreover, the DO (Dissolved Oxygen) values also show a significant difference. In Thailand's rivers, the DO ranges from 4.4 to 5.7 mg/L, whereas in Japan's rivers, the DO ranges from 4.5 to 12.6 mg/L. This demonstrates that the water in Japan's rivers has a much higher DO compared to the water in Thailand's rivers.

Keywords: Water Quality; River; Khlong Chang River

1. Introduction

Thailand and Japan are both countries that place importance on water resource management. Because water is an important factor in life, agriculture, industry and environmental protection. However, the two countries have different geographies, climates, and levels of development. This affects the water quality and water management of each country. A comparison of water quality between Thailand and Japan was undertaken to study differences in management practices and factors affecting water quality in various contexts.

2. Methodology

Water samples were collected from 5 points in the study area (3 replications were analyzed at each point)

Measure the following parameters:

- pH
- Temperature
- Turbidity
- Dissolved Oxygen

The water analysis method in the research is shown in **Table 1** according to the standard criteria for water sample analysis.

Table 1. Analysis of river sample

Parameter	Method of analysis
pH	pH Meter
Temperature	Thermometer measurement during sampling
Turbidity	Turbidity Meter
DO (Dissolved oxygen)	Azide Modification

3. Results

Table 2. Water quality in Japan

Quality of water			
Point	pH	Turbidity (NTU)	DO (mg/L)
1	7.9	22.3	7.8
2	8.2	40.2	8.7
3	7.4	22.2	4.5
4	9.3	25.3	11.7
5	9.2	21.4	12.6

Table 3. Water quality in Thailand

Quality of water						
Point	Temperature (°C)		pH	Turbidity (NTU)	DO (mg/L)	Conductivity (µS/cm)
	Water Surface	Water				
1	30.2	32.6	6.8	22.7	4.4	252
2	31.8	34.7	7	26.5	4.8	184
3	30.6	37.1	7.1	23.1	5	173.7
4	31	36.8	7	23.6	5.7	185.6
5	30.5	35.2	7	31.3	4.9	218

4. Discussion

From the analysis of water quality between Thailand and Japan, it was found that the pH values differ significantly. In the case of Chang Canal, Trang Province, Thailand, the pH ranges from 6.8 to 7.1, while in rivers in Japan, the pH ranges from 7.4 to 9.3. This indicates that the water in Thailand's rivers is neutral, whereas the water in Japan's rivers is more alkaline.

Moreover, the DO (Dissolved Oxygen) values also show a significant difference. In Thailand's rivers, the DO ranges from 4.4 to 5.7 mg/L, whereas in Japan's rivers, the DO ranges from 4.5 to 12.6 mg/L. This demonstrates that the water in Japan's rivers has a much higher DO compared to the water in Thailand's rivers.

5. Conclusion

The geographical location and climate have an impact on pH changes. During August to October, Thailand experiences its summer season, while Japan is in its rainy season. Additionally, differences in riverbed composition—soil-based versus concrete—may play a role. It is possible that limestone reacts with water to form calcium hydroxide, which is alkaline, thereby influencing an increase in pH levels.

Furthermore, air temperature affects DO (Dissolved Oxygen) levels. Thailand's higher temperatures compared to Japan lead to increased movement of particles in the water, reducing the oxygen content. As a result, the DO levels in Thailand's water are lower than those in Japan.

6. Acknowledgements

The collaborative research between Thailand and Japan was successfully conducted with the kind support of Princess Chulabhorn Science High School Trang, Thailand, and Hyogo Prefectural Akashi-Kita High School, Japan, which facilitated and promoted this research project.

7. References

American Water Works Association/ American Public Works Association/Water Environment

Federation. Standard methods for the examination of water and wastewater. 22nd ed. Washington, D.C.; 2012.

Sunanta Narakam, Sunantha Laowansiri. (2018). Comparison of Water Quality of Waterfalls in PhuRuea National Park. <https://shorturl.asia/E2iSK>

The Differences between Japanese rice and Thai rice in making rice resin

Nanami Matsunaga¹, Nanami Ogawa¹, Jitraphat Chanakul², Phakhin Chantayothin²

¹*Yamaguchi Prefectural Tokuyama Senior High School (Japan)*

²*Princess Chulabhorn Science High School Trang (Thailand)*

Abstract:

Rice resin is becoming a more sustainable alternative to traditional plastics, supporting the United Nations' Sustainable Development Goal (SDG) 12, which encourages responsible consumption and production. This study looks at the differences between Japanese rice and Thai rice in making rice resin, focusing on their properties. Japanese rice is known for its sticky texture and high starch content, while Thai rice is known for its fragrant aroma and lower starch content. These differences affect how the rice resin behaves, such as its strength and durability. The report also explores how these rice varieties impact the efficiency of making rice resin, helping to reduce our dependence on plastic made from oil. Additionally, the study shows that the average weight from rice resin which was made from Japanese rice and Thai rice is 7 kilograms. By examining the properties of Japanese and Thai rice, this report offers insights into developing sustainable bioplastics that align with global sustainability goals and promote responsible production methods.

Keywords: Japanese rice, Thai rice, Rice Resin, Weight load

1. Introduction

In recent years, there has been a growing interest in finding sustainable alternatives to plastic, which is harmful to the environment. One such alternative is rice resin, a bioplastic made from rice, which is biodegradable and eco-friendly. Rice is widely grown around the world, and two popular types—Japanese rice and Thai rice—have unique characteristics that might affect the properties of rice resin.

Japanese rice is known for its sticky texture and high starch content, while Thai rice is famous for its fragrant aroma and lower starch content. These differences may influence the strength, durability, and processing of rice resin. This study compares these two rice varieties to understand how their properties impact rice resin production.

By examining Japanese and Thai rice, this research aims to offer insights into making better, more sustainable bioplastics. This is in line with the United Nations Sustainable Development Goal (SDG) 12, which promotes responsible consumption and production, as shown in Figure 1. The findings may help reduce the need for plastic made from oil and encourage the use of environmentally materials.



Figure 1. Rice resin exhibited at Sustainable Material Expo

2. Methodology

2.1. Preparation of plastic samples

Heat the hotplate or fire to 300 °C, then let the biodegradable plastic melt. Once melted, mix the plastic with rice flour (Japanese rice for Japan, Thai rice for Thailand) in a 1:1 ratio until the mixture is evenly distributed. Then, pour the processed plastic into a square mold measuring 8x8 cm and 0.5 cm thick, and let it cool and harden. The resulting product is called “Rice resin.”

2.2. Strength testing

The next step is to test the strength of rice resin by weighing it, as shown in the experimental diagram in Figure 2. In this step, we tie a rope to rice resin, place a weight on the rope, and record the maximum weight that rice resin can load. Afterward, we compare the maximum weight that rice resin can load using both Japanese rice and Thai rice.

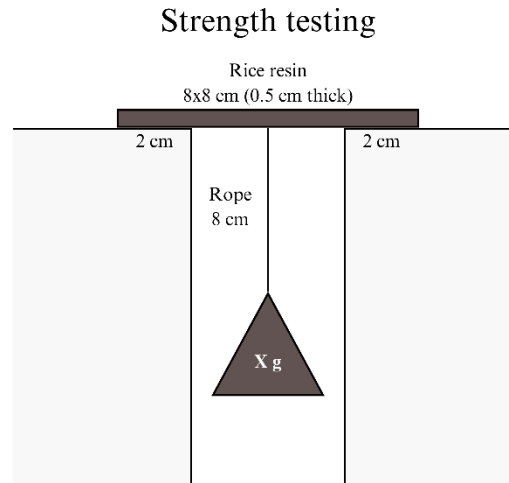


Figure 2. Experimental diagram

3. Results

From the strength test, the average weight from rice resin which was made from Japanese rice and Thai rice. The experimental results can be recorded in Table 1.

Table 1. Experimental results: Weight that rice resin can load

	Japanese rice resin	Thai rice resin
Average Weight(kg)	7	7

4. Discussion

The average weight from rice resin which was made from Japanese rice and Thai rice is 7 kilograms.

5. Conclusion

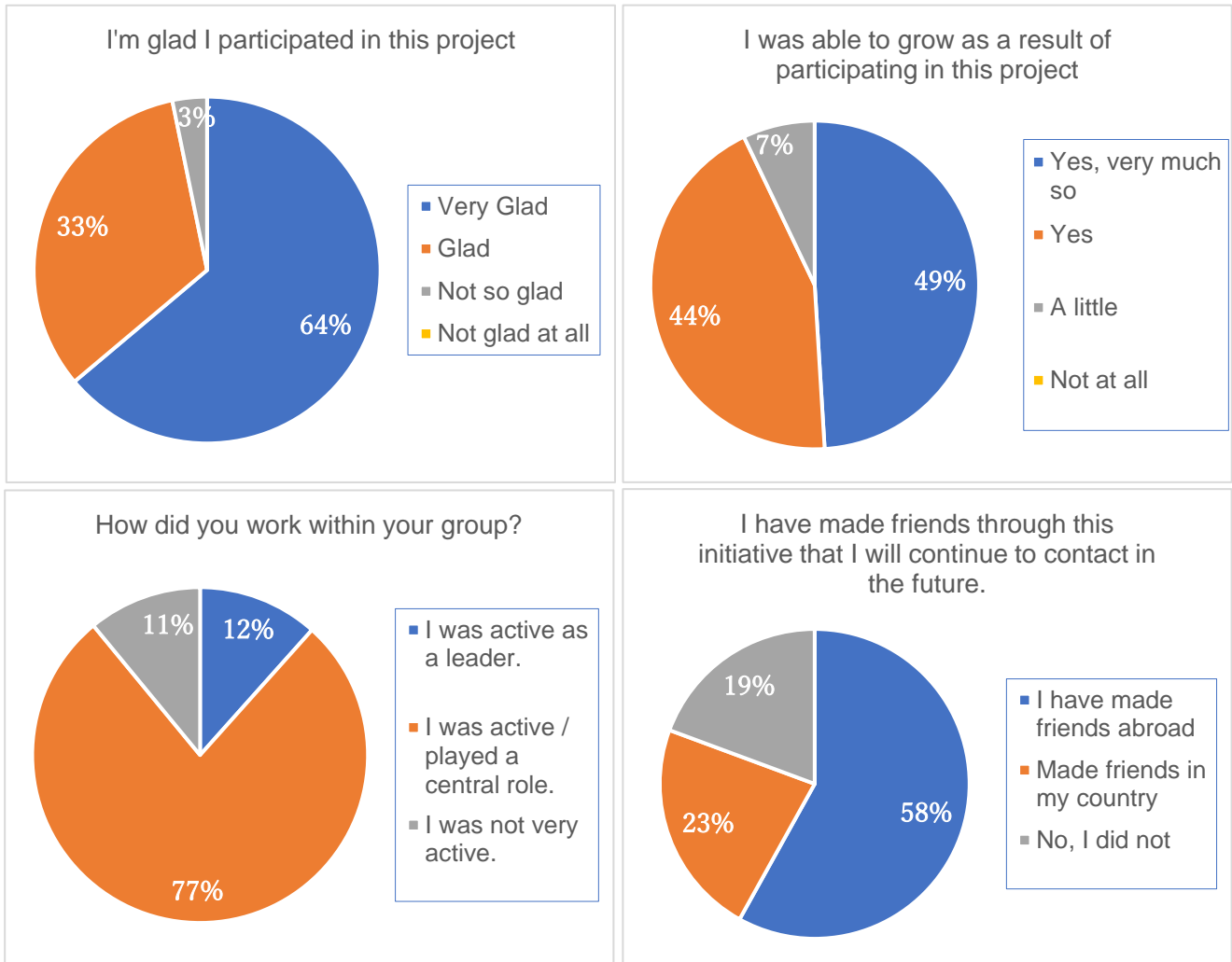
This study looks at the differences between Japanese rice and Thai rice in making rice resin, focusing on their properties. Japanese rice is known for its sticky texture and high starch content, while Thai rice is known for its fragrant aroma and lower starch content. These differences affect how the rice resin behaves, such as its strength and durability. And the result is also showed that the average weight from rice resin which was made from Japanese rice and Thai rice is 7 kilograms.

6. References

- Dayi Qian, Nuohan Wang, Qunhui Wang, Tianlong Zheng, Xiaona Wang, & Yongsheng Li. (2024, 12 23). Research Hot Spots and Development Trends of Biodegradable Plastics. *ScienceDirect*. <https://www.sciencedirect.com>
- ITPO Tokyo. (n.d.). Rice Resin. *UNIDO*. <https://itpo-tokyo.unido.org>
- Thai Plastics Industries Association. (n.d.). Activities: Rice Resin Development for Sustainable Plastics. *Thai Plastics Industries Association*. <https://thaiplastics.org>
- United Nations. (n.d.). Sustainable Development Goals. *United Nations*. <https://sdgs.un.org>

Post Survey Results

The following pie graphs are the results of the survey taken after the International Collaborative Research Fair. The results of the overseas students and Japanese students were combined for a total of 155 students (79 overseas students, 76 Japanese students).



The percentage of affirmative responses to the questions "I'm glad I participated in this project." was 97% and "I was able to grow as a result of participating in this project" was 93%, indicating that the participating students highly evaluated the project. The percentages of "very glad" and "Yes, very much so" were also high at 64% and 49%, respectively, indicating that the International Collaborative Research project has a significant impact on the students' growth and that they feel a sense of accomplishment and satisfaction. In the question "How did you work within the group?" 12% of the students were able to take an active role as a leader, whereas 77% of the students were able to be active and play a central role in an international research group. When asked if they had made lasting friends through this program, almost 60% of the students made friends overseas, indicating that the program was effective in building an international network.

This initiative has aimed to develop international leaders through the following four objectives.

- Discuss objectives and methods from a broad and high-level perspective
- Communicate in English with group members
- Enhance coordination skills to divide roles and share opinions with each other
- Make friends without concern about national borders

We believe that the above four objectives were achieved at a high level. We hope that more high school students will continue to experience international collaborative research during their high school years, feel the importance of cooperation beyond national borders, and expand their future activities.

Here are some of the comments from the participants.

- Over the past seven months, I've seen significant personal and professional growth. Positively, I've improved my communication and teamwork skills, particularly in overcoming language and cultural barriers. I've also developed a deeper appreciation for cultural diversity and its role in enriching collaborative work. On the downside, balancing the demands of this project with other commitments was challenging at times, but it taught me better time management and prioritization.
- Aside from the technical skills I've developed from doing this project, I was able to emotionally grow and really empathize and see the beauty in transcending language barriers for a common purpose. But of course, along with that came adversities, most of which stemmed from role conflicts and time constraints which might have affected some of my other pursuits.
- I've become incredibly inspired by the power of diversity and international collaboration, and I intend to continue exploring this in my future years at college. My communication skills have increased significantly, and I have become more open-minded. Though language and culture barriers were difficult to get over, I now see them as opportunities to learn about other people rather than obstacles to overcome.
- As for me, there's a lot of positive changes that occurred during my journey with this project — such as communication skills, empathy for others, respect for each other, and being able to share each other's cultures.
- I have learned the format of a formal essay, and how to analyze the data. Moreover, I found how to demonstrate my results in a way that even those unfamiliar with the topic could understand.
- I have learned a lot from the report about doing research. Not only did my knowledge improve, but I also learned how to get along with others and manage time better.
- Participating in ICRF for seven months was an enriching and fulfilling experience. I felt proud to be part of such a dynamic and impactful initiative. There were moments of challenge, especially with the demands of collaboration, but they were outweighed by the excitement of contributing to meaningful work and forming strong connections with others.
- These past few months created a long-lasting memory between me and my friends. It has helped me develop bonds that I would've never gotten had I not joined. Additionally, the project

has made me less anxious to communicate with others abroad.

- I'm glad that I got the chance to join such an incredible project. I've never thought I could participate in an international research project. I got to improve my science skills and also build relationships with Japanese students.
- Participating in this project made me reflect on my own actions and appreciate the excellence of those around me. I had many moments of frustration and self-doubt, but it was a stimulating and valuable experience. I'm really glad I took part. *(translated from Japanese)*
- Through ICRF, I made friends from overseas and had more opportunities to use English, which was truly beneficial for me. It also made me realize how amazing the research being done at other Japanese schools is. I now want to use English more going forward. Thank you for giving us such a wonderful opportunity. *(translated from Japanese)*
- Although I faced many challenges over these past seven months—things didn't go as planned, and the language barrier was tough—I kept believing I was growing, and I did my best. There are still parts of the research I want to explore further, so I hope I get the chance to participate in a project like this again. *(translated from Japanese)*
- This project helped me realize the responsibility and pressure that comes with leading a group, and most importantly, that this role actually suits me. I want to take on leadership roles more proactively from now on. *(translated from Japanese)*
- There were many difficulties, like communication issues with teammates and experiments not going well, but completing a full research project gave me a huge sense of achievement. I also developed planning and communication skills that will help me in the future. I'm truly glad I participated. *(translated from Japanese)*
- It was my first time working with international students, and everything felt new and exciting! I'd like to continue becoming someone who collaborates with people around the world instead of staying only in Japan. *(translated from Japanese)*
- Unlike classroom experiments, there's no right answer in research, and it was much harder than I imagined. But completing today's presentation gave me a big sense of accomplishment, and I'm now motivated to keep pursuing things I'm interested in. *(translated from Japanese)*
- Through regular communication, I gained vocabulary and improved both my everyday and academic English. The learning materials we received also helped me improve my scientific presentation skills. These experiences gave me confidence and a solid foundation for future research. *(translated from Japanese)*
- I gained the ability to approach challenges with perseverance—whether through experimentation or preparing presentations. I feel this experience helped me develop valuable resilience for life. *(translated from Japanese)*

2024-2025 International Collaborative Research Project Report

Issued March 2025

Issued by Ritsumeikan High School

1-1-1 Choshi Nagaokakyo City, Kyoto, JAPAN

TEL : +81-75-323-7111 FAX : +81-75-323-7123